A comparative study between Pt and Rh for the electro-oxidation of aqueous SO_2 and other model electrochemical reactions

M Potgieter

20463294

Dissertation submitted in partial fulfilment of the requirements for the degree *Magister Scientiae* in Chemistry at the Potchefstroom Campus of the North-West University

Supervisor: Dr RJ Kriek

Co-supervisor: Prof V Ramani

May 2014

Acknowledgements

Firstly, I would like to give glory to my Heavenly Father for all the opportunities and privileges He has granted me and for the strength and hope needed during my studies.

I would like to thank the following people:

- My husband Renier Potgieter, for all the love, support and patience throughout this study
- My baby girl, Maylene, you give me hope
- Parents, Marianne Allen and Hannes Smit, for believing in me and the sacrifices to allow me the opportunity to follow my dreams
- Adri Young, for all the support, help and working together
- Vasilica Lates, for all the help and advice during this study
- My study leaders, Cobus Kriek and Vijay Ramani for the leadership

I would also like to thank the following institutions for funding, without which this project would not have been possible:

Abstract

The ever increasing demand for a clean and renewable energy source has stimulated research for alternatives for the use of fossil fuels, which contribute significantly to global warming. The SO_2 oxidation reaction was studied for production of hydrogen as a clean and renewable energy carrier. This reaction occurs at a lower standard electrode potential (0.158 V vs. SHE) than normal water electrolysis (1.23 V vs. SHE). This is a theoretical indication that the SO_2 oxidation reaction has possible potential when compared to normal water electrolysis, since hydrogen production may occur at lower potentials and therefore lower cost. Rh was compared with Pt for the SO_2 oxidation reaction since little research has been done on this catalyst and many studies exist in which Pt was used as catalyst. The oxygen reduction reaction and ethanol oxidation reaction were also included in this study to create a foundation for the catalysts studied, since the SO_2 oxidation reaction is complicated by different adsorbed species that can form according to various mechanisms.

The electrochemical techniques employed in this study to characterize the catalysts included cyclic voltammetry from which onset potentials and limiting current densities were determined, as well as from which some qualitative analysis was done. Linear polarization experiments were used during rotating disk electrode studies from which Levich and Koutecky-Levich analyses were done and the number of electrons transferred calculated and compared between the two catalysts. From the Koutecky-Levich analysis the kinetic current density was also obtained for use in Tafel analysis for further comparison between catalysts.

It was found that Rh showed good behaviour for the oxygen reduction reaction when compared to Pt with similar onset potentials and limiting current densities. From Levich analysis it was concluded that both catalysts achieved diffusion limitation at high overpotentials. However, from the calculated number of electrons transferred it was evident that a difference in mechanism existed between catalysts and that the mechanism for both changed in the potential range studied, which is confirmed by the Tafel slopes.

For the ethanol oxidation reaction it was shown that Rh exhibited very low catalytic activity in comparison with Pt. However, it was concluded from cyclic voltammetry and rotating disk electrode studies that more adsorbed species were present on the surface of Rh than on Pt. These results confirmed the possibility of using Rh as a co-catalyst together with Pt since it was shown from rotating disk electrode studies that low adsorption of ethanol and its oxidation products caused species to be transported away from the surface of the electrode during rotation.

For the SO_2 oxidation reaction it was found that Rh exhibited very poor catalytic activity together with being very susceptible to poisoning by adsorbed species. Pt showed very good behaviour, which corresponded well with what had been observed in literature. Levich analysis revealed that Pt did not exhibit diffusion limitation and Koutecky-Levich analysis revealed that a 2 electron reaction occurred on Pt, which corresponds with the SO_2 oxidation reaction during which 2 electrons are transferred.

It was, therefore, shown that Rh could exhibit good behaviour and act as a suitable catalyst in certain circumstances. However, for the SO_2 oxidation reaction, which was the main focus of this study it was shown that Rh is not a suitable catalyst, either alone or as co-catalyst.

Opsomming

Die toenemende vraag na skoon en hernubare energiebronne het navorsing oor alternatiewe vir die gebruik van fossielbrandstowwe, wat aansienlik bydra tot aardverwarming, gestimuleer. Die SO_2-oksidasiereaksie vir die produksie van waterstof as 'n skoon en hernubare energiedraer is bestudeer. Hierdie reaksie vind by 'n laer standard-elektrodepotensiaal (0,158 V mvn SWE) as die normale waterelektrolise plaas (1.23 V mvn SWE). Dit is 'n teoretiese aanduiding dat die SO_2-oksidasiereaksie moontlik potensiaal het in vergelyking met normale waterelektrolise aangesien waterstofproduksie mag voorkom by 'n laer potensiaal, en dus teen laer koste .Rh is vergelyk met Pt vir die SO_2-oksidasiereaksie aangesien min navorsing oor hierdie katalisator gedoen is, terwyl vele studies oor Pt as katalisator bestaan. Die suurstof-reduksiereaksie en etanol-oksidasiereaksie is ook in hierdie studie ingesluit om 'n grondslag te skep vir die studie van die katalisators aangesien die SO_2-oksidasiereaksie ingewikkeld is, met verskillende geadsorbeerde spesies wat volgens verskeie meganismes kan vorm.

Die elektrochemiese tegnieke in hierdie studie gebruik om die katalisators te karakteriseer het ingesluit sikliese voltammetrie waaruit aanvangspotensiale en limiet-stroomdigthede bepaal is, sowel as kwalitatiewe analises. Lineêre polarisasie-eksperimente is gebruik in roterende-skyfelektrode-studies waarin Levich- en Koutecky-Levich analises gedoen is en die aantal elektrone oorgedra, bereken kon word en die twee kataliste vergelyk kon word. Van die Koutecky-Levich-analise is die kinetiese stroomdigtheid vir gebruik in Tafel-analises vir verdere vergelyking tussen katalisators ook verkry.

Daar is gevind dat Rh vir die suurstof reduksie-reaksie goeie gedrag openbaar het wanneer dit vergelyk word met Pt met soortgelyke aanvangspotensiale en die limiet-stroomdigthede. Vanaf die Levich-analise is die gevolgtrekking gemaak dat beide katalisators diffusie-limiete by hoë oorpotensiale bereik. Maar uit die berekende aantal elektrone oorgedra, was dit duidelik dat daar 'n verskil in meganisme tussen die katalisators bestaan en dat die meganisme vir beide verander in die potensiaalgebied wat bestudeer is, en wat bevestig word deur die Tafel-hellings.

Vir die etanol-oksidasiereaksie is getoon dat Rh baie lae katalitiese aktiwiteit in vergelyking met Pt toon. Daar is egter mbv sikliese voltammetrie en roterende-skyfelektrode-studies waargeneem dat meer geadsorbeerde spesies op die oppervlak van Rh teenwoordig is as op Pt. Hierdie bevindinge bevestig die moontlikheid van die gebruik van Rh as 'n mede-katalisator saam met Pt, want met roterende-skyfelektrode-studies is gevind dat lae adsorpsie van etanol en sy

oksidasieprodukte veroorsaak dat spesies weg van die oppervlak van die roterende elektrode vervoer word.

Vir die SO_2-oksidasiereaksie is bevind dat Rh baie swak katalitiese aktiwiteit toon, tesame met die feit dat dit baie vatbaar is vir vergiftiging deur geadsorbeerde spesies. Pt het baie goeie gedrag getoon, wat ooreenstem met wat in die literatuur gevind is. Levich-analise het aangedui dat Pt nie diffusiebeperking toon nie en Koutecky-Levich-analise het aan die lig gebring dat 'n 2-elektron-reaksie op Pt plaasvind, wat ooreenstem met die SO_2-oksidasiereaksie waartydens 2 elektrone oorgedra word.

Dit is dus getoon dat Rh goeie gedrag kan openbaar as 'n geskikte katalisator onder sekere omstandighede. Maar vir die SO_2-oksidasiereaksie, wat die hooffokus van hierdie studie was, is aangetoon dat Rh nie 'n geskikte katalisator is nie, hetsy op sy eie of as mede-katalisator.

Keywords: Rhodium, Platinum, Polycrystalline, SO_2 oxidation, Rotating disk electrode, Levich, Koutecky-Levich, Tafel

Table of Contents

Table of Contents continued

Table of Contents continued

List of Tables

List of Figures

Abbreviations and Symbols

Symbol/Abbreviation	Description	Unit
i_0	Exchange Current Density	mA.cm^{-2}
i_k	Kinetic Current Density	mA.cm^{-2}
i_{lim}	Limiting Current Density	mA.cm^{-2}
i_f	Current Density of forward scan	mA.cm^{-2}
i_b	Current Density of backward scan	mA.cm^{-2}
A	Electrode Area	cm^2
Au	Gold	
C	Concentration	mol.L^{-1}
CA	Chronoamperometry	
CE	Counter Electrode	
CH_3COOH	Acetic Acid	
CO	Carbon Monoxide	
CO_2	Carbon Dioxide	
CO_3^{2-}/HCO_3^-	Carbonate/Bicarbonate	
CV	Cyclic Voltammogram	
D_0	Diffusion Coefficient	cm^2.s^{-1}
DFT	Density Functional Theory	
e^-	Electron	
E^0	Standard Electrode Potential	V
E_{LOW}	Lower Potential Value	
EOR	EtOH Oxidation Reaction	
EtOH	EtOH	
F	Faraday's Constant	C.mol^{-1}

H^+	Proton	
H_2	Hydrogen	
H_2O	Water	
H_2O_2	Hydrogen Peroxide	
H_2SO_4	Sulphuric Acid	
$HClO_4$	Perchloric Acid	
HyS	Hybrid Sulphur	
Ir	Iridium	
K-L	Koutecky-Levich	
KOH	Potassium Hydroxide	
LP	Linear Polarization	
N	Number of Electrons	
O_2	Oxygen	
OH	Hydroxide	
ORR	Oxygen Reduction Reaction	
Pd	Palladium	
PEM	Proton Exchange Membrane	
Pt	Platinum	
PtO	Platinum Oxide	
R	Gas constant	$J.K^{-1}.mol^{-1}$
RDE	Rotating Disk Electrode	
RE	Reference Electrode	
Rh	Rhodium	
RhO	Rhodium Oxide	
RRDE	Rotating Ring Disk Electrode	
Ru	Ruthenium	
SCE	Standard Calomel Electrode	

SDE	Sulphur Dioxide Depolarized Electrolyzer	
SHE	Standard Hydrogen Electrode	
SO_2	Sulphur Dioxide	
T	Temperature	K
WE	Working Electrode	
XRD	X-Ray Diffraction	
v	Kinematic Viscosity	$cm.s^{-1}$
α	Transfer Coefficient	
η	Overpotential	V
θ	Coverage by an adsorbate	
ω	Rotation Rate	s^{-1}

1 Introduction

The world's current energy sources consist mainly of fossil fuels which contribute largely to global warming. There also exists a fear of the depletion of fossil fuels in the near future. Another source of energy has to be found that is not only environmentally friendly, but also renewable. Hydrogen is a very promising energy carrier since it has a high energy of combustion and the only by products formed are water and oxygen. The production and storage of hydrogen are still problems that need attention since they are still very expensive.

Hydrogen can be produced from the electrochemical splitting of water and is represented by the following reaction and standard electrode potential (Atkins & de Paula, 2006:1005):

$$2H_2O \rightarrow O_2 + 4H^+ + 4e^- \quad | \quad E^0 = 1.23\,V\ (vs\ SHE) \quad | \quad (1)$$

The hybrid sulphur (HyS) cycle is a thermochemical cycle for the production of hydrogen for which the net reaction is the splitting of water to form hydrogen and oxygen. During this process, sulphuric acid is decomposed thermally (via nuclear or solar heat sources) to produce SO_2 and an acid electrolyser (more commonly known as a sulphur dioxide depolarized electrolyser (SDE)) oxidises SO_2 electrochemically to produce H_2 and H_2SO_4 (Gorensek *et al.*, 2009). The following reactions occur at the following standard electrode potentials inside the SDE:

Anode	$SO_{2(aq)} + 2H_2O \rightarrow H_2SO_4 + 2H^+ + 2e^-$	$E^0 = 0.158\,V\ (vs\ SHE)$	(2)
Cathode	$2H^+ + 2e^- \rightarrow H_{2(g)}$	$E^0 = 0.0\,V\ (vs\ SHE)$	(3)

As can be seen, hydrogen production can theoretically occur at much lower potential values inside the SDE (0.158 V) by the electrochemical oxidation of SO_2 when compared to normal water electrolysis (1.23 V).

The main focus of this study is the electro-oxidation of sulphur dioxide (SO_2), i.e. the reaction occurring at the anode of the SDE. It is of importance to achieve high current densities in the electrolyser at the lowest possible overpotential to produce adequate amounts of hydrogen at a low cost. An optimal target current density of 500 mA.cm^{-2} at a potential of 0.6 V was proposed by Gorensek & Summers (2009). One of the factors that influence the performance of an electrolyser is the type of catalyst used. A suitable catalyst will yield high current densities at lower overpotentials to keep costs as low as possible. The most used catalysts studied for this reaction were Pt, Au, Pd and carbon ((Seo & Sawyer, 1965), (Samec & Weber,

1975), (Appleby & Pinchon, 1979), (Lu & Ammon, 1980)). Since the variety of catalysts studied are very limited, it was decided to do a comparison between polycrystalline Rh and polycrystalline Pt. Pt has been studied most extensively and Rh has not been studied much as a catalyst for this reaction. A comparative study will be done in order to determine if Rh may possibly be a suitable catalyst for the oxidation of SO_2. The results obtained can then be used to determine the possibility of using Rh together with Pt in future studies in an alloy for the oxidation of SO_2. The variables that will be determined to compare effectively the two catalysts include onset potential and limiting current density, since a better catalyst will achieve higher current densities at lower potentials. igh current density achieved by a catalyst is also an indication of faster reaction kinetics. The peak potential (potential corresponding to the peak current density) of each catalyst will also be compared, since a lower peak potential at higher current densities is ideal. The number of electrons transferred during the reaction can also be calculated by use of K-L and Levich analyses, and these techniques will be used to compare the selectivity of each catalyst toward a reaction. To compare if a reaction occurs faster on a specific electrode, the reaction kinetics can be determined for each catalyst by calculating the kinetic current density (from K-L analysis). Tafel analysis (conducted from kinetic current densities calculated from K-L analysis) will then give information regarding the type of mechanism followed on each catalyst.

Complex mechanisms are proposed by various authors and the exact mechanism followed by the SO_2 oxidation reaction is not entirely agreed upon ((Seo & Sawyer, 1965), (Appleby & Pinchon, 1979)). There are also several intermediate species involved in the reaction that may adsorb onto the surface and take part in the reaction or poison the electrode's surface. Pt has been widely studied for many different types of reactions and has been used most commonly as an electrocatalyst in different types of fuel cells as well as in the SDE. Most problems are expected to arise while investigating Rh, since little research has been done on it, especially for the SO_2 oxidation reaction.

The approach taken in this study is to first investigate the behaviour of Rh compared to Pt for model reactions, i.e. the oxygen reduction reaction (ORR, acidic and alkaline medium) and EtOH oxidation reaction (EOR, acidic and alkaline medium) and to characterize the two catalysts, based on the results for different reactions. The ORR will be investigated first, since it is a well-studied reaction with limited problems and it has been studied on various catalysts including Pt and Rh. The general reaction and standard electrode potential for the ORR as part of a low temperature fuel cell, is the following:

Cathode	$O_2 + 4H^+ + 4e^- \rightarrow 2H_2O$	$E^0 = 1.23\ V\ (vs\ SHE)$	(4)

There also exist intermediate species formed during the reaction, along with multiple reaction pathways (Song & Zhang, 2008). The ORR is, therefore, an appropriate reaction to study first.

The second reaction that will be studied is the EOR. This reaction was chosen, since it is more complex than the ORR with different reaction pathways that can be followed, as well as the formation of different intermediate species that may adsorb onto the electrode's surfaces (Antolini, 2007). This is valuable since many different adsorbed species may be present in the study of the oxidation of SO_2. Thus the results from the ORR and EOR may be good preparation for work that has to be done.

These two catalysts will be compared for the above-mentioned reactions by means of certain electrochemical techniques. Firstly, each electrode's surface will be characterized using cyclic voltammetry (CV) experiments in a clean electrolyte solution. From these results, information can be gathered on the surface like potentials at which hydrogen adsorption and desorption occur, as well as oxidation and reduction of the surfaces. Further CV experiments will then be done in the presence of the electro-active species (O_2, EtOH or SO_2) to determine onset potentials and limiting current densities. The second type of technique used will be linear polarization (LP) experiments during which different rotation rates will be applied to the rotating disk electrode (RDE). From these results, Koutecky-Levich (K-L) plots can be drawn in order to determine the number of electrons transferred, as well as the kinetic current density. Levich plots can be drawn to confirm the number of electrons transferred. A difference or similarity in these values gives valuable information about the possible mechanism the reaction follows on a given surface. The main focus of the study was not to determine the mechanism, only to compare the activities of the two catalysts (Pt, Rh) in the different reactions.
Each reaction will be discussed separately, with every chapter containing of its literature survey, experiment description, results and discussion, and conclusions sections. A final chapter will give a brief summary of the different reactions studied and main conclusions will be made regarding the catalysts studied.

2 The electro-reduction of oxygen (ORR) on Pt and Rh

2.1. LITERATURE

2.1.1. Background

In proton exchange membrane (PEM) fuel cells, electricity is generated by the conversion of hydrogen and oxygen to water. At the anode of the fuel cell, hydrogen is oxidised to form protons which migrate through a membrane to the cathode (see Figure 2.1.).

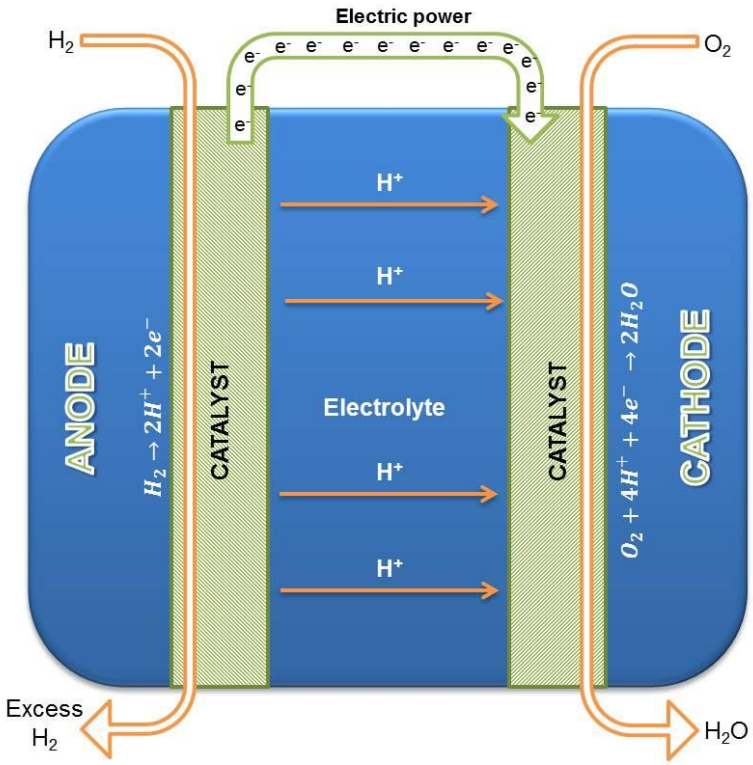

Figure 2.1: Schematic representation of a low temperature PEM fuel cell

At the cathode, oxygen is reduced and combined with these protons to form the final product, water. These reactions and their standard electrode potentials are represented as follows;

$H_2 \rightarrow 2H^+ + 2e^-$	$E^0 = 0.0\ V\ (vs\ SHE)$	(5)
$O_2 + 4H^+ + 4e^- \rightarrow 2H_2O$	$E^0 = 1.23\ V\ (vs\ SHE)$	(6)

The most commonly used catalyst for use in fuel cells is Pt. There are however, still problems with the efficiency of fuel cells, since a high overpotential is caused at the cathode when compared to the anode. An overpotential as close as possible to the standard electrode potential for the reduction of oxygen (1.23 V) is ideal to keep costs as low as possible. The high overpotential is due to slow reaction kinetics during the ORR, caused by the stability of adsorbed oxygen at high potentials (low overpotential) (Norskov *et al.*, 2004). Therefore, the

reduction of oxygen can only start once the potential is taken to more negative values, i.e. higher overpotentials.

2.1.2. Mechanism of the ORR and role of electrode surface

Many studies have been conducted on the ORR to try and determine the mechanism in order to identify the cause of the above-mentioned overpotential. The formation of different intermediate species during the reduction of oxygen could be responsible for this and the reaction paths that are followed play an important role in the kinetics of the reaction, as will be discussed in this section.

A DFT study was done by Norskov *et al.* (2004) and two types of mechanisms were proposed for the ORR, an associative and a dissociative mechanism (M denotes an electrode surface site):

Dissociative mechanism		**Associative mechanism**	
$O_2 + M \rightarrow MO$	(7)	$O_2 + M \rightarrow MO_2$	(10)
$MO + H^+ + e^- \rightarrow MOH$	(8)	$MO_2 + H^+ + e^- \rightarrow MO_2H$	(11)
$MOH + H^+ + e^- \rightarrow H_2O + M$	(9)	$MO_2H + H^+ + e^- \rightarrow H_2O + MO$	(12)
		$MO + H^+ + e^- \rightarrow MOH$	(13)
		$MOH + H^+ + e^- \rightarrow H_2O + M$	(14)

Dissolved oxygen can either dissociate before adsorbing onto the metal surface, wherafter hydrogenation occurs with H_2O forming as final reaction product, or it can also adsorb onto the metal surface as an O_2 molecule whereafter hydrogenation occurs with H_2O_2 forming as an intermediate. Norskov *et al.* (2004) conclude that it is possible for both these mechanisms to occur on an electrode surface, depending on the applied potential and electrode material used. During the dissociative mechanism, H_2O is formed as the only reaction product and during the associative mechanism, H_2O_2 may also form during step (12) or it can be reduced to H_2O. When working in aqueous electrolyte solutions, two main reaction pathways may be followed during the electro-reduction of O_2 (Song & Zhang, 2008) (Markovic & Ross Jr, 2002). These pathways are summarised in Figure 2.2, as shown in a review article by Markovic & Ross (2002). The first pathway involves a 4 electron reaction with H_2O as final product (a). The second pathway involves the formation of H_2O_2 (b) during a 2 electron reaction which can be further reduced to water (c), decomposed back to O_2 (d) or desorbed from the electrode's surface as final product (e).

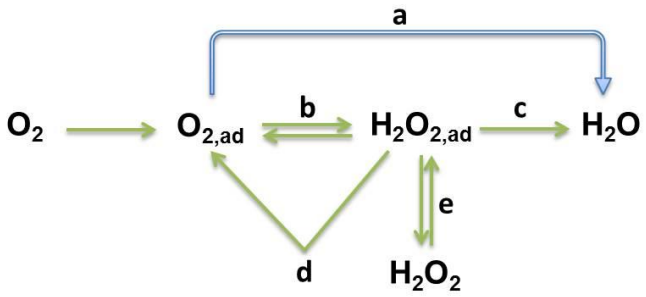

Figure 2.2: Schematic representation of pathways that may be followed during the ORR

Genshaw *et al.* (1967) studied the ORR on a Rh electrode, specifically regarding the H_2O_2 species that might form either as a reaction intermediate or as a reaction product. They described the parallel pathways as being very similar than that proposed by Markovic & Ross (2002):

$$O_2 \overset{i}{\rightarrow} H_2O$$

$$O_2 \overset{ii}{\rightarrow} H_2O_2 \overset{iii}{\rightarrow} H_2O$$

$$O_2 \overset{ii}{\rightarrow} H_2O_2 \overset{iv}{\rightarrow} to\ solution$$

Firstly, oxygen can either undergo a direct reduction to the final product, H_2O, which is represented by (i). The other pathway that may be followed is the formation of H_2O_2 as an intermediate species (ii), which then may undergo further reduction to the final product (iii), H_2O, or it may become a reaction product that diffuses away from the electrode surface (iv) into the electrolyte solution. These authors determined the role of H_2O_2 on Rh and found that it was formed as an intermediate species in insufficiently purified acid solutions, where no H_2O_2 was formed if the acid solution had been sufficiently purified. In alkaline solutions, H_2O_2 formed as a reaction intermediate with partial reduction to water (Genshaw *et al.*, 1967).

Sawyer & Day (1963) found that each of these two reaction products formed on a different electrode surface in a study on Pt, Pd and silver electrodes, i.e. that H_2O was mainly formed on a pre-oxidised surface and that H_2O_2 was mainly formed on a pre-reduced surface. Also, the mechanism on the pre-oxidised surface changed to one observed on a pre-reduced surface, since the surface was reduced as the potential was taken to smaller values during the reduction of oxygen. They proposed the following mechanisms on the two types of electrode surfaces:

Pre-oxidised electrode		**Pre-reduced electrode**	
$M(OH)_2 + 2e^- \rightarrow M + MOH^-$	(15)	$M(OH_2)_n + O_2 + e^- \rightarrow M(OH_2)_{n-1}(OH)^- + OH_2$	(17)

$2M + O_2 + 2H_2O \rightarrow 2M(OH)_2$	(16)	$M(OH_2)_{n-1}(OH)^- + H_2O \rightarrow M(OH_2)_n + OH^-$	(18)
		$2HO_2 \rightarrow H_2O_2 + O_2$	(19)

They found that during the ORR experiment, the reactions (15) and (16) that occurred on a pre-oxidised electrode surface were replaced by reactions (17), (18) and (19) as the potential was taken to more negative values. This indicated that the electrode surface was being reduced during the course of the reaction and therefore, two types of mechanisms were present on one electrode surface that started at a potential value where an oxidised surface was present. Furthermore, the electrode itself was involved in the reduction of O_2 when it was pre-oxidised which was not the case for a pre-reduced electrode.

This was confirmed by Markovic *et al.* (1995), using the rotating ring disk electrode (RRDE) technique, where they observed that very little H_2O_2 formed on a Pt electrode surface at potentials above 0 V (vs. SCE). Below this potential, the reaction products consisted mainly of H_2O_2. These two potential ranges correspond to the above-mentioned types of electrode surfaces, i.e. oxide-covered and oxide-free surfaces.

The different pathways that can be followed in acidic and alkaline electrolytes, together with their standard electrode potentials (vs. SHE), are given below (Song & Zhang, 2008) (Bard & Faulkner, 2001):

- Acidic electrolyte:

$O_2 + 4H^+ + 4e^- \rightarrow H_20$	$E^0 = 1.23\,V$	(20)
$O_2 + 2H^+ + 2e^- \rightarrow H_2O_2$	$E^0 = 0.70\,V$	(21)
$H_2O_2 + 2H^+ + 2e^- \rightarrow 2H_2O$	$E^0 = 1.76\,V$	(22)

- Alkaline electrolyte:

$O_2 + 2H_2O + 4e^- \rightarrow 4OH^-$	$E^0 = 0.401\,V$	(23)
$O_2 + H_2O + 2e^- \rightarrow HO_2^- + OH^-$	$E^0 = -0.065\,V$	(24)
$HO_2^- + H_2O + 2e^- \rightarrow 3OH^-$	$E^0 = 0.867\,V$	(25)

Another important factor to consider when studying the ORR is the presence of the metal oxides that form at high potentials. This reaction for Pt can be represented as follows (Song & Zhang, 2008):

$$Pt + {}^{1}/_{2}\,O_2 \rightarrow PtO \quad \left| \quad E^0 = 0.88\,V\ (vs\ SHE) \right. \quad (26)$$

Therefore, any electrode material will have the oxide present during ORR studies, due to the very high standard reduction potential of oxygen (1.23 V). This has to be taken into consideration, since the electrode surface will not only consist of the pure metal but also its oxide (Song & Zhang, 2008:112).

Regarding the kinetics and mechanism of the ORR, generally, two Tafel slopes can be obtained, -60 mV.dec^{-1} and -120 mV.dec^{-1} (Song & Zhang, 2008). The presence of these two Tafel slopes is dependent on the potential range, as well as the electrode material that is being used and the existence of different Tafel slopes in the same potential range confirms that different mechanisms can be operational on an electrode in a single potential range. Sepa & Vojnovic (1981) studied the kinetics and mechanism of the ORR in acidic and alkaline media on a Pt rotating disk electrode and obtained a Tafel slope of -60 mV.dec^{-1} in the higher potential region, where the electrode structure consisted of Pt and PtO. A Tafel slope of -120 mV.dec^{-1} was observed in the lower potential region where the electrode surface consisted mainly of Pt. Another study done on the ORR on a Rh wire as catalyst also found a Tafel slope of close to -120 mV.dec^{-1} in the lower potential region and -60 mV.dec^{-1} in the higher potential region (Martinovic *et al.*, 1988). These results were obtained for the oxygen reduction reaction in acidic and alkaline media. This difference in the Tafel slope for the different potential regions is an indication that a different mechanism operates on a clean electrode surface and a surface partially covered with oxide.

2.1.3. Overview of catalysts studied

The mechanism and kinetics regarding oxygen reduction have been studied most extensively on Pt as catalyst (Song & Zhang, 2008) (Markovic & Ross Jr, 2002).

Other noble metals have been studied thoroughly as well, including Pd and its alloys (Shao *et al.*, 2006) where it was found that Pd supported on various other metals showed increasing activity in the following order: Pd/Ru(0001) < Pd/Ir(111) < Pd/Rh(111) < Pd/Au(111) < Pd/Pt(111). Sawyer *et al.* (1963) also studied the ORR on Pd, together with Pt and silver electrodes regarding the mechanism and kinetics on pre-reduced and pre-oxidised electrode surfaces as already discussed in section 2.1.2.

Zurrilla *et al.* (1978) studied the ORR on a Au electrode in alkaline electrolyte and confirmed that the only mechanism present on a Au surface, involved reactions (23) and (24) where HO_2^- was formed as an intermediate and was further reduced to OH^-.

The kinetics (Martinovic *et al.*, 1988) and mechanism (Genshaw *et al.*, 1967) of the ORR have been studied on a Rh electrode. Regarding the kinetics of the reaction on Rh, Martinovic *et al.* (1988) determined Tafel slopes at high and low overpotentials in alkaline and acidic electrolytes and found them to be similar to that obtained for Pt. Genshaw *et al.* (1967) investigated the mechanism of the reaction on Rh in alkaline and acidic electrolytes, especially regarding the H_2O_2 that might form as an intermediate or as a reaction product.

Therefore, many noble metals have been investigated as catalysts for the ORR and numerous studies exist to which results in this chapter can be compared. Different techniques can be used during comparison Rh and Pt for the ORR, as well as the other reactions done in this study (Chapters 3 and 4). These techniques will be discussed briefly below.

2.1.4. Analyses of catalysts

2.1.4.1. Basic descriptions

A standard three-electrode setup is used during the experiments and this setup can be seen in Figure 2.3 as adapted from Bard & Faulkner (2001:26).

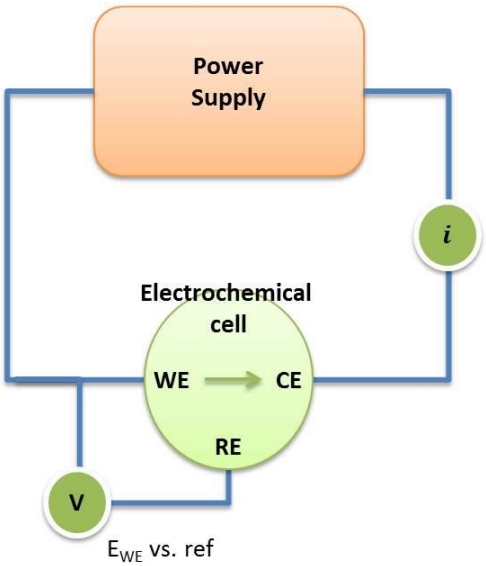

Figure 2.3: Schematic representation of a three-electrode electrochemical cell (Bard & Faulkner, 2001)

This setup consists of a working electrode (WE), counter electrode (CE) and a reference electrode (RE). A potential is applied to the working electrode by means of a potentiostat (power supply), where the reaction occurs and the electrode material acts as a catalyst during a oxidation or reduction reaction. The potential of the working electrode is measured against a reference electrode of which the potential is known. The current generated by electron transfer during the electrochemical reaction is passed between the working electrode and the counter electrode. The actual oxidation or reduction reaction being studied will be taking place on the surface of the working electrode and species from an electrolyte solution (for the ORR, 0.1 M $HClO_4$ for acidic and 0.1 M KOH for alkaline studies) have firstly to be transported to the surface of the electrode where adsorption occurs for electron transfer to be possible. Active species have to be adsorbed strongly enough for the electron transfer to be possible, but also not too strong since surface sites will then be blocked and electron transfer will be inhibited (Pletcher, 2009:36-38). The working electrode used in this study will be a rotating disk electrode (RDE), since studies can be conducted where the electrode is rotated and mass-transfer of electrolyte is limited due to increased convection to the surface. Therefore, the higher the rotation rate of the electrode, the higher the rate of transport to the surface of the electrode.

To compare the activity of the two catalysts from results obtained, the onset potential, peak potential, peak current density and limiting current density can be determined. These features are represented in Figure 2.4.

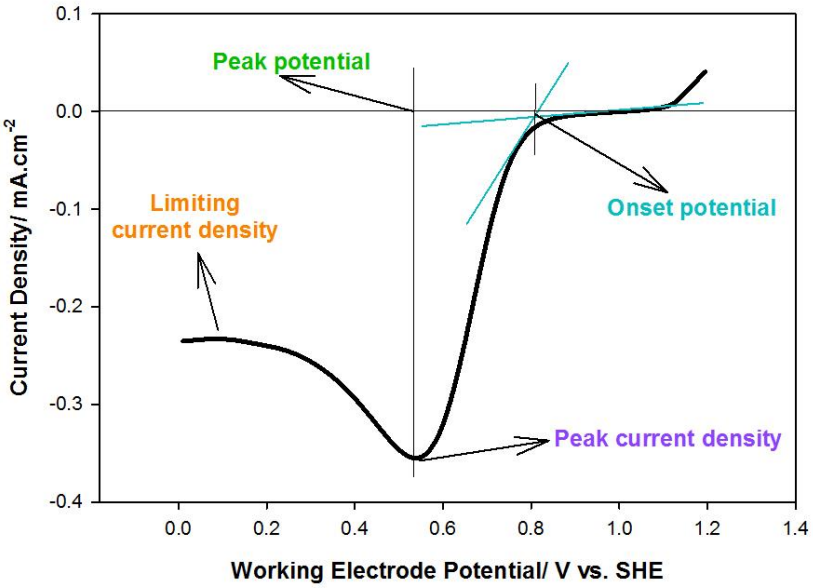

Figure 2.4: **Representation of a LP experiment to demonstrate which parameters are used to compare catalysts**

The onset potential of a catalyst is the potential at which the reaction initiates and the peak potential is the potential corresponding to the peak current density (see Figure 2.4.). The peak current density is found where a maximum current density is reached and the limiting current density is where the potential no longer influences the rate at which the reaction takes place (Pletcher, 2009:30). Therefore, a more active catalyst will have an earlier onset potential (more positive potential for a reduction reaction and more negative potential for an oxidation reaction), as well as a higher limiting current density or peak current density (higher cathodic current for reduction reaction and higher anodic current for oxidation reaction) at a lower peak potential. In cases where a limiting current density is not achieved, the peak current density can serve as a measure of the activity of a catalyst. It is necessary for the reaction to proceed at a potential as close as possible to the reaction's standard electrode potential for the catalyst to be effective in a reaction. Problems with catalysts usually arise when the applied potential needed to drive a reaction deviates significantly from the reaction's standard electrode potential, i.e. a high overpotential is present.

Different control regions are operational on rotating electrode surfaces, i.e. the kinetic, mixed transport-kinetic and mass transport control regions (see Figure 2.5).

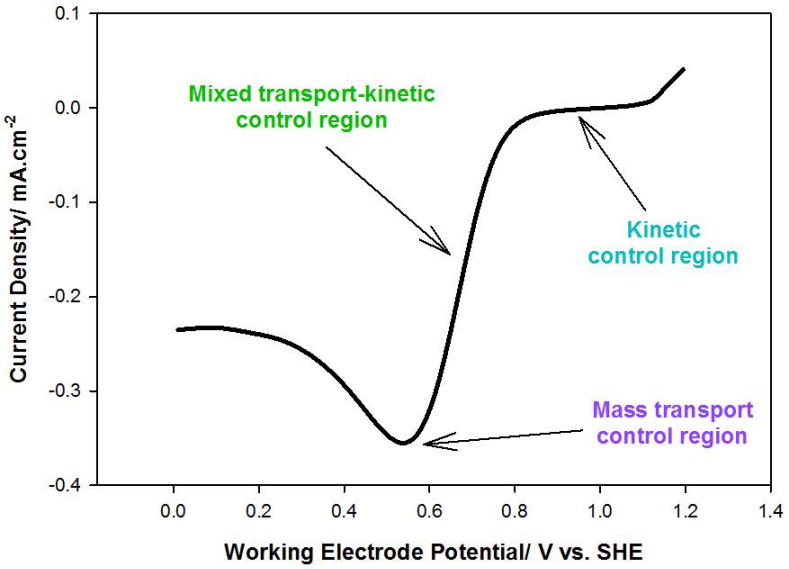

Figure 2.5: **Representation of a LP experiment to demonstrate the different control regions operational on an electrode**

At low potentials where current density is initially zero, the surface concentration of the reactant is still very high (the same as the bulk electrolyte) and electron transfer can occur (Pletcher, 2009:30). The current density at this potential is not yet dependent on the rotation rate of the electrode (Pletcher, 2009:165) and is therefore governed by kinetic control. As the potential is taken to higher values, the surface concentrations of reagents decrease due to oxidation/reduction of these species. An increase in current density can then be observed up until a point where the concentration of the surface species become zero and a plateau is reached. Here the current density is independent of the applied potential and an increase can be achieved by transport of reagents from the electrolyte to the surface of the electrode by means of rotation. This region is called the mass transport controlled region. In between these two control regions, mixed control governs where the current density becomes increasingly dependent on the rotation rate as the potential is increased (Pletcher, 2009:165).

2.1.4.2. Levich analysis

A valuable technique for comparing the reaction on both catalysts is by using the Levich plot. It describes the reaction in the mass transport controlled region (see Figure 2.5) of the reaction studied (Pletcher, 2009:164). The Levich equation describes the diffusion limiting current on the catalyst.

The Levich equation can be described as follows:

$$i_{lim} = 0.620nFAD_0^{2/3}v^{1/6}\omega^{1/2}c^* \qquad \text{(I)}$$

with n the number of electrons transferred, F Faraday's constant (C.mol^{-1}), A the electrode area (cm^2), D_0 the diffusion coefficient (cm^2.s^{-1}), c^* the concentration of active species at the electrode surface (mol.dm^{-2}), v the kinematic viscosity of the electrolyte solution (cm.s^{-1}) and ω the rotation rate (s^{-1}).

A plot of limiting current density (i_{lim}) versus square root of rotation rate ($\omega^{1/2}$) can be drawn and this relation should give a straight line through the origin. This indicates that the reaction is mass transport controlled (Pletcher, 2009:164), together with current density that is independent of potential. The number of electrons transferred can be calculated from the slope of the Levich plot. Similarity between the numbers of electrons transferred, calculated from Levich plots and from K-L plots, is an indication that the reaction is proceeding via a single step charge transfer mechanism (Treimer *et al.*, 2002). If a discrepancy is observed for the number of electrons transferred between K-L and Levich plots, it will indicate the presence of a multiple charge transfer reaction occurring, i.e. a complex reaction mechanism or electron transfer regime.

2.1.4.3. Koutecky-Levich (K-L) analysis

The number of electrons transferred, as well as the kinetic current density achieved by each catalyst can be determined from K-Levic analysis. The number of electrons transferred will be used to confirm that the correct reaction is occuring on the catalyst. It will also be possible to determine which of the parallel reactions is occuring on the specific catalyst, the 2 electron or 4 electron reaction. The kinetic current density can be used in order to compare the activity of Rh and Pt and will be used for Tafel analysis.

The K-L equation can be represented as follows:

$$\frac{1}{i} = \frac{1}{i_K} + \frac{1}{0.62nFAD_0^{2/3}c^*v^{1/6}\omega^{1/2}} \qquad \text{(II)}$$

with n the number of electrons transferred, F Faraday's constant (C.mol^{-1}), A the electrode area (cm^2), D_0 the diffusion coefficient (cm^2.s^{-1}), c^* the concentration of active species at the

electrode surface (mol.dm^{-2}), v the kinematic viscosity of the electrolyte solution (cm.s^{-1}) and ω the rotation rate (s^{-1}) of the electrode.

A plot of the inverse of current density ($\frac{1}{i}$) versus the inverse of the square root of the rotation rate ($\frac{1}{\omega^{1/2}}$) can be drawn for different overpotentials in the mixed-control (kinetic + diffusion control) region of the LP scans obtained at different rotation rates. The kinetic current can be calculated from the y-intercept and the number of electrons transferred from the slopes of the K-L plot (Song & Zhang, 2008). The kinetic current density corresponding to different overpotentials can therefore be calculated to serve as an indication of the kinetics of the catalyst toward the reaction studied. Thus, the higher the value obtained for kinetic current at a given overpotential, the faster the reaction is taking place.

This technique is mainly used for insight into the mechanism of a reaction on a catalyst. However, to be able to further compare the catalysts by means of Tafel analysis the kinetic current density is needed from K-L analysis.

2.1.4.4. Tafel analysis

Tafel analysis is a helpful tool when comparing catalysts since the Tafel slope can be derived from these plots. The Tafel slope is another tool for comparison of the mechanism between catalysts.

The general Tafel equation can be given by the following and shows that current is exponentially related to overpotential (Bard & Faulkner, 2001:92):

$$\eta = a + b\log i$$

with $a = \frac{2.3RT}{\alpha F}\log i_0$ and $b = \frac{-2.3RT}{\alpha F}$ (Bard & Faulkner, 2001:102). This behaviour is valid at large overpotentials and a representation of a Tafel plot of $\log i$ vs. η can be seen in Figure 2.6 as adapted from (Pletcher, 2009).

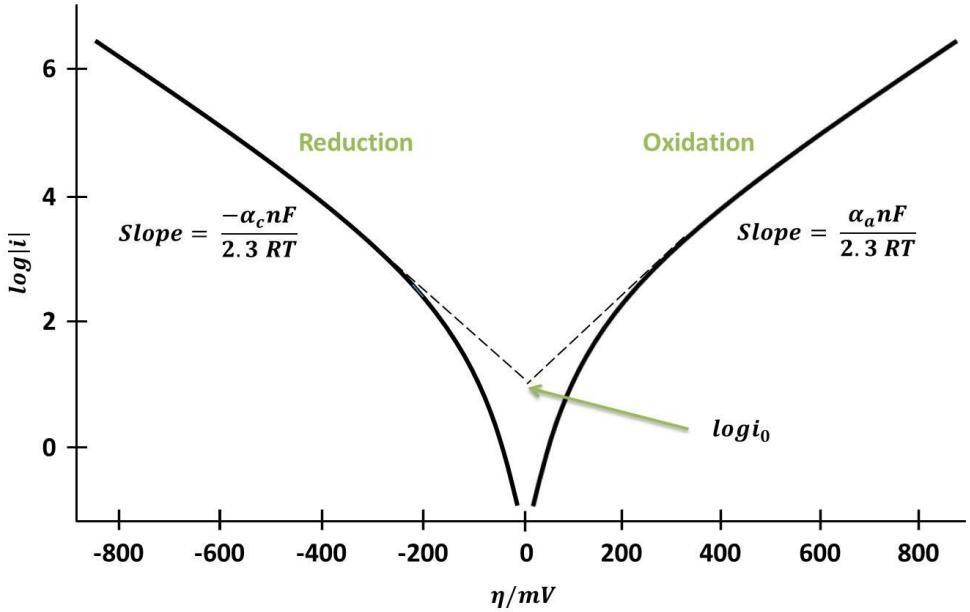

Figure 2.6: Tafel plots to show slopes and exchange currents for anodic and cathodic reactions

The Tafel equation for a cathodic (reduction) reaction like the ORR will look as follows (Pletcher, 2009:17):

$$\log(-i_c) = logi_0 - \frac{\propto_c nF}{2.3RT}\eta$$

with i_c the reaction current density (mA.cm^{-2}), i_0 the exchange current density (mA.cm^{-2}), $\propto_c$ the transfer coefficient (usually 0.5 for simple electron transfer reactions (Pletcher, 2009:14)), n the number of electrons transferred during the rate determining step, F Faraday's constant (C.mol^{-1}), R the gas constant (J.K^{-}1.mol^{-1}), T the temperature (K) and η the overpotential (V).

The Tafel slope can be obtained from the slope of a plot of the logarithm of the current density ($\log(i_c)$) versus overpotential (η) as can be seen in Figure 2.6.

2.1.5. Focus of the study

A comparison between polycrystalline Rh and Pt for the ORR is to be conducted so as to analyze each catalyst employing different electrochemical techniques that will be described in more detail in the next section.

Cyclic voltammetry and linear polarization will be used to electrochemically study each catalyst toward the reduction of oxygen, obtaining onset potentials, peak potentials, and limiting current

densities from these experiments. Further, rotating disk electrode (RDE) experiments will also be done in order to be able to employ the K-L, Levich and Tafel analysis techniques.

The results obtained from these analyses will be used to compare Rh and Pt for the reduction of oxygen from onset potentials, peak potentials, limiting current density, number of electrons transferred calculated from Levich and K-L plots, kinetic current density at various overpotentials from K-L plots, as well as Tafel slopes.

2.2. EXPERIMENTAL

2.2.1. Electrochemical Setup

A standard three-electrode setup was used in the electrochemical experiments (see Figure 2.7).

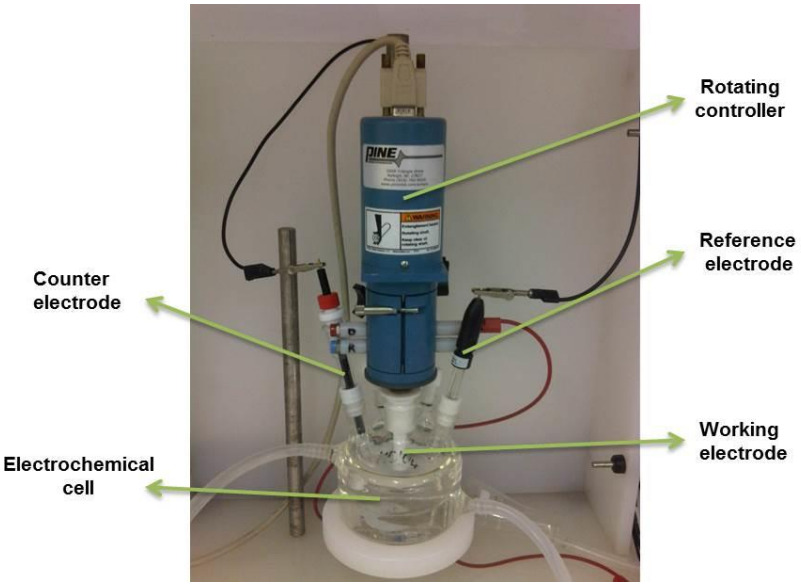

Figure 2.7: Three-electrode electrochemical setup used in the experiments

The working electrodes were polycrystalline Rh and Pt rotating disk electrodes (Pine instruments, 5 mm diameter). The counter electrode is a Pt wire (Pine instruments) and the reference electrode a Ag/AgCl (0.205 V vs SHE) electrode (Radiometer Analytical). All potentials referred to in this study are given versus the Standard Hydrogen Electrode (SHE). A potentiostat (Bio Logic VSP science instrument) was used to control the potential on the working electrode. All experiments were carried out at 25˚C and atmospheric pressure. A Julabo F12 temperature controller was used to regulate the temperature of the electrochemical cell. For the study in acidic electrolyte, 0.1 M $HClO_4$ (70 % Merck) was used and for the study in alkaline electrolyte, a 0.1 M KOH (Merck) solution.

The XRD spectra for the Rh and Pt working electrodes can be seen in Figure 2.8. From these graphs the polycrystallinity of the electrodes could be confirmed.

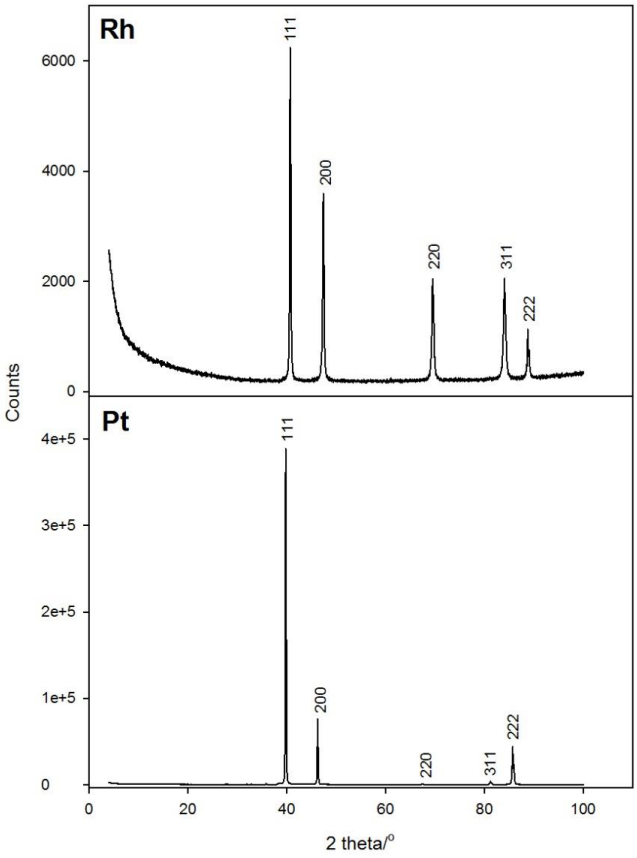

Figure 2.8: XRD graphs for polycrystalline Rh and Pt

2.1.6. Preconditioning Procedures

Preconditioning of the electrodes is extremely important to ensure reproducible results. A suitable procedure was established by a series of experiments during which the reproducibility of a combination of procedures was tested. This included a combination of cyclic voltammetry (CV) and chronoamperometry (CA) experiments. The best preconditioning procedure was found to be as follows: The working electrode was first polished using 5.0 µm and then 0.05 µm alumina polishing solutions (Buehler). The electrode was polished by moving it in a figure of 8 to ensure consistent polishing of the electrode surface. The electrode was then sonicated in ultrapure water for 5 minutes and thereafter rinsed with water and dried using a nitrogen stream.

All solutions were deaerated by bubbling nitrogen for 10 minutes prior to doing the preconditioning experiments to remove all dissolved oxygen in solution. The electrolyte solutions were made using deionized water (prepared by a MIilliQ purifying system).

Regarding electrochemical cleaning of the electrode, a CA experiment was first run on each electrode with the potential being held constant for 2 minutes each time at a potential of 0.0 V (for acidic electrolyte) or -0.78 V (for alkaline electrolyte) to ensure that the electrode surfaces were in the reduced state before continuing with CVs.

A CV was then carried out on the electrode in 0.1 M $HClO_4$ (70 % Merck) or 0.1 M KOH solutions (Merck) in the potential ranges 0.0 V < E < 1.2 V (for acidic electrolyte) and -0.78 V < E < 0.47 V (for alkaline electrolyte) to electrochemically clean the electrode to its original state. 10 cycles were done at a sweep rate of 50 $mV.s^{-1}$ until a stable CV was obtained to ensure electrode surface reproducibility each time before an experiment was carried out.
The above-mentioned procedure was carried out prior to each run.

2.1.7. Rotating disk electrode (RDE) experiments

Linear polarization (LP) experiments were conducted at different rotation rates in either a 0.1 M $HClO_4$ or a 0.1 M KOH solution saturated with oxygen. The saturation was achieved by bubbling oxygen gas for 20 minutes prior to each run.

For the reaction in acidic electrolyte, the potential range studied was 0.0 V < E < 1.2 V. For alkaline electrolyte, the potential range studied was -0.78 V < E < 0.47 V. These LP experiments were done at a sweep rate of 10 $mV.s^{-1}$.

The following different rotation rates were studied: 0 rpm, 100 rpm, 400 rpm, 900 rpm and 2500 rpm.

2.2. RESULTS AND DISCUSSION

2.2.1. Cyclic voltammetry

The CVs done in acidic electrolyte in the absence of oxygen on Rh and Pt can be seen in Figure 2.9.

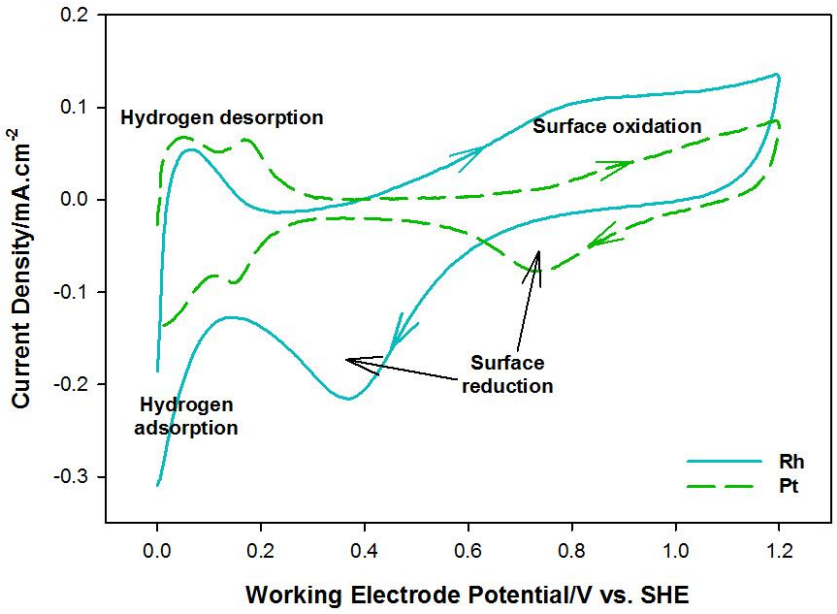

Figure 2.9: CVs on Rh and Pt in 0.1 M $HClO_4$ at a scan rate of 50 $mV.s^{-1}$ in the absence of O_2

Hydrogen desorption peaks could be seen during the forward scan, as well as the surface oxidation peak. During the backward scan the surface reduction peaks, as well as hydrogen adsorption peaks could clearly be seen for both metals. This was the shape the CV had each time before an experiment was run after the preconditioning procedure had been done. The features mentioned should be present every time before an experiment was conducted to be certain of the same electrode surface each time.

It could clearly be seen that Rh oxide species were already formed at much lower potentials than Pt oxide species (an onset of ~ 0.4 V for Rh versus ~ 0.6 V for Pt). Reduction of this oxide then took much longer to occur again during the backward sweep (Peaks at ~ 0.35 V for Rh versus ~ 0.75 V for Pt). Much higher oxidation and reduction current densities could also be seen for Rh than for Pt. This could be an indication that a more stable metal oxide was formed on Rh than on Pt since Rh oxide did not reduce as quickly. This is important to note, since the metal oxide would be present on the electrode surface in the potential range studied for the oxygen reduction reaction.

The CVs done in alkaline electrolyte in the absence of oxygen on Rh and Pt can be seen in Figure 2.10.

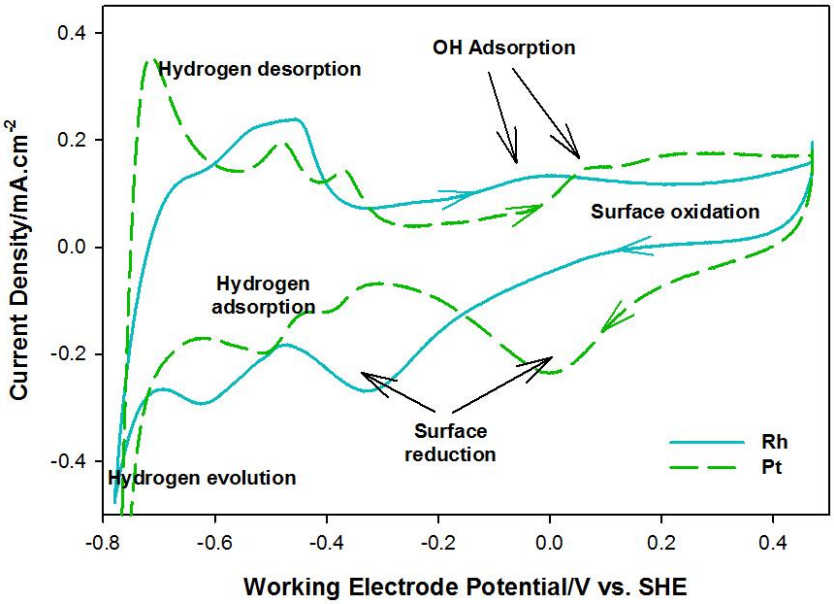

Figure 2.10: CVs on Rh and Pt in 0.1 M KOH at a scan rate of 50 mV.s^{-1} in the absence of O_2

The same features were observed as mentioned for the acidic electrolyte, with the exception of a small OH adsorption peak for both catalysts (at about ~ -0.05 V for Rh and ~ 0.05 V for Pt). Once again, Rh oxide was formed at lower potentials than Pt oxide (with an onset at ~ -0.2 V for Rh versus ~ -0.05 V for Pt) with reduction thereof starting much later than for Pt (Peaks of ~ -0.35 V for Rh versus ~ 0.0 V for Pt).

When the CVs on Rh and Pt in acidic and alkaline electrolytes were compared, it could be seen that in alkaline electrolyte a more active surface was obtained for both catalysts since higher current densities were obtained in the hydrogen adsorption/desorption region.

2.2.2. Rotating Disk Electrode (RDE) experiments

Experiments were conducted on Rh and Pt in acidic and alkaline electrolyte at different rotation rates as discussed in the experimental section. The results will be given and discussed separately below for acidic and alkaline electrolytes.

2.2.2.1. Acidic electrolyte

The RDE results on Rh and Pt in acidic electrolyte (0.1M $HClO_4$) can be seen in Figure 2.11.

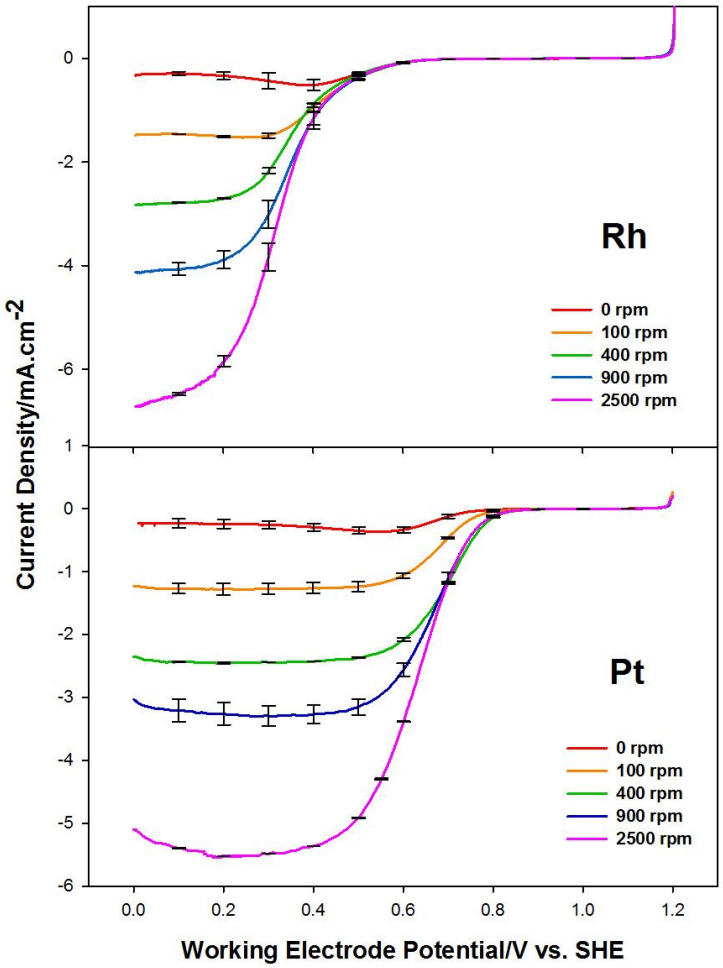

Figure 2.11: RDE experiments on Rh and Pt in 0.1 M $HClO_4$ at a scan rate of 10 $mV.s^{-1}$

Firstly, both Rh and Pt showed the expected trend of increasing current density with an increase in rotation rate. At 0 rpm, a peak was present where after the limiting current density was reached. A plateau was directly formed at all the other rotation rates, except for Rh at 100 rpm, with increasing current density as the rotation rate was increased. This was due to increased transport of electrolyte to the surface of the electrode and, therefore, the higher the rotation rate, the more species were brought to the surface to take part in the reaction. Diffusion limitations were a minimum and this was where the limiting current density was reached. Good reproducibility was found for both catalysts as can be seen in Figure 2.11.

- **Onset potential and limiting current density**

At a rotation rate of 0 rpm, Rh has a higher onset potential and higher limiting current density than Pt (see Table 2.1.). Therefore, a higher current density is reached on Rh, which is favourable since this is an indication of faster reaction kinetics. However, a much higher overpotential is needed for the reaction to initiate, which is unfavourable since it takes a much longer time for Rh to reach a point where the reaction is occurring faster than on Pt.

Table 2:1: Comparison of onset potentials and limiting current densities in acidic electrolyte for Rh and Pt

	Rh	Pt
Onset potential (V)	0.662	0.790
Overpotential (V)	0.568	0.440
Limiting current density ($mA.cm^{-2}$)	0.291	0.229

There may be many different reasons for a difference in onset potential between different catalysts. A few possible reasons will be stated briefly below, since a more in-depth study will be needed to be able to elucidate more clearly what happens on each electrode surface – which is beyond the scope of this project.

The higher onset potential of Rh may be due to the higher reduction potential of Rh oxide as discussed in Section 2.1 when compared to Pt, since surface sites may be blocked for longer by the presence of the more stable Rh oxide species. Sawyer & Day (1963) stated that the mechanism followed on a pre-oxidised electrode surface gave way to the mechanism followed on a pre-reduced electrode surface as the surface oxide was reduced during the course of the oxygen reduction reaction. Therefore, since the reduction of surface oxides occur in the same potential range than the ORR, the possibility exists that competition between the reduction of surface oxide and reduction of oxygen occurs, which leads to the delayed onset of oxygen reduction on Rh.

Another possibility is that the onset potential is dependent on the adsorption of reagents and/or intermediate species of the reaction. This is due to the Sabatier principle which involves that reagents should bind strong enough to a catalyst surface for a reaction to occur to produce intermediates and/or products. These binding energies should also be low enough to allow the species formed during the reaction to leave the surface of the catalyst for new reagents to be able to bind to the surface (Laursen *et al.*, 2012) (Laursen *et al.*, 2011). Therefore, during the ORR, if O_2 (in its molecular or dissociated form) or any of the formed intermediate species

bind too strongly to the electrode's surface, the reaction will be inhibited and the onset potential will likely be influenced.

- **Levich plots**

Levich plots for Rh and Pt in acidic electrolyte can be seen in Figure 2.12. These plots were drawn using values for the limiting current density of each rotation rate for the two catalysts in the diffusion limited region of the LP.

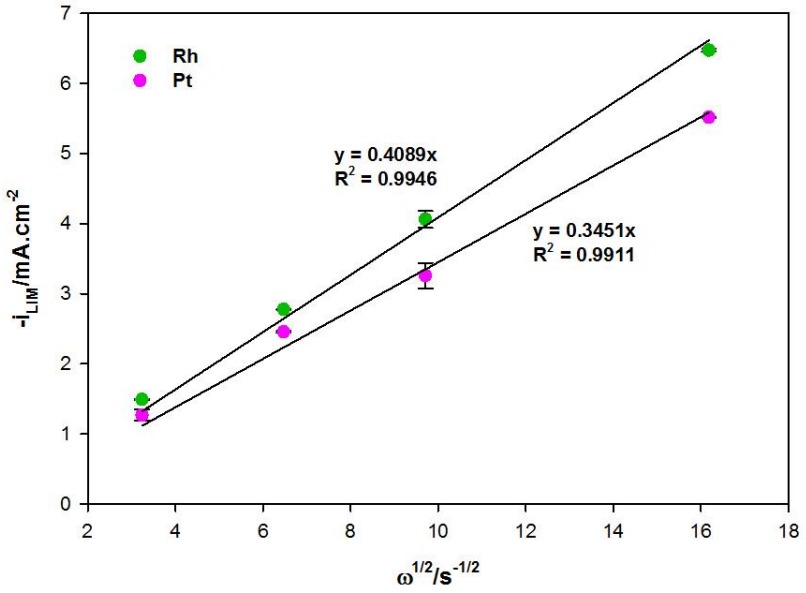

Figure 2.12: Levich plots on Rh and Pt in acidic electrolyte (0.1 M $HClO_4$)

Linearity of these plots is an indication of a mass transport controlled reaction (Pletcher, 2009:164) occurring on the electrode. The number of electrons transferred was calculated from the slopes of the Levich plots shown in Figure 2.11 (see Appendix for calculation). For Rh, the number of electrons transferred was found to be 3.501 and for Pt it was found to be 2.955. The first thing that is evident from these two values obtained, is that a different mechanism is followed for the ORR on each catalyst since different values for the number of electrons transferred was found. Further investigation is needed to be able to determine exactly which mechanism is followed and will not be included in this study. These values can, however, be compared to values obtained for the number of electrons transferred from K-L analyses and further comparison of catalysts can be done.

- **K-L plots**

K-L plots can be drawn from the RDE data to determine the kinetic current density. The number of electrons transferred can also be calculated to compare the mechanism on the two catalysts. These plots for Rh and Pt in acidic electrolyte can be seen in Figure 2.13.

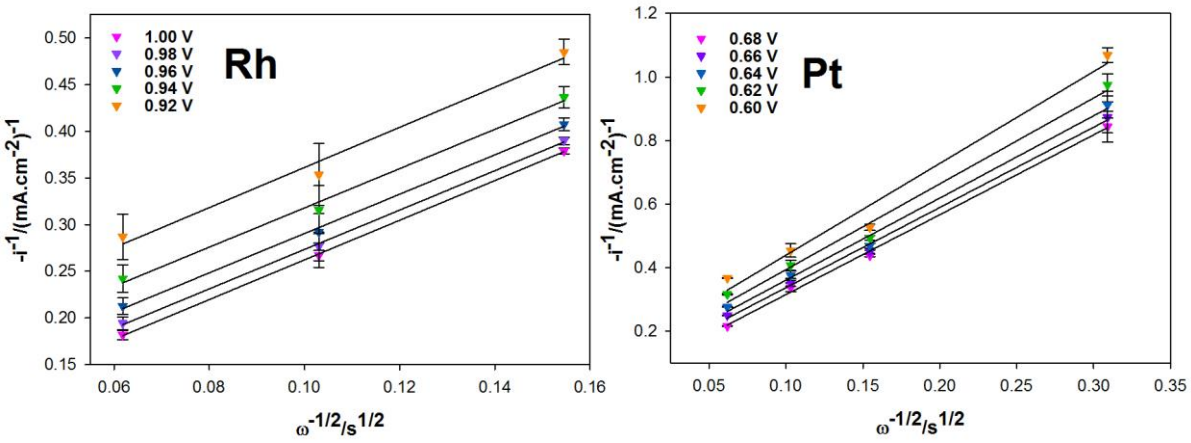

Figure 2.13: K-L plots on Rh and Pt in acidic electrolyte (0.1 M $HClO_4$)

The overpotential values used were chosen from the mixed-transport kinetic control region of the LP results to be able to accurately determine the number of electrons transferred, as well as the kinetic current density. The absolute values for current density were used, since a cathodic reaction was being studied. For Rh, 100 rpm was left out of the analysis, since it showed similar behaviour than 0 rpm where it did not seem to be much dependent on rotation rate and a peak was present before the limiting current density was reached which indicated that the current in this region was not completely dependent on the rotation rate.

A series of parallel straight lines were obtained for Rh, where the lines deviated from parallelism at certain overpotentials for Pt. This was an indication that a single mechanism was followed on Rh in the mixed transport-kinetic control region, where the mechanism on Pt in this region changed as the overpotential was changed (since similar slopes will lead to similar calculated number of electrons transferred). The calculated number of electrons transferred and kinetic current densities for the potential range studied for K-L analysis are shown in Table 2.2 for both catalysts.

The number of electrons transferred was calculated from the slopes of the K-L plots (values can be seen in Tables 1 and 2 of the Appendix) for the two catalysts. The following values were used in the calculations for 0.1 M $HClO_4$ at 25 °C: diffusion coefficient of O_2 (1.93×10^{-5} $cm^2.s^{-1}$), kinematic viscosity (0.01 $cm^2.s^{-1}$) and solubility of O_2 (1.26×10^{-3} $mol.L^{-1}$) (Shao *et al.*, 2006).

Table 2:2: Calculated number of electrons transferred for Rh and Pt in acidic electrolyte from K-L plots

Rh			Pt		
Potential (V)	**Overpotential (V)**	**n**	**Potential (V)**	**Overpotential (V)**	**n**
0.230	1.000	4.035	0.550	0.680	3.420
0.250	0.980	4.062	0.570	0.660	3.405
0.270	0.960	4.070	0.590	0.640	3.322
0.290	0.940	4.077	0.610	0.620	3.182
0.310	0.920	3.989	0.630	0.600	2.974

When comparing the calculated number of electrons transferred for Rh and Pt (see Appendix for calculation), it can be seen that the values on Rh vary between 3.989 and 4.035, therefore it can be said that a 4 electron transfer reaction occurs on Rh in the mixed transport-kinetic control region. This corresponds to the 4 electron reaction described for the ORR where H_2O is formed as the final product (see Section 2.1.2). On Pt, however, the calculated number of electrons transferred vary between 2.974 and 3.420, which is an indication that the mechanism is changing while the overpotential is rising. The mechanism followed on Pt is also different than the mechanism followed on Rh, since the number of electrons transferred differ. These results agree well with initial assumptions made from parallelism of K-L plots.

In comparison with results obtained from Levich analysis, for both catalysts, the mechanism in the mixed transport-kinetic control region (K-L analysis) is different from the mechanism in the diffusion limited region (Levich analysis) as seen from the difference in values for number of electrons transferred. These results are also confirmed by the literature survey since various authors concluded that different mechanisms were operative on both Rh's and Pt's surfaces in the same potential region (Norskov *et al.*, 2004), (Genshaw *et al.*, 1967), (Sawyer & Day, 1963), (Martinovic *et al.*, 1988).

The kinetic current densities were calculated from the y-intercepts of the K-L plots and can be seen in Table 1 in the Appendix. These values were used in the following section during Tafel analysis to be able to do further comparison of the catalysts.

- **Tafel analysis**

The Tafel plots can be seen in Figure 2.14 in acidic electrolyte derived from the kinetic current densities and corresponding overpotentials obtained from K-L analysis.

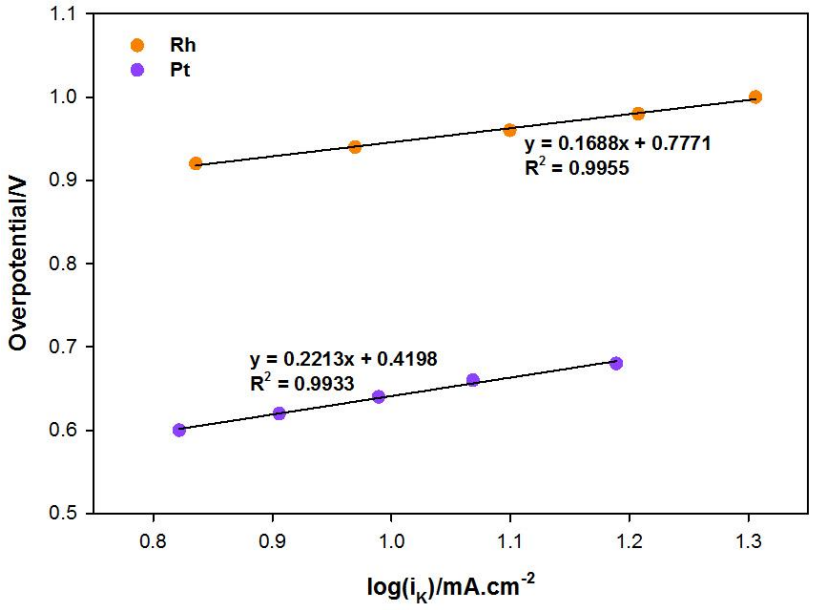

Figure 2.14: Tafel plots on Rh and Pt in acidic electrolyte (0.1 M $HClO_4$)

A linear plot was obtained from which the Tafel slope could be determined from the slope of the straight line. From the slopes of the Tafel plots for Rh and Pt, a Tafel slope of 168.8 mV.decade^{-1} was found for Rh and 221.3 mV.decade^{-1} was found for Pt. The difference in values for the Tafel slopes of the two catalysts confirms the assumptions made during Levich and K-L analyses that a different mechanism is followed on Rh when compared to Pt.

2.2.2.2. Alkaline electrolyte

The RDE results on Rh and Pt in alkaline electrolyte at different rotation rates can be seen in Figure 2.15. The expected trend of increasing current density with an increase in rotation rate was also obtained as described in the previous section for acidic electrolyte. Good reproducibility was also found for both catalysts in alkaline electrolyte.

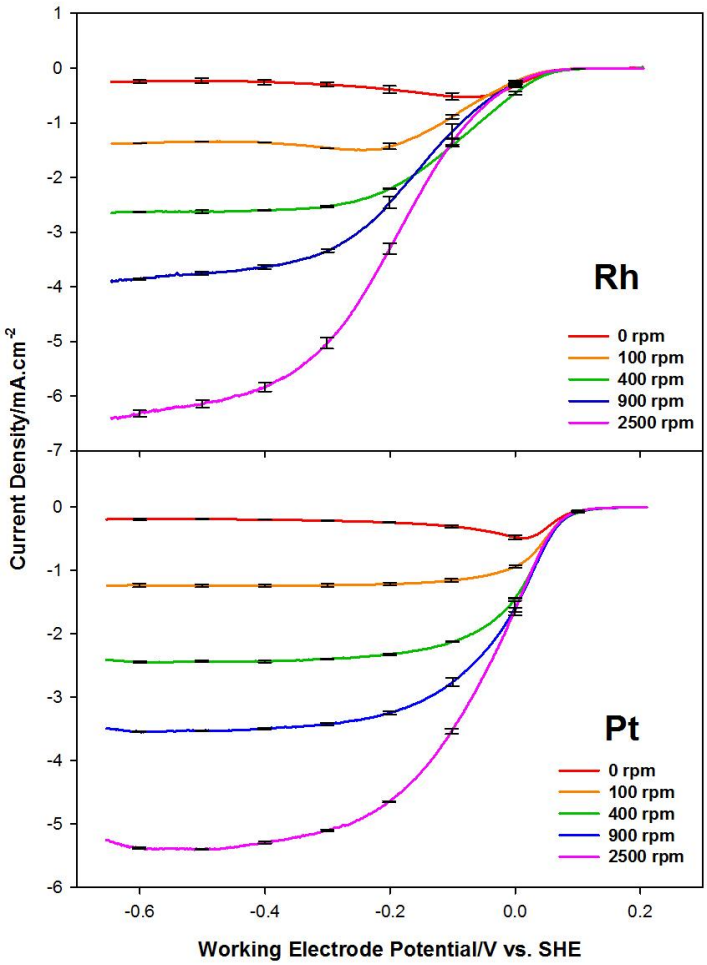

Figure 2.15: RDE experiments on Rh and Pt in 0.1 M KOH at a scan rate of 10 mV.s^{-1}

- **Onset potential and limiting current density**

At 0 rpm similar behaviour could be observed than for acidic electrolyte. Rh had a higher onset potential with higher limiting current density than Pt as can be seen in Table 2.3.

Although slightly higher current densities were reached on Rh than on Pt, the higher onset potential achieved on Rh indicated that it was less suitable for this reaction than Pt. It should be mentioned that the current densities, as well as overpotential values obtained on Rh were very close to the values obtained on Pt, which suggests that in alkaline electrolyte Rh has behaviour very comparable with Pt.

Table 2:3: **Comparison of onset potentials and limiting current densities in acidic electrolyte for Rh and Pt**

	Rh	Pt
Onset potential (V)	0.074	0.131
Overpotential (V)	0.327	0.270
Limiting current density (mA.cm^{-2})	0.228	0.201

- **Levich analysis**

The Levich plots for Rh and Pt in alkaline electrolyte can be seen in Figure 2.16.

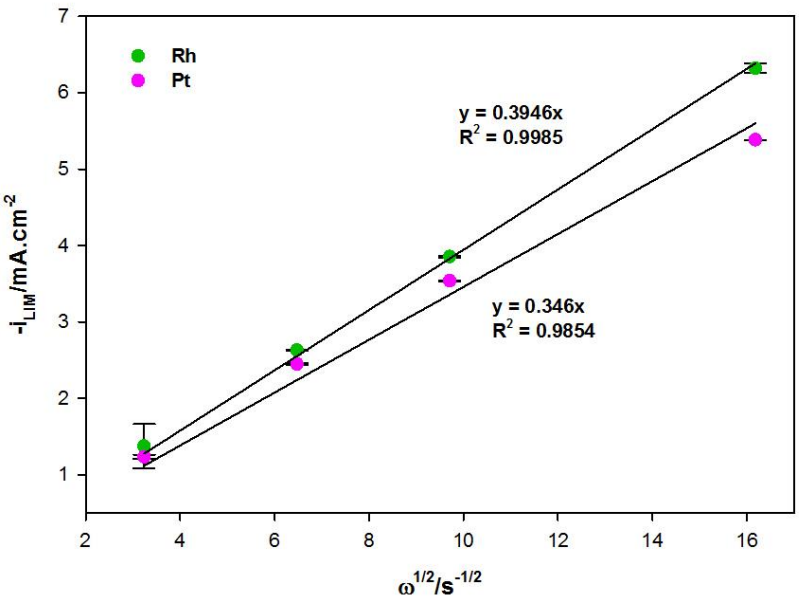

Figure 2.16: **Levich plots on Rh and Pt in alkaline electrolyte (0.1 M KOH)**

As for acidic electrolyte, linearity of these plots indicates that the reaction in this region was mass-transport limited. The number of electrons transferred calculated from the slopes for Rh and Pt, was found to be 3.584 and 3.143, respectively. Hence in alkaline electrolyte, a different mechanism is also followed on each electrode for the ORR since the number of electrons transferred on each is different.

- **K-L analysis**

The same approach was taken for the K-L analysis in alkaline electrolyte as discussed for acidic electrolyte in Section 2.2.2.1. The RDE results were used in order to draw K-L plots to determine the kinetic current density, as well as number of electrons transferred. As with the

analysis in acidic electrolyte, 100 rpm was left out since it showed behaviour that was not entirely dependent on rotation rate as for the other rotation rates.

The K-L plots for Rh and Pt in alkaline electrolyte can be seen in Figure 2.17.

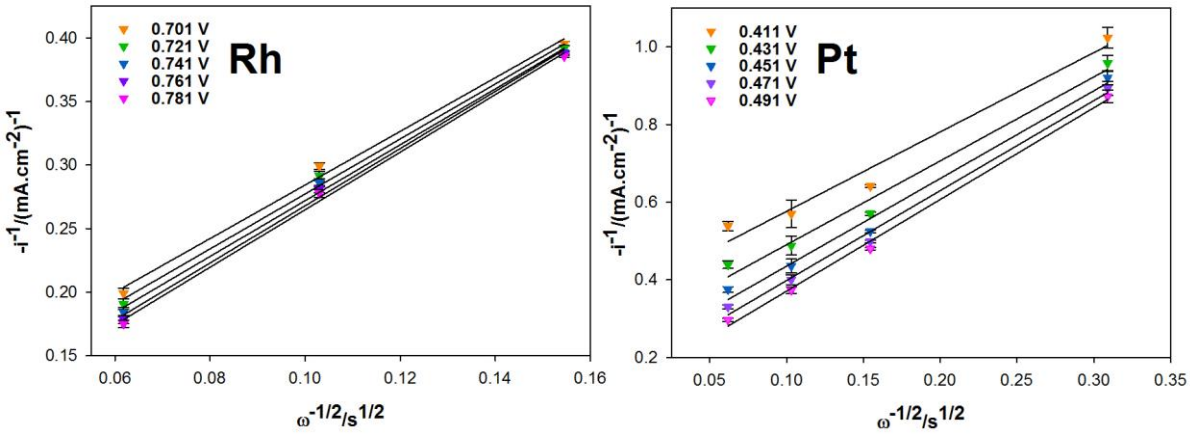

Figure 2.17: K-L plots on Rh and Pt in alkaline electrolyte (0.1 M KOH)

A series of non-parallel straight lines were obtained for both metals (R^2 values can be found in table 3 and 4 of the Appendix). As for the results on Pt in acidic electrolyte, this was an indication of a change in the mechanism in the overpotential range used. Table 2.4 shows the number of electrons transferred calculated from the slope of K-L plots together with corresponding potentials and overpotentials (Slopes and y-intercepts can be seen in Table 3 and 4 of the Appendix).

The number of electrons transferred for Rh and Pt was calculated from the slopes of the K-L plots. The following values were used in the calculations for 0.1 M KOH at 25 °C: diffusion coefficient of O_2 (1.9 x 10^{-5} $cm^2.s^{-1}$), kinematic viscosity (0.01 $cm.s^{-1}$) and solubility of O_2 (1.2 x 10^{-6} $mol.L^{-1}$) (Song & Zhang, 2008:99).

Table 2:4: Calculated number of electrons transferred for Rh and Pt in acidic electrolyte from K-L plots

Rh			Pt		
Potential (V)	**Overpotential (V)**	**n**	**Potential (V)**	**Overpotential (V)**	**n**
-0.300	0.701	4.320	-0.010	0.411	4.461
-0.320	0.721	4.211	-0.030	0.431	4.218
-0.340	0.741	4.146	-0.050	0.451	4.035
-0.360	0.761	4.048	-0.070	0.471	3.934
-0.380	0.781	4.024	-0.090	0.491	3.859

When comparing the number of electrons transferred during the ORR on Rh and Pt, the calculated values for Rh varies between 4.024 and 4.320 and for Pt it varies between 3.859 and 4.461. The differences in the values for both catalysts over the overpotential range for each confirm the initial observations made from the non-parallelism of K-L plots that the mechanism changes over the mixed transport-kinetic control region The mechanism followed on Rh is also different from the mechanism followed on Pt since the values obtained are different. These values are also different from the number of electrons transferred, calculated from Levich plots. Thus the mechanism changes on each catalyst when moving into the diffusion limited region. As for the results obtained in acidic electrolyte, the results here confirm that a changing mechanism is operative on the surfaces of Rh and Pt in the same potential region (see Section 2.1.2).

The kinetic current densities were calculated from the y-intercept of the K-L plots and can be seen in Table 3 and 4 in the Appendix. These values were used in the following section during Tafel analysis to be able to compare the mechanism and kinetics of each catalyst.

- **Tafel analysis**

The Tafel plots for Rh and Pt in alkaline electrolyte can be seen in Figure 2.18 and the same approach was taken as for acidic electrolyte in Section 2.3.2.1. The kinetic current densities obtained from the y-intercepts of K-L plots were used to draw these Tafel plots.

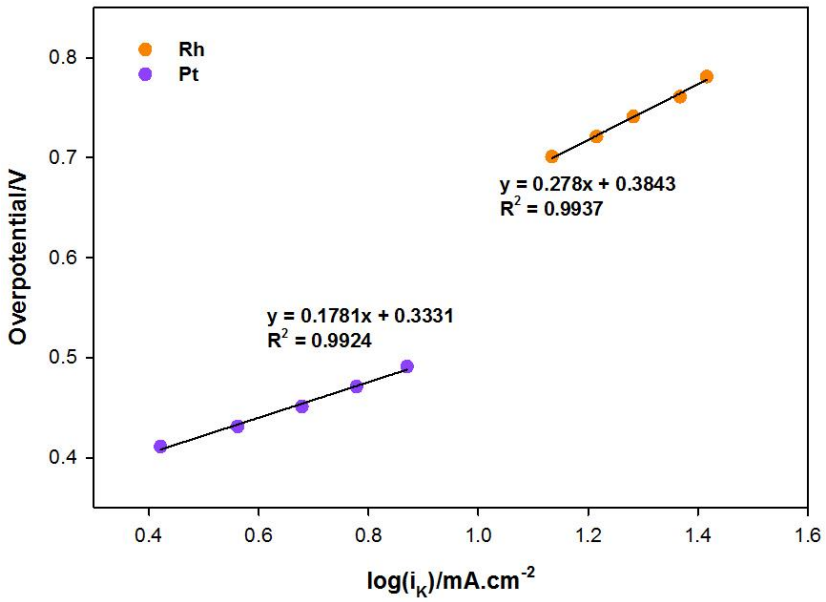

Figure 2.18: Tafel plots on Rh and Pt in alkaline electrolyte (0.1 M KOH)

The values for the Tafel slopes were found as 278 mV.decade^{-1} for Rh and 178.1 mV.decade^{-1} for Pt. The difference in these values for the two catalysts is a confirmation of the assumptions made during Levich and K-L analyses of different mechanisms operating on these two catalysts in the potential region of the ORR.

2.3. CONCLUSIONS

2.3.1. Onset potentials and limiting current density

It was shown that in acidic electrolyte, Pt was kinetically more favourable than Rh since the reaction occurred at a lower overpotential (0.440 V vs. 0.568 V for Rh) with the limiting current density reached much quicker than on Rh, even though Rh reached slightly higher current densities (0.229 mA.cm^{-2} vs. 0.291 mA.cm^{-1} for Rh). In alkaline electrolyte similar results were obtained, with the exception that the onset potential on Rh was much closer to that observed for Pt (0.270 V for Pt vs. 0.327 V for Rh). Slightly higher current densities were also achieved on Rh than on Pt (0.228 mA.cm^{-2} for Pt vs. 0.201 mA.cm^{-2} for Rh).

2.3.2. Levich, K-L and Tafel analysis

From Levich analysis, it was found that both catalysts became diffusion limited at high overpotentials (from linearity of these plots). The calculated number of electrons transferred for Rh and Pt from Levich plots compared to the calculated number of electrons transferred from K-L plots in both acidic and alkaline electrolyte revealed that a complex mechanism was followed on both catalysts with a changing number of electrons as the overpotential was increased. This is in agreement with studies mentioned in Section 2.1.3 where authors found a changing mechanism on Rh and Pt as seen from a change in the Tafel slope in different potential regions. These analyses also revealed a difference in mechanism between the two catalysts studied since the number of electrons transferred for these two was different. A more in-depth investigation will be needed to determine the exact mechanism followed on each catalyst, but since this was only a basic comparative study further investigation will not be done.

Regarding the Tafel slopes obtained for each catalyst, the values for Rh were different than that obtained for Pt. This was observed in both acidic and alkaline electrolytes for each

catalyst, which was also a confirmation of assumptions made from Levich and K-L analyses that a difference in mechanism existed between the two catalysts.

2.3.3. General conclusions

Determination of the mechanism was not in the scope of this study, but these observations may be used in possible future studies where a more in-depth investigation may be done regarding the mechanism. It was shown that in acidic electrolyte Rh was not a suitable catalyst for the ORR due to much higher onset potentials. Generally, Rh exhibited similar activity for the ORR in alkaline electrolyte with onset potential and limiting current density values close to that of Pt.

To answer the question if it is possible for Rh to be used alone or as part of an alloy in low-temperature fuel cells, it can be concluded that Rh shows similar behaviour than Pt in the sense that a changing mechanism is operative on its surface in the potential range studied for the ORR. Rh also produces high current densities in alkaline electrolyte, which suggests that it may be possible to use Rh as catalyst or co-catalyst for the ORR.

3 The electro-oxidation of Ethanol (EOR)

3.1. LITERATURE

3.1.1. Background

Ethanol (EtOH) is a more promising fuel for low-temperature fuel cells when compared to methanol, due to the fact that (a) methanol is very toxic (Antolini, 2007), (b) ethanol can be produced in large quantities from agricultural products, for example sugar cane, and (c) ethanol has a higher energy density than methanol (Shen *et al.*, 2010), which makes it very desirable for use in fuel cells, especially when complete oxidation to CO_2 takes place, as a high yield is reached for ethanol during complete oxidation to CO_2 (Lamy *et al.*, 2002), (Lamy *et al.*, 2004).

The standard electrode reaction for the oxidation of ethanol at a fuel cell anode involves the transfer of 12 electrons. The produced protons are then combined with reduced O_2 at the cathode of the fuel cell in the presence of air. The standard electrode potentials are given below for the cathode and anode reactions (Lai *et al.*, 2010):

Anode	$C_2H_5OH + 3H_2O \rightarrow 2CO_2 + 12H^+ + 12e^-$	$E^0 = 0.1\ V$	(27)
Cathode	$O_2 + 4H^+ + 4e^- \rightarrow 2H_2O$	$E^0 = 1.23\ V$	(28)

The electro-oxidation of EtOH occurs according to a parallel reaction mechanism involving a total oxidation path and a partial oxidation path (Antolini, 2007):

$CH_3CH_2OH \rightarrow [CH_3CH_2OH]_{ad} \rightarrow C1_{ad}, C2_{ad} \rightarrow CO_2$ (total oxidation)

$CH_3CH_2OH \rightarrow [CH_3CH_2OH]_{ad} \rightarrow CH_3CHO \rightarrow CH_3COOH$ (partial oxidation)

During the formation of CO_2, fragments with one or two carbon atoms may form, $C1_{ad}$ and $C2_{ad}$. There is much controversy about the exact path the reaction follows, as well as on the nature of the intermediates. Something that is generally agreed upon is that a very important aspect during EtOH oxidation is that the C-C bond has to be broken for the reaction to be completed to form the main product, namely CO_2. Pt, however, is not effective enough in breaking the C-C bond, with the result of acetaldehyde and acetic acid occurring as products. Another problem with Pt as catalyst for the EOR is its susceptibility to poisoning by strongly adsorbed intermediates. Consequently, many studies have been conducted on the EOR by

combining other metals, like Ru and Sn, with Pt (Vigier *et al.*, 2004), (Antolini, 2007) in order to overcome the problems that exist with using Pt alone.

Lai & Koper (2009) propose that the EOR follows a dual pathway during which acetaldehyde and acetic acid are formed; with the production of acetic acid being considered a 'dead-end' since further oxidation is very difficult. They further confirm that the C-C bond has to be broken to form a single carbon adsorbed species, i.e. CO_{ad} or $CH_{x,ad}$, which can both be oxidised further to CO_2.

3.1.2. Acidic electrolyte

Most of the studies mentioned in a review by Antolini (2007) were conducted in acidic electrolyte solutions, and numerous catalysts were compared. A known problem that exists is breaking of the C-C bond in order to completely oxidise EtOH to CO_2, as mentioned in section 3.1.1. Pt alone is not efficient enough to break this bond and the use of a co-catalyst may aid Pt with oxidation of EtOH by better breaking of the C-C bond and thus facilitating formation of more CO_2. Characteristics of a good catalyst, as described by Gupta & Datta (2006), should include better breakage of the C-C bond, as well as being able to better oxidise CO_{ad} to CO_2, since adsorbed CO species can easily contribute to poisoning of the catalyst surface when further oxidation is difficult.

Kutz *et al.* (2011) studied the EOR on polycrystalline Pt, investigating the mechanism and pathways involved. The summary of the proposed pathways are shown in Figure 3.1 and a brief overview of their results is given below.

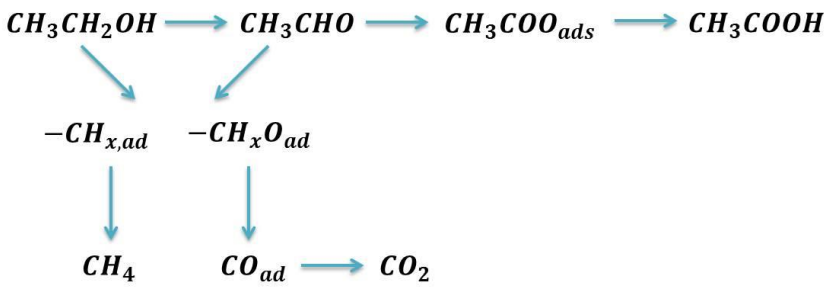

Figure 3.1: Reaction pathways for the EOR in acidic medium

Different products are formed at low potentials (E < 0.4V) compared to products formed at high potentials (E > 0.4V). At low potentials, CO is the main reaction product, whereas acetate is the main product at high potentials. The acetate can be further oxidised to acetic acid, which diffuses away from the electrode surface and is seen as a 'dead-end' to the reaction,

since it cannot be further oxidised. The C-C bond is also easily broken at low potentials, but oxidation of the $–CH_x$ fragment is more difficult than the oxidation of the $–CH_xO$ fragment and methane can be formed at very low potentials from reduction of $-CH_x$. Concerning the supporting electrolyte, the authors revealed that lower current densities were achieved in H_2SO_4 than in $HClO_4$. This was due to co-adsorption of bisulfate in H_2SO_4 solutions.

There have been studies conducted in which Rh was employed as a co-catalyst, for instance in the study done by Gupta & Datta (2006). They found that a PtRh (specifically $Pt_{74}Rh_{26}$) electrode showed better EtOH oxidation behaviour than Pt alone. The reason for this is better breaking of the C-C bond (Markovic *et al.*, 1995), which has also been mentioned by Kowal *et al.* (2009). In another study done on Pt, Rh and PtRh (de Souza *et al.*, 2002) the EOR was enhanced by the presence of Rh by increasing the amount of CO_2 as final product of the reaction.

3.1.3. Alkaline electrolyte

It is worthwhile to also study the EOR in alkaline media as well, since it has been found that the efficiency of the reaction increased in alkaline compared to acidic media (Lai & Koper, 2009). Non-Pt catalysts can also be used in alkaline fuel cells which are an advantage, since Pt is very expensive. The challenges with using alkaline fuel cells are being overcome and more research is being done on them and it has been shown that it is possible to use EtOH as a fuel in alkaline fuel cells (Verma & Basu, 2005).

Numerous studies have been undertaken on the EtOH oxidation reaction in alkaline electrolytes on various catalysts. Pd has been investigated in alkaline media, since it showed increased catalytic activity compared to Pt (Xu *et al.*, 2010). A similar problem exists when using Pd as catalyst, like Pt, in that it suffers from poor C-C bond breakage ability (Liang *et al.*, 2009), (Fang *et al.*, 2010).

Co-catalysts, therefore, have to be used together with Pt, which is able to break this bond as mentioned in section 3.1.2. Pt and Pd have been studied together, mostly in alkaline media, but various other catalysts have also been investigated (Antolini, 2007). More recently, Rh have received more attention for use as a co-catalyst together with Pt in alkaline media. This is due to the ability of Rh to break the C-C bond better and facilitate the complete oxidation of EtOH to CO_2. More specifically, Suo & Hsing (20110 reported a Rh/C catalyst that showed much higher activity towards the EOR than Pd-Rh/C or Pd/C catalysts at low potentials and

that different mechanisms might exist on the different catalysts. This might then lead to different reaction products being formed on each catalyst.

Another study in alkaline medium employed PtRh catalysts in comparison with Pt (Shen *et al.*, 2010). Their results showed that Pt_2Rh/C was more active than Pt/C. They also ascribed this to better breaking of the C-C bond as well as better kinetics of the oxidation of CO_{ad} to CO_2, which was limited on Pt.

Rh should therefore be able to better accomplish the following when compared to Pt:

- Achieve better breaking of the C-C bond
- Show increased kinetics of CO_{ad} oxidation to CO_2

3.1.4. Focus of the study

It has been shown from literature that Rh was a promising co-catalyst together with Pt; however, no clear results were found about the activity of pure polycrystalline Rh. In this regard a comparison between Rh and Pt for the EOR will be done, using cyclic voltammetry and linear polarization techniques similarly to what was done for the ORR.

The EOR has been chosen to be included in this study after the ORR, but before the SO_2 oxidation reaction will be studied, since it is more complicated, with intermediate species that can be formed and which can adsorb onto the surface and influence the pathway of the reaction. This is in preparation for SO_2 oxidation, during which many different adsorbed intermediates may be present in the potential range studied.

This study will include basic comparisons of the catalysts under question toward the electro-oxidation of EtOH in order to create a base from which further studies can be done on PGM group alloys. This study can be referred to during future work where combinations of metals will be used in order to look at each metal's contribution. However, the work done on the mechanism in the literature is of great importance since the ideas and results of these authors can be used to identify possible problems and explain behaviour of the catalysts.

The techniques used to compare the two catalysts will include cyclic voltammetry and linear polarization electrochemical measurements from which the Levich, K-L and Tafel analyses will be done. The onset potentials and limiting current densities will also be compared for Rh and Pt to compare the activity of each catalyst toward the reaction being studied.

A more detailed study will be done during cyclic voltammetry experiments for alkaline electrolyte solutions, since adsorbed OH that forms on the electrode surface may play an important role during the reaction as shown by Liang *et al.* (2009). Therefore, different concentrations of alkaline electrolyte will be included in this study.

3.2. EXPERIMENTAL

3.2.1. Electrochemical Setup

A standard three-electrode setup was used in the electrochemical experiments (see Figure 2.6). The working electrodes were polycrystalline Rh and Pt rotating disk electrodes, 5 mm in diameter (Pine Instruments). The counter electrode was a Pt wire (Pine Instruments) and the reference electrode a saturated calomel (0.241 V vs SHE) electrode (Radiometer Analytical). All potentials referred to in this study are given versus the Standard Hydrogen Electrode (SHE). A potentiostat (Bio Logic VSP science instrument) was used to control the potential on the working electrode. All experiments were carried out at a temperature of 25 ˚C and atmospheric pressure. A Julabo F12 refrigerated temperature controller was used to regulate the temperature of the electrochemical cell. For the study in acidic electrolyte, a 0.1 M $HClO_4$ (70 % Merck) solution was used and for the study in alkaline electrolyte, 1 M and 0.1 M KOH (Merck) solutions were used.

The XRD graphs for the Rh and Pt working electrodes can be seen in Figure 2.7 in Chapter 2 where the polycrystallinity of the catalysts can be confirmed.

3.2.2. Preconditioning Procedures

Preconditioning of the electrodes is extremely important to ensure reproducible results. A suitable procedure was established by a series of experiments during which the reproducibility of a combination of procedures was tested. This included a combination of cyclic voltammetry (CV) and chronoamperometry (CA) experiments. The best preconditioning procedure was found to be as follows: The working electrode was first polished using 5.0 µm and then 0.05 µm alumina polishing solutions (Buehler). The electrode was polished by moving it in a figure of 8 to ensure consistent polishing of the electrode surface. The electrode was then sonicated in ultrapure water for 5 minutes and thereafter rinsed with water and dried using a nitrogen stream.

All solutions were deaerated by bubbling nitrogen for 10 minutes prior to doing the preconditioning experiments in order to remove all dissolved oxygen in the solution. The electrolyte solutions were made using deionized water (prepared by a MIilliQ purifying system).

Regarding electrochemical cleaning of the electrode, a CA experiment was first run on each electrode with the potential being held constant for 2 minutes each time at a potential of 0.0 V (for acidic electrolyte) or -0.78 V (for alkaline electrolyte) to ensure that the electrode surfaces were in the reduced state before continuing with CVs. A CV was then carried out on the electrode in 0.1 M $HClO_4$ (70 % Merck) or 0.1 M KOH solutions (Merck) in the potential ranges 0.0 V < E < 1.2 V (for acidic electrolyte) and -0.78 V < E < 0.47 V (for alkaline electrolyte) to electrochemically clean the electrode to its original state. 10 cycles were done at a sweep rate of 50 $mV.s^{-1}$ until a stable CV was obtained to ensure electrode surface reproducibility each time before an experiment was carried out.

The above-mentioned procedure was done prior to each run.

3.2.3. Cyclic voltammetry experiments

3.2.3.1. Acidic electrolyte

Acidic electrolyte solutions were made by adding the appropriate amounts of $HClO_4$ (70 % Merck) and EtOH (Absolute Merck) to ultrapure water. All solutions were deaerated before the experiments by bubbling nitrogen for 10 minutes prior to the run.

CV experiments were done on Rh and Pt in 0.1 M $HClO_4$ solutions containing 1 M EtOH to be able to determine the activity of each metal in acidic media. The concentration of 0.1 M for $HClO_4$ was chosen, since it is most commonly used and higher current densities are obtained in $HClO_4$ than in H_2SO_4 (Kutz *et al.*, 2011). The reaction was studied in the potential range 0.0 V < E < 1.2 V at a scan rate of 10 $mV.s^{-1}$.

The preconditioning procedure, described in section 3.2.2., was followed prior to any CV experiment. The CV was then conducted, first in the clean electrolyte solution and then in an EtOH-containing electrolyte solution in order to determine if the catalyst showed activity towards the EOR and to compare the observed peaks to that of the catalyst in the clean electrolyte.

This was only done to determine and compare the activity of Rh, towards the EOR, to that of Pt. In this regard the onset potentials and peak potentials were compared.

3.2.3.2. Alkaline electrolyte

Alkaline electrolyte solutions were made up by adding the appropriate amounts of KOH pellets and EtOH to ultrapure water. All solutions were deaerated by bubbling nitrogen for 10 minutes prior to the run.

For experiments conducted in alkaline medium, a different approach was taken than in acidic medium. Different concentrations of KOH (0.1 M and 1 M) as electrolyte were investigated, since the adsorption of OH^- has a significant role to play during the oxidation of EtOH and different OH^- concentrations will, therefore, influence the reaction differently. Liang *et al.* (2009) propose that the kinetics of the EOR is influenced by OH^- ions at high potentials. These different KOH concentrations were also used to determine the effect on current density, as well as on the reproducibility of the results.

CV experiments were subsequently conducted after the preconditioning procedure was followed as described in section 3.2.2. The potential range chosen was $-0.75\ V < E < 0.47\ V$ at a scan rate of 10 $mV.s^{-1}$.

3.2.4. Rotating disk electrode (RDE) experiments

Different rotation rates were studied for use in Levich- and K-L analyses. Linear polarization (LP) experiments were conducted at different rotation rates in 0.1 M $HClO_4$, 0.1 M KOH or 1 M KOH solutions each containing 1 M EtOH.

For the RDE experiments, acidic and alkaline, the same potential ranges were used as for the CV experiments at a sweep rate of 10 $mV.s^{-1}$. The following rotation rates were studied: 0 rpm, 100 rpm, 400 rpm, 900 rpm and 2500 rpm.

3.3. RESULTS AND DISCUSSION

3.3.1. Cyclic voltammetry

3.3.1.1. Acidic electrolyte

It has been mentioned that Rh shows limited catalytic activity towards the EOR in acidic electrolytes, but that it shows good behaviour when used together with another metal, like Pt (de Souza *et al.*, 2002). It enhances the reaction in that better C-C bond breakage is achieved, compared to when only Pt is used as catalyst and it increases the total yield of CO_2 production.

The CV results for the EOR on Rh and Pt are shown in Figure 3.2. The CV of the clean electrolyte (0.1 M $HClO_4$) is shown together with the EtOH-containing (1 M EtOH) perchloric acid solution. The shape of the CV obtained on Pt for the EOR was similar to that found by Kutz *et al.* (2011). During the forward sweep a hump and two distinct peaks can be observed as well as a peak during the backward scan. At the potential where surface oxides are formed, the oxidation current decrease until it is inhibited completely by blockage of surface sites by Pt-O species. The peak during the backward scan has an onset at exactly the potential where surface oxides start to reduce and is inhibited again when too low potentials are reached for any oxidation to occur. For Rh it is evident that it shows some activity towards the EOR in $HClO_4$ solutions, although with very low current densities. The exact same features are present on Rh as on Pt, namely the hump followed by the two distinct peaks. This behaviour suggests that a similar mechanism is followed on Rh as on Pt. However, Rh doesn't show a peak during the backward sweep like Pt, which might be due to the presence of more stable surface oxide species formed by Rh, as can be seen from the much lower surface reduction potential. Therefore, at the potential where Rh's surface oxide species are reduced, the potential is already too low for EtOH oxidation to occur. Another aspect that can be observed is that the currents are suppressed on Rh in the hydrogen adsorption/desorption region which suggests that some species are present on the surface which block sites in this region.

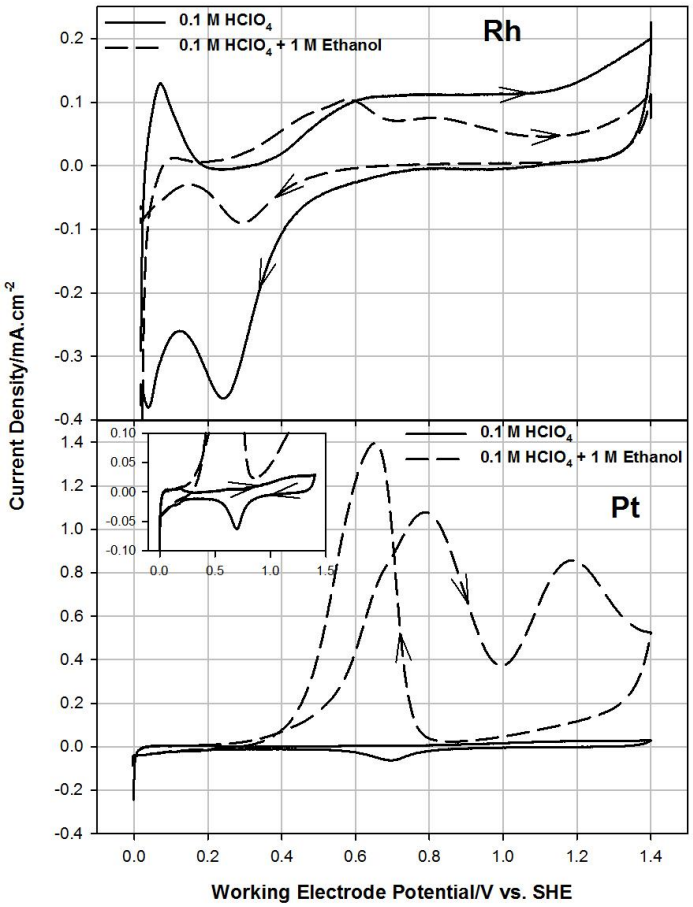

Figure 3.2: CVs on Rh and Pt in 0.1 M HClO4 and 0.1 M HClO4 + 1 M EtOH solutions at a sweep rate of 10 mV.s^{-1}

When comparing the onset potentials of Rh and Pt, it can be seen that Rh shows a lower onset potential (0.2 V) than Pt (0.3 V). It can therefore be said that Pt follows a less favoured pathway than Rh, since most of the reaction occurs at higher potentials than Rh. A significant difference worth mentioning is that all three features on Rh during the forward sweep show lower peak potentials (0.46 V, 0.58 V and 0.81 V) than the three features on Pt (0.65 V, 0.78 V and 1.18 V). This is an indication that the EOR follows a lower-energy pathway than on Pt, since the oxidation occurs at lower potentials. However, Rh shows very limited activity toward the EOR in acidic electrolyte and is therefore not very suitable for use as catalyst on its own, as already mentioned. The potential of Rh acting as a suitable co-catalyst is confirmed by the lower potentials at which EtOH is oxidized on Rh than on Pt, together with a lower onset potential.

3.3.1.2. Alkaline electrolyte

The effect of different concentrations (1 M and 0.1 M) of alkaline electrolyte will be highlighted to demonstrate what effect this has on the oxidation of EtOH for each catalyst. This will also be used to determine which concentration is most suitable and shows good reproducibility for further studies.

3.3.1.2.1. Comparison between Rh and Pt for 1 M KOH + 1 M EtOH

In Figure 3.3, the EOR is shown in 1 M KOH on Rh and Pt. For both catalysts the CVs for 1 M KOH containing 1 M EtOH are compared to the CVs in the clean electrolyte solutions.

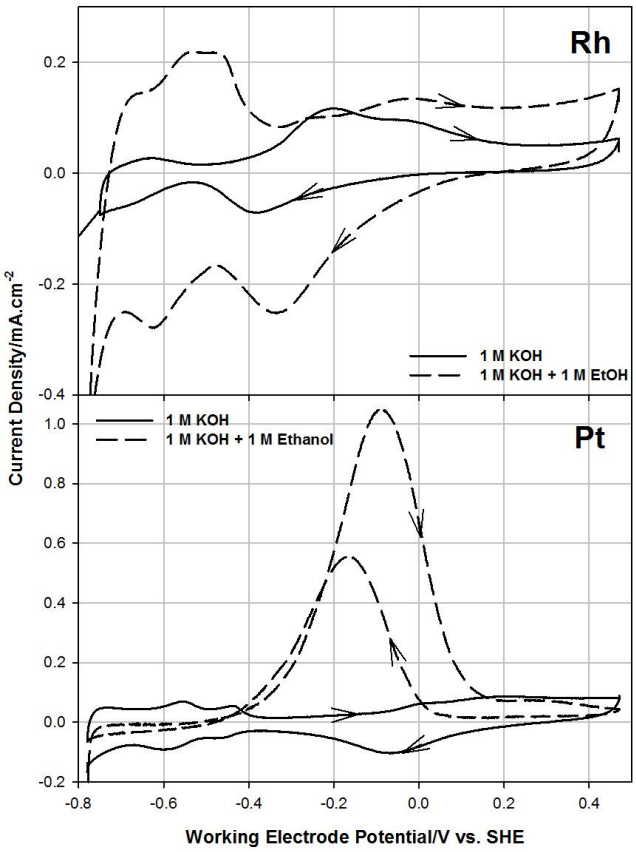

Figure 3.3: CVs on Rh and Pt in 1 M KOH and 1 M KOH + 1M EtOH at a sweep rate of 10 mV.s^{-1}

On Rh, it can be seen that the features in the hydrogen adsorption/desorption region was completely suppressed in the electrolyte containing 1M EtOH. This may be due to strong adsorption of species present in the electrolyte solution. Furthermore two peaks can be seen on Rh in the forward sweep although with very low current densities. There is no peak present in the backward sweep. On Pt it can be seen that the peaks in the hydrogen

adsorption/desorption region is also suppressed. This is in agreement with results obtained by Lai & Koper (2009) where they observed similar surface blocking and ascribed this to adsorption of the decomposition products of EtOH. For Pt a peak is present during the forward sweep as well as in the backward sweep.

Evaluation of the catalysts is done by comparing the onset potentials, peak potentials and peak current densities for both Rh and Pt. Similar to the approach taken by Shen *et al.* (2010) the ratio of the peak current density of the forward scan (i_f) to the peak current density of the backward scan (i_b) will also be compared for Rh and Pt. Adsorbed species are formed during the forward scan by incomplete oxidation of EtOH. This ratio (i_f/i_b) mentioned above is an indication of the extent to which these species are removed during the backward scan from the surface of the electrode (Shen *et al.*, 2010).

The onset potentials, peak potentials, peak current densities and i_f/i_b ratios are tabulated below (Table 3.1.).

Table 3:1: Onset potentials, peak potentials, current densities and i_f/i_b ratios for Rh and Pt in 1 M KOH containing 1 M EtOH

	Onset Potential (V)	Peak Potential (V)	Current Density (mA.cm^{-2})	i_f/i_b ratio
Rh	-0.4	-0.198	0.117	-
Pt	-0.371	0.088	1.051	1.891

The onset potential for Rh is slightly lower than for Pt, which is an indication that the reaction initiates faster on Rh than on Pt. The lower peak potential of Rh indicates that the reaction takes place at a lower potential when compared to Pt. A i_f/i_b ratio could not be calculated for Rh since no peak was present during the backward scan. This may by an indication that a more complete reaction occurred on Rh or it may just be the result of poor catalytic activity. The current density is so low for Rh when compared to Pt that it cannot be considered as a suitable catalyst in this concentration of electrolyte solution.

A more detailed description of what is observed will be given in section 3.3.1.2.3 during a comparison between the different concentrations of electrolyte.

3.3.1.2.2. Comparison between Rh and Pt for 0.1 M KOH + 1 M EtOH

In Figure 3.4 the electro-oxidation of EtOH is shown in 0.1 M KOH on Pt and Rh. For both catalysts, the CVs in 0.1 M KOH containing 1 M EtOH are compared to the CVs in the clean

electrolyte solutions. The CV in clean electrolyte solution for Pt can be seen more clearly in the insert.

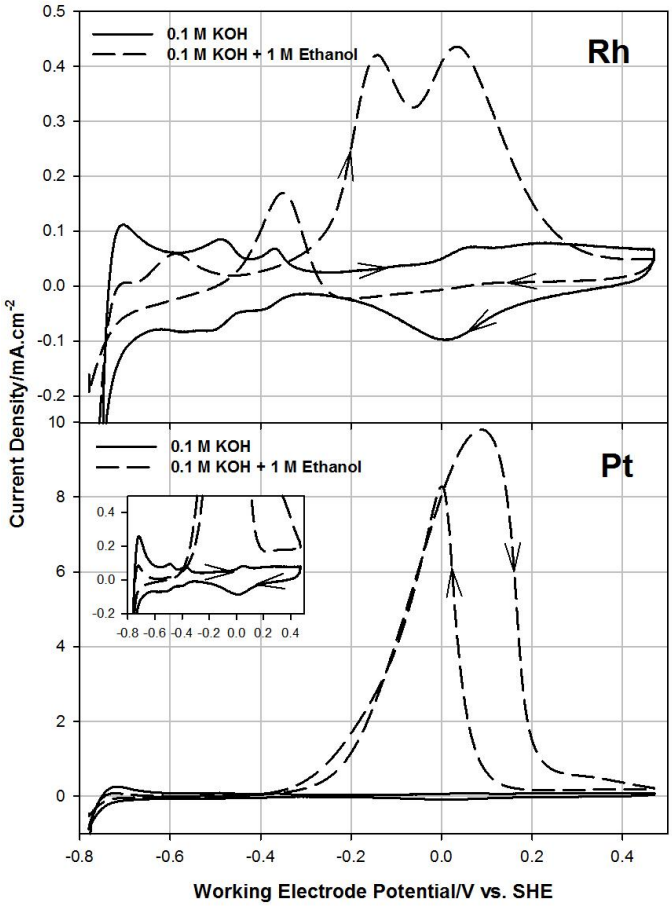

Figure 3.4: CVs on Rh and Pt in 0.1 M KOH and 0.1 M KOH + 1 M EtOH at a sweep rate of 10 mV.s^{-1}

Firstly, the same behaviour was observed in the 0.1 M KOH electrolyte solution on the two catalysts in the sense that the peaks in the hydrogen adsorption/desorption region are being suppressed due to the decomposition products of EtOH (Lai & Koper, 2009).

The onset potentials, peak potentials, peak current densities and i_f/i_b ratios can be seen in Table 3.2.

Table 3:2: Onset potentials, peak potentials, current densities and i_f/i_b ratios for Rh and Pt in 0.1 M KOH containing 1 M EtOH

	Onset Potential (V)	Peak Potential (V)	Current Density (mA.cm^{-2})	i_f/i_b ratio
Rh	-0.32	0.032	0.436	2.569
Pt	-0.40	0.088	9.802	1.184

It can be seen clearly that the onset potential for Pt is lower than for Rh, which indicates that the reaction is initiated much quicker on Pt than on Rh. Another aspect that can clearly be seen is the significantly higher current density that is achieved by Pt compared to Rh. Therefore, in this concentration of electrolyte, Pt exhibited faster reaction kinetics as concluded from the higher current density achieved. However, the peak potential of the reaction on Rh is much lower than on Pt which suggests that the reaction may occur earlier on Rh. This, together with the higher i_f/i_b ratio obtained on Rh may indicate that a more complete reaction is occurring compared to Pt since adsorption products of EtOH may be more completely oxidised to CO_2 (Shen *et al.*, 2010).

From further qualitative comparison between Rh and Pt, it can be seen that Rh presented two peaks during the forward scan, where Pt only had one peak. This is consistent with results obtained by Shen *et al*. (2010) on Pt/C and Rh/C electrodes and may be an indication of a different mechanism operating on the two catalysts studied.

3.3.1.2.3. Comparison between Rh and Pt for 0.1 M KOH and 1 M KOH

An important similarity for Pt in both cases (1 M KOH and 0.1 M KOH) is that the reverse sweep shows current densities very close to the current density of the forward sweep below a certain potential. For 1 M this can be seen at potentials lower than -0.2 V and for 0.1 M at potentials lower than 0.0 V. This was also observed in the study by Lai & Koper (2009) on Pt in alkaline electrolyte solutions. They mentioned that possible explanations for this might be that for alkaline solutions the oxidation of adsorbed species did not play a significant role during the EOR. When considering the results for Rh, it is clear that this effect is not present, since for the 1 M KOH electrolyte solution no backward peak is even present and for the 0.1 M KOH electrolyte solution the peak in the reverse sweep is at completely different potentials than in the forward sweep, which may indicate that a different reaction occurs during the backward sweep. This may possibly be the oxidation of adsorbed intermediate species formed during the oxidation of EtOH during the forward sweep. Lai & Koper (2009) also mentioned that a significant part of the current density on Pt might be due to the formation of acetate as product which did not adsorb strongly on the surface. This might indicate that on Rh the acetate species were not formed and a more complete oxidation towards CO_2 as final product might occur. This is a confirmation of observations made from the values of i_f/i_b for Rh and Pt where it was said that adsorbed species were not completely oxidized by Pt or did not play a significant role during the reaction.

Furthermore, for Pt, the peak potential shifts to more positive values in the 1 M KOH electrolyte solution. The current density also reaches much higher values in the 0.1 M KOH solution compared to the 1 M KOH solution. During the backward scan, the same behaviour is observed as for 1 M KOH, where the oxidation is resumed at the potential where surface reduction occurs up to a potential where the surface is fully reduced. For Rh, in 0.1 M KOH electrolyte, the surface is not blocked to the same extent than in the 1 M KOH electrolyte solution (seen from suppression of hydrogen adsorption/desorption peaks) and much better activity is therefore observed. This may be due to adsorption of species present in the electrolyte solution, i.e. the intermediate species formed during the EOR that adsorbs onto the surface. Another possibility is higher adsorption of OH^- due to the higher concentration of electrolyte. Further investigation will have to be conducted to be able to confirm this, but will not be included here since this is only a simple comparison of Rh and Pt for different reactions.

From these results it can be seen that adsorbed species formed during the oxidation of EtOH play a more significant role on Rh than on Pt.

3.3.2. Rotating disk electrode (RDE) experiments

3.3.2.1. Acidic electrolyte

Although Rh showed activity toward the EOR (see Figure 3.5) in acidic electrolyte solutions, the current obtained was so low that no increase in current density could be observed with increasing rotation rate during RDE experiments. Therefore, the increase in transport of EtOH to the surface of the electrode could not enhance the reaction with increase in rotation rate. Some rotation rates for Rh are shown to demonstrate that its activity was too low in order for a proper RDE analysis to be conducted. Only 900 and 1600 rpm results are shown, together with 0 rpm to illustrate the effect of increased rotation rate.

It can be seen that when the electrode is rotated, the current density of the first peak decreases with no difference being observed in the second peak. The current densities of both peaks stay unchanged as the rotation rate is increased even further. The initial decrease in the current density of the first peak could be due to species being transported away from the surface as the electrode is rotated due to low adsorption products formed during the oxidation of EtOH or of EtOH itself (Hayes *et al.*, 2008). EtOH that does not adsorb very strongly is then transported away from the surface due to the rotation of the electrode.

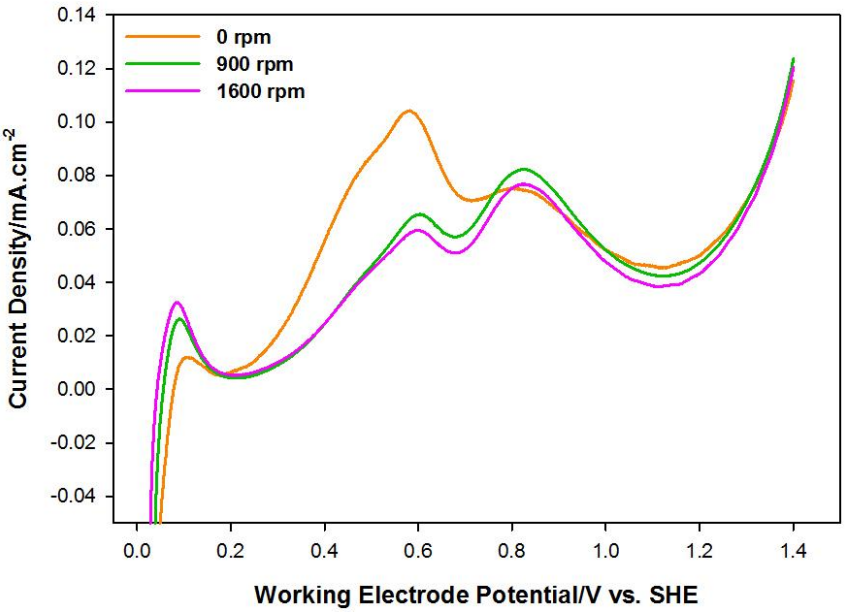

Figure 3.5: RDE experiments on Rh in 0.1 M $HClO_4$ containing 1 M EtOH at a scan rate of 10 $mV.s^{-1}$

The low activity of Rh in acidic electrolyte solutions may be due to the already mentioned poor adsorption of EtOH and intermediate species formed during oxidation of EtOH. Pt showed good activity toward the EOR in acidic electrolyte, but the RDE experiments will not be included here since a comparison of Rh and Pt cannot be made as RDE experiments on Rh could not be completed.

In comparison with Pt, Rh exhibited very limited catalytic activity toward the EOR in acidic electrolyte (as seen in CV results in Section 3.3.1). Therefore, Rh alone does not prove to be a promising catalyst for the EOR in acidic electrolyte when compared to Pt

3.3.2.2. Alkaline electrolyte

Levich and K-L analyses were attempted (at different rotation rates) to determine the number of electrons transferred, as well as the kinetic current density so as to conduct a Tafel analysis and to compare Tafel slopes.

3.3.2.2.1. 1 M KOH and 1 M EtOH

The results for the RDE experiments in 1 M KOH electrolyte solutions containing 1 M EtOH can be seen in Figure 3.6.

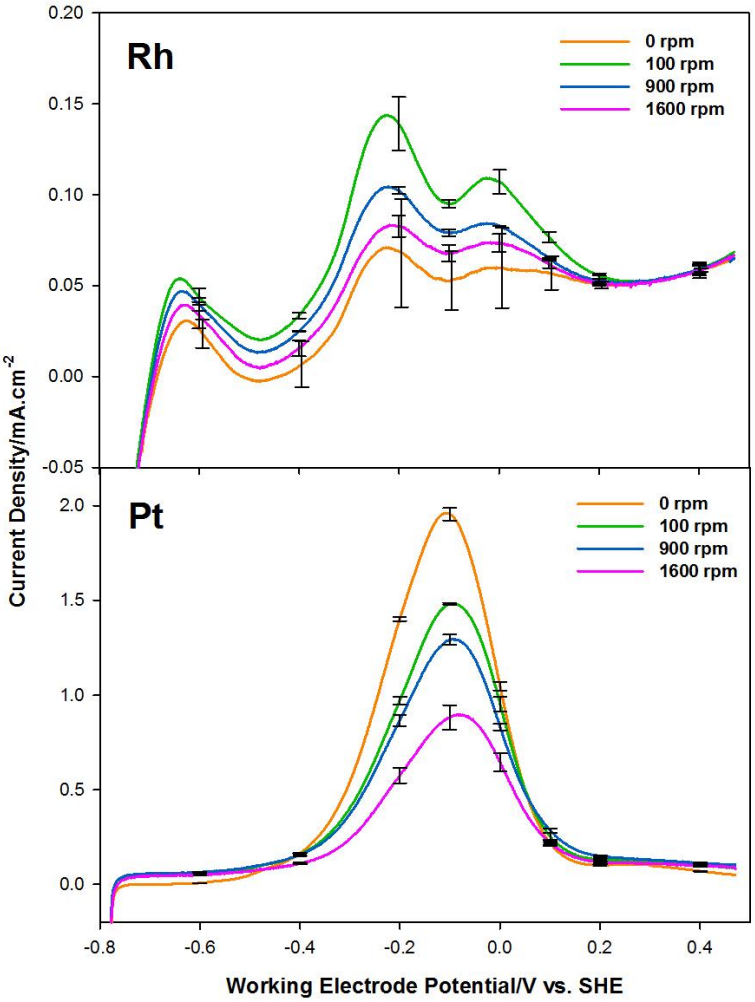

Figure 3.6: RDE experiments on Rh and Pt in 1 M KOH containing 1 M EtOH at a scan rate of 10 mV.s^{-1}

Good reproducibility of results is observed for Rh and Pt, with the exception of 0 rpm (for Rh) which does not seem to be very reproducible. For both catalysts a clear trend could be observed during RDE studies. This is, however, not the expected trend where an increase in current density is seen with an increase in rotation rate as species are transported to the surface to be oxidized, but the exact opposite. A decrease in current density is observed with an increase in rotation rate for both Rh and Pt. Rh exhibits an initial increase in current density, which suggests that by rotating the electrode an increase in adsorption of species is seen. However, when going to even higher rotation rates, a decrease in the current density is seen, like that for Pt. This is due to the EtOH and products of EtOH oxidation being transported away from the surface as the rotation rate is increased due to low adsorption of these species. This trend was also observed by Hayes *et al*. (2008) during a study of the methanol oxidation reaction on Pt where they also observed a decrease in current density with an increase in rotation rate. They ascribed this to reaction intermediates being swept into the bulk electrolyte due to rotation of the electrode.

3.3.2.2.2. 0.1 M KOH and 1 M EtOH

Both Rh and Pt exhibited improved activity in the 0.1 M KOH electrolyte solution when the current density was taken into consideration. However, reproducibility of RDE experiments was so poor that the results obtained could not be used in any kinetic analysis or to make any conclusions. No trend of increasing current density with increasing rotation rate could be observed for Rh or Pt. The trend observed for 1 M KOH electrolyte solution could also not be observed here. The results obtained for Rh and Pt in the 0.1 M KOH electrolyte can be seen in Figure 3.7. The error only for 100 rpm is included here as illustration to the irreproducibility of the results.

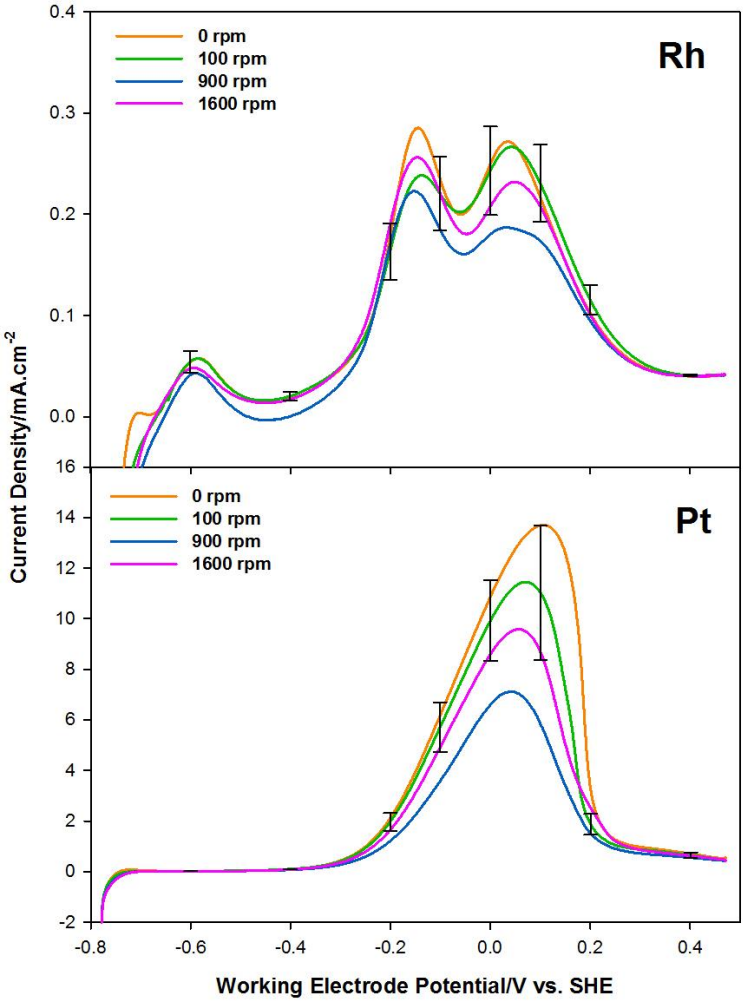

Figure 3.7: RDE experiments on Rh and Pt in 0.1 M KOH containing 1 M EtOH at a scan rate of 10 mV.s^{-1}

3.3.3. Tafel analysis

Ideally, the Tafel plots have to be drawn from the kinetic current densities obtained from K-L analysis like they were done for the ORR in Chapter 2. In this study, however, the K-L analysis could not be completed due to the results obtained from the RDE studies where an increase in current density could not be achieved with increasing rotation rate. Using the kinetic current density is ideal, since all the rotation rates are taken into consideration for Tafel plots. However, the results for 0 rpm will be used here for Tafel analyses and a comparison between catalysts will be made.

3.3.3.1. Acidic electrolyte

Tafel plots for Rh and Pt in acidic electrolytes can be seen in Figure 3.8. These plots were drawn by plotting the working electrode potential against the logarithm of the current density and the linear part of the plot is shown.

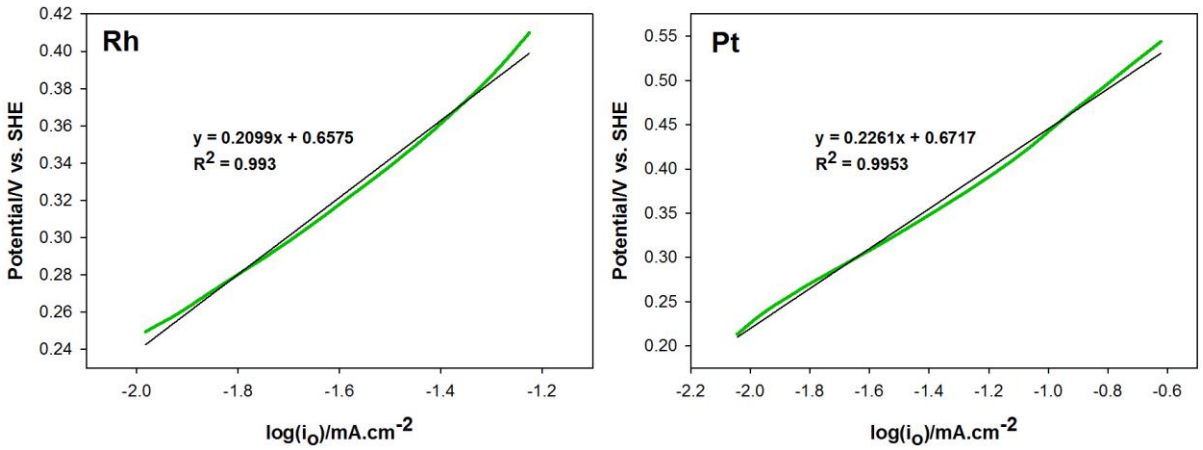

Figure 3.8: Tafel plots for Rh and Pt in 0.1 M $HClO_4$ + 1 M EtOH

It can be seen that only one Tafel slope is obtained for both Rh and Pt with 209.9 mV.decade^{-1} for Rh and 226.1 mV.decade^{-1} for Pt. The differences between the values for the two catalysts are not significant enough to indicate different reaction mechanisms operating on the two catalysts. These Tafel regions for both Rh and Pt can only be observed in a potential region before surface oxides are formed. Therefore, in acidic electrolytes, on Rh and Pt, the mechanism of the EOR is influenced by the presence of surface oxides and a similar reaction mechanism is operative on both catalysts.

3.3.3.2. Alkaline electrolyte

3.3.3.2.1. 1 M KOH and 1 M EtOH

Tafel plots for Rh and Pt in 1 M KOH electrolyte can be seen in Figure 3.9. These plots were drawn by plotting the working electrode potential against the logarithm of the current density. The linear part of the plot is shown.

It is quite clear that a different behaviour existed on Rh compared to that on Pt. Only one Tafel slope could be obtained on Rh, whereas Pt exhibited two Tafel slopes. The Tafel slope obtained for Rh was 165.1 mV.decade^{-1} and the Tafel slopes on Pt were 123.1 mV.decade^{-1} (in a lower potential region) and 192.4 mV.decade^{-1} (in a higher potential region).

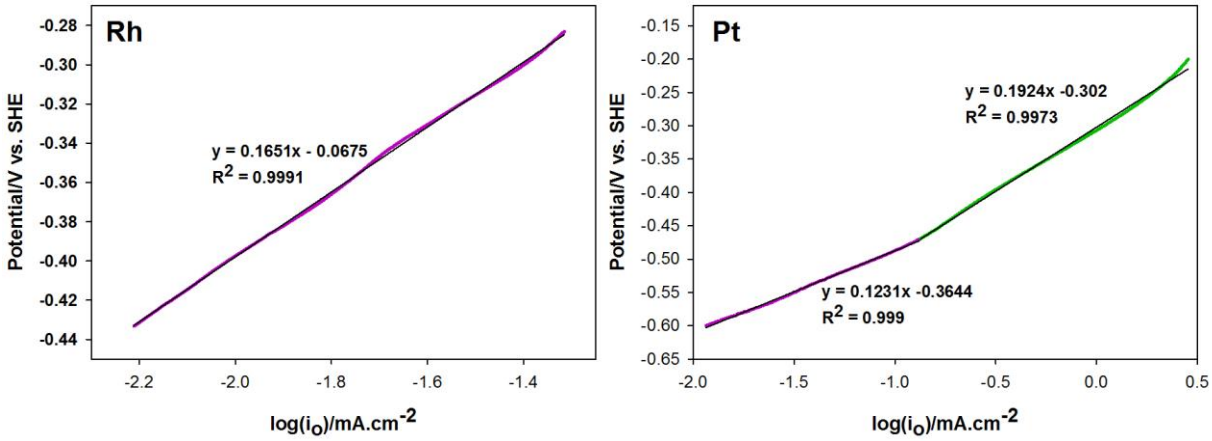

Figure 3.9: Tafel plots for Rh and Pt in 1 M KOH + 1M EtOH

For Rh, the Tafel slope observed is already in the potential region where surface oxide has started to form. This may be due to the low onset potential of the formation of Rh oxide on the electrode surface. Therefore, only one reaction mechanism can be present on the Rh surface since only one Tafel slope is present. For Pt, both Tafel slopes are present in a potential region where no surface oxide is present. The Tafel slope increases as the potential is taken to higher values, which is an indication of a different mechanism operating at higher potentials. This may be an indication that different reactions are taking place on a Pt electrode.

3.3.3.2.2. 0.1 M KOH and 1 M EtOH

Tafel plots for Rh and Pt in 0.1 M KOH electrolyte will not be included in this study due to the irreproducibility in this concentration of electrolyte, since any results and values obtained will then be unreliable.

3.4. CONCLUSIONS

3.4.1. Acidic electrolyte

In an acidic electrolyte solution, Rh showed a lower onset potential compared to Pt (0.2 V for Rh vs. 0.3 V for Pt) which indicates that the reaction was initiated earlier than on Pt. Lower peak potentials are also observed on Rh which may be an indication that the reaction took place earlier. But due to the very low current densities achieved by Rh, it is not suitable for use as a catalyst for the EOR since this is an indication of very slow reaction kinetics. It may be of use when employed as co-catalyst together with Pt due to its lower onset and peak potentials.

3.4.2. Alkaline electrolyte

In general, higher current densities were achieved on Rh and Pt in 0.1 M KOH electrolyte solution than in the 1 M KOH electrolyte solution with a shift in the peak potentials to more positive values in the higher concentration of electrolyte. However, the results obtained in the 0.1 M KOH electrolyte solution were much less reproducible than the results obtained in the 1 M KOH electrolyte solution. These differences might be due to the presence of strongly adsorbed intermediate species present in the different concentrations of electrolyte solutions.

For the 0.1 M electrolyte solution, Pt showed a lower onset potential than Rh (-0.32 V for Rh vs. -0.4 V for Pt). Therefore, the reaction was initiated earlier on Pt than on Rh. Rh showed lower peak potentials although with much lower current densities, which indicate slower reaction kinetics. A higher i_f/i_b ratio on Rh suggested that a more complete reaction occurred than on Pt, as well as that adsorbed species played a more significant role on Rh than on Pt. These findings confirm that Rh shows promise for use as a co-catalyst to enhance the behaviour of Pt for the EOR.

For the RDE results, Rh and Pt showed a decrease in current density as the rotation rate was increased which might be an indication that the active species were being transported away from the surface with rotation of the electrode. However, Rh showed an initial increase in

current density which might be an indication that more adsorption occurred initially than on Pt, with these species swept away from the surface at higher rotation rates. This can be confirmed in further studies by means of rotating ring disk electrode studies.

From Tafel analysis, one Tafel slope was obtained on Rh (165.1 mV.decade^{-1}) and two Tafel slopes were obtained on Pt (123.1 mV.decade^{-1} and 192.4 mV.decade^{-1}) which is an indication that different mechanisms operated on the two catalysts with multiple reactions possibly occurring on Pt.

4 The electro-oxidation of SO_2 on polycrystalline Rh and Pt as catalysts

4.1. LITERATURE

4.1.1. Background

4.1.1.1. The HyS process

The world's current energy sources consist mainly of fossil fuels which contribute largely to global warming. There also exists a fear of the depletion of fossil fuels in the near future. Another source of energy has to be found that is not only environmentally friendly but also renewable. Hydrogen is a very promising energy carrier since it has a high energy of combustion and the only by products formed are water and oxygen. The production and storage of hydrogen are still problems that need attention due to the high cost thereof.

The hybrid sulphur (HyS) cycle is a thermochemical cycle for the production of hydrogen for which the net reaction is the splitting of water into hydrogen and oxygen. During this process, sulphuric acid is decomposed thermally (via nuclear or solar heat sources to produce SO_2) and an acid electrolyser employs electrical energy to oxidise SO_2 electrochemically to produce H_2 and O_2, hence the hybrid cycle (Gorensek *et al.*, 2009). Figure 4.1 shows schematically the working of the hybrid sulphur process.

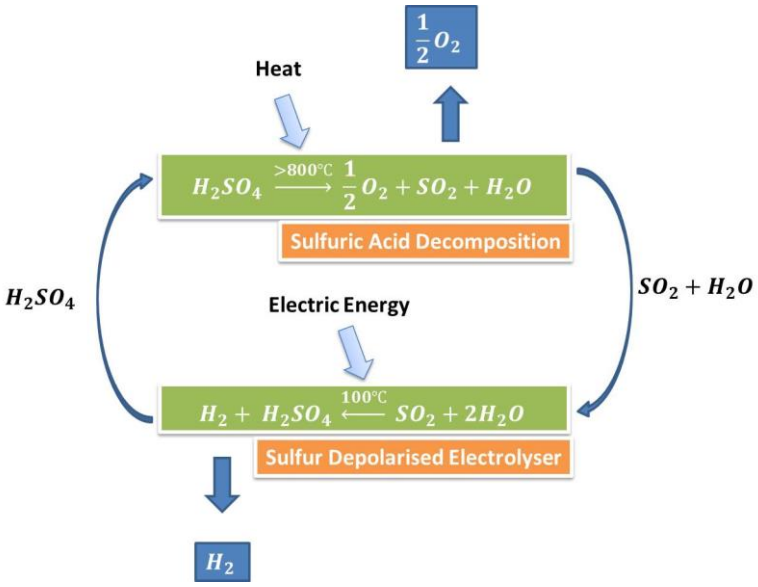

Figure 4.1: Schematic representation of the hybrid sulphur process (Gorensek & Summers, 2009)

Sulphuric acid is decomposed at high temperatures (±800˚C) to give SO_2 and O_2, after which the SO_2 is separated from the O_2, combined with H_2O and recycled H_2SO_4. This mixture is then fed to the anode where the SO_2 is oxidised to H_2SO_4 and H^+ inside a sulphur depolarised electrolyser (SDE). The H_2SO_4 is recycled and used again during the decomposition step.

The complete oxidation to hydrogen occurs via two steps and at the following standard electrode potentials inside the SDE:

Anode	$SO_{2(aq)} + 2H_2O \rightarrow H_2SO_4 + 2H^+ + 2e^-$	$E^0 = 0.158V\ (vs.SHE)$	(29)
Cathode	$2H^+ + 2e^- \rightarrow H_{2(g)}$	$E^0 = 0.0V\ (vs.SHE)$	(30)

These formed protons migrate through a proton exchange membrane (PEM) to the cathode of the SDE, where it undergoes reduction to form H_2 gas (see Figure 4.2).

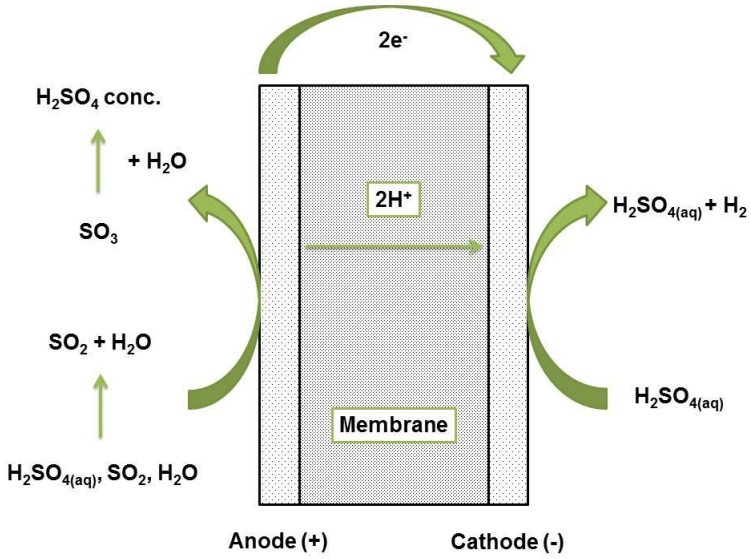

Figure 4.2: Schematic representation of the sulphur depolarized electrolyser (SDE)

The oxidation of SO_2 for use in hydrogen production is worth studying, since if compared to normal water electrolysis (E^0 = 1.23V (vs. SHE)) it is seen that SO_2 oxidises to form protons at a much lower overpotential (E^0 = 0.158V (vs. SHE)).

The most important factor for the development of the HyS process is to improve the efficiency of the electrolyser. A performance of 500 mA.cm^{-2} is the ideal current density to be achieved at an overpotential of 0.6 V (Gorensek & Summers, 2009). Thus far, the highest performance reached, has been a current density of 200 mA.cm^{-2} (O'Brien *et al.*, 2010). It was also noted that most of the overpotential responsible for the low performance of the electrolyser, arose from the reaction at the anode (where SO_2 oxidation takes place). A few studies have been

done in order to determine the effect of different anode catalysts on the overpotential of the reaction and it was found that, in the presence of noble metals (in particular Pt), the reaction was enhanced when compared to carbon materials (O'Brien *et al.*, 2010).

Catalysts, studied for the oxidation of SO_2, include Pd, Pt, Al and Au. Of these, Pt and Au have received the most attention. During various studies by Quijada *et al.* (Quijada *et al.*, 2000) (Quijada *et al.*, 1995) (Quijada *et al.*, 2000) on Au, they found that it was more active than Pt and much higher current densities were reached. This is due to different mechanisms that operate on Pt and Au.

4.1.1.2. Cleaning of waste gases from industries that contain SO_2

SO_2 gas released into the atmosphere by industries using fossil fuels is an increasing concern, since it contributes to pollution and is also responsible for acid rain. The importance of cleaning these waste gases that industries produce has stimulated research into possible cleaning techniques and this is where the SO_2 oxidation reaction comes into play. The oxidation of SO_2 to form sulphuric acid can be implemented to reduce SO_2 in air, with the resultant sulphuric acid recycled.

4.1.2. Sulphuric acid concentration

Struck *et al*. (1980) reported that a decrease in current density was observed with an increase in sulphuric acid concentration and they proposed that in order to achieve proper catalytic activity, a sulphuric acid concentration of less than 60 wt.% would have to be used. The same was observed by Scott & Taama (1999) during a study of the anodic oxidation of SO_2 and they reported a decrease in current density with an increase in sulphuric acid with 0.5 M sulphuric acid giving the highest current density (compared to 3 and 5 M).

Therefore, an appropriate sulphuric acid concentration has to be chosen, since it has the ability to influence the SO_2 oxidation reaction since the presence and behaviour of adsorbed species have such an important role to play. Another aspect that is significant when choosing the correct sulphuric acid concentration is the solubility of SO_2 since the gas will be dissolved in sulphuric acid. The solubility of SO_2 differs in different sulphuric acid solutions.

4.1.3. Cyclic voltammetry

Cyclic voltammetry results obtained by various authors in the literature will be discussed briefly together with general trends found. As discussed in the review done by O'Brien *et al.* (2010), most authors found that the SO_2 oxidation reaction occurred in two regions in the potential range studied. The first of which was in the double layer region of the catalyst and the second occurred in the potential range where electrode surface oxides were formed.

Seo & Sawyer (1965) mentioned the presence of two types of oxidation occurring on Pt and Au electrodes, the first of which was a pure electron-transfer reaction that occurred in the double-layer region where no surface oxides were present and the second of which was in the potential range of surface oxidation, where a chemical reaction occurred between a surface oxide species and the electrolyte. Spotnitz *et al.* (1983) also reported two processes occurring on smooth Pt electrodes in the same two potential regions as already mentioned above. They called an electrode on which the peak in the double-layer region was visible an 'activated' electrode. They investigated the effect of different lower and higher potential limits and showed the influence when starting scans at low potential values and attributed the effect to adsorbed sulphur species, as will be discussed in the following section. The effect of changing the higher potential limits could be seen during the reverse sweeps at low potentials where reduction peaks were present. Quijada *et al.* also mentioned the presence of two regions of oxidation on Pt and Au electrodes in various studies ((Quijada *et al.*, 2000), (Quijada *et al.*, 1995 a), (Quijada *et al.*, 1995b) (Quijada *et al.*, 1996)). They showed the effects of different potential, especially the effect of different lower potential values and these will also be discussed in the following section.

It is, however, important to note that there is general agreement among all these studies about the regions where SO_2 oxidation takes place, and the effect that different polarization scenarios have on these two regions of oxidation.

4.1.4. Influence of adsorbed species

4.1.4.1. Adsorbed sulphur species

Adsorbed sulphur is formed when SO_2 is reduced at low potentials according to the following reaction:

$$SO_2 + 4H^+ + 4e^- \rightarrow S + 2H_2O \quad \left| \quad E^0 = 0.45\ V\ (vs\ SHE) \right. \quad (31)$$

This may have an influence on the oxidation of SO_2, since it may form in the same potential region where SO_2 oxidation occurs. In the study done by Spotnitz *et al.* (1983) on the electro-oxidation of SO_2 on Pt, they reported that two processes were involved, with the first being described as oxidation on an 'activated' electrode and the second overlapping with electrode surface oxidation. The formation of the surface oxide eventually inhibited the reaction. They found that the mentioned activation of the electrode of the oxidation reaction was due to the formation of a species at potentials lower than 0.1 V, i.e. sulphur formation. When the potential moved into the region of surface oxidation, accumulation of sulphur was prevented since the adsorbed sulphur would be oxidised. The extent of the sulphur coverage achieved depended on the time spent at potentials lower than 0.1 V. However, at a certain point an optimum amount was reached and above that amount of coverage the reaction would be inhibited.

A number of years later Quijada *et al.* (1995b and 1996) also investigated the effect of adsorbed sulphur species on the SO_2 oxidation reaction on Pt electrodes. The earlier study (Quijada *et al.*, 1995) included a study of the effect of adsorbed sulphur by looking at different lower potential values and the effect on the SO_2 oxidation reaction. They also found that the presence of adsorbed sulphur enhanced the reaction and that an excess amount influenced the reaction negatively of both the oxidation and reduction of bulk SO_2. Something that they mentioned that was important was the fact that when doing SO_2 oxidation reaction studies, both the processes present in the bulk phase, as well as the behaviour of adsorbed species, should be accounted for. The following study by the same authors (Quijada *et al.*, 1996) further investigated the effect of adsorbed sulphur on the oxidation of SO_2 and followed three different methods to deposit sulphur onto the electrode's surface. They observed different coverages formed by the different methods and the effect on the oxidation reaction. It was reported that when θ_s was lower, with an inevitably higher θ_{SO_2}, the reaction was inhibited since more surface sites were available for the adsorption of SO_2 and the negative effect too much adsorbed SO_2 had on the reaction. They further concluded that adsorbed sulphur enhanced the SO_2 oxidation reaction (most enhancements are found at the bilayer level) but excessive sulphur deposition, however, led to loss of catalytic activity.

In 1975 Samec & Weber studied the SO_2 oxidation reaction on Au and found that as for Pt, the presence of adsorbed sulphur (reduced SO_2) species had an enhancing effect on the reaction ((Samec & Weber, 1975a), (Samec & Weber, 1975b)). They proposed that two forms of adsorbed SO_2 were present, one of which was strongly adsorbed SO_2, the other was weakly adsorbed SO_2. The presence of reduced SO_2 inhibited the strong adsorption of SO_2 and in turn better oxidation could occur, since too much adsorbed SO_2 hindered the reaction.

Seo & Sawyer mentioned two processes occurring during the oxidation of SO_2, the one being pure electron transfer and the other chemical oxidation involving metal oxide during oxidation (Seo & Sawyer, 1965)

Two studies were done by Quijada *et al.* (2000) on the SO_2 oxidation reaction on Au and the effect of adsorbed sulphur ((Quijada *et al.*, 2000a), (Quijada *et al.*, 2000b)). In the first study they formed sulphur adlayers in a single cycle by varying the lower potential value during the following cycle: 0.5 V < E_{LOW} < 0.55 V. By varying the lower potential value, the amount of coverage reached could be controlled. In the later study these authors investigated the effect of different sulphur coverages in more detail. Sulphur was adsorbed onto the Au surface similar to what has been described above, and then characterized in the absence of SO_2 and it was shown that the adsorbed sulphur could be desorbed in one cycle. The effect that the different coverages of sulphur had on the oxidation of SO_2 was then investigated. They found that for a maximum of $\theta = 0.5$ the most enhancements could be obtained regarding the catalytic activity of Au toward the oxidation of SO_2 and this value corresponded to a monolayer of sulphur on the electrode surface.

In conclusion they found that adsorbed sulphur in certain amounts did indeed increase the catalytic activity of Au toward the SO_2 oxidation reaction.

4.1.4.2. Adsorbed molecular SO_2

The adsorption and behaviour of adsorbed molecular SO_2 are important, since they play a significant role in the SO_2 oxidation reaction and the types of adsorbed SO_2 have an influence on the reaction and the potentials at which they occur, as well as the poisoning of the electrode surface. Authors mentioned that adsorbed SO_2 could have a poisoning effect on the electrode and limited oxidation will take place.

Moraes *et al.* (1997) studied the nature of adsorbed SO_2 species on polycrystalline Pt by means of FTIR spectroscopy and found that adsorbed sulphur, as well as adsorbed molecular SO_2 was present and both could be formed in the potential where the SO_2 oxidation reaction was studied. It is important to know in which form SO_2 was present on the surface of electrodes since it would influence conclusions made.

When the influence of adsorbed SO_2 as the only sulphur species is to be studied, the formation of adsorbed sulphur on the electrode surface has to be limited. In the review done by O'Brien *et al.* (2010) they mentioned that at potentials of ~0.65 V and above SO_2 would not be reduced

to form sulphur. Therefore if a study has to be done on the SO_2 oxidation reaction in the absence of adsorbed sulphur, a potential range has to be chosen with a lower potential limit higher than 0.65 V.

Quijada *et al.* (1994) studied the SO_2 oxidation reaction on Pt (111) and focused on the behaviour of adsorbed SO_2 species. They first adsorbed SO_2 onto the electrode's surface by cycling in the following potential range: 0.65 V → 1.35 V → 0.62 V. They then went on to characterize the adsorbed SO_2 that was formed, by cyclic voltammetry in sulphuric acid solution and found that more than 6 sweeps were necessary to remove the adsorbed SO_2. They observed that the presence of adsorbed SO_2 was responsible for structural changes to the electrode's surface, like the formation of Pt (110) and Pt (100) defects. The adsorption of oxygen onto these defect sites was also responsible for the surface changes observed. They then studied the effect of sulphur-oxygen adsorbed species on the SO_2 oxidation reaction and found that the adsorption of SO_2 played an important role in the behaviour shown by Pt electrodes toward the SO_2 oxidation reaction (Quijada *et al.*, 1995). They referred to the poisoning effect that adsorbed SO_2 had on the reaction and mentioned that contrary to what had been stated in literature, that SO_2 was a poisoning agent and not dithionate. They stated that a prewave (at about 0.85 V) was present in cyclic voltammetry experiments that was increased when the lower potential limit was decreased (at potentials lower than 0.65 V) until another peak was formed. This second peak was usually present when adsorbed sulphur was formed during the reduction of SO_2 at lower potentials. The authors made the conclusion that SO_2 was responsible for surface poisoning, since the presence of adsorbed sulphur might block sites that had previously been occupied by SO_2 and the adsorbed sulphur was able to facilitate better the oxidation of bulk SO_2. During a study done on Au, they reported that a possible reason for the better performance of Au toward the SO_2 oxidation reaction when compared to Pt might be due to the lack of the ability of SO_2 to strongly adsorb onto a Au surface (Quijada *et al.*, 2000). The presence of adsorbed sulphur was, however, able to enhance the SO_2 oxidation reaction on Au.

The adsorption of SO_2 onto catalyst's surfaces is an important factor that has to be taken into account when studying the SO_2 oxidation reaction, since adsorbed sulphur can be formed at low potentials with an enhancing effect on the reaction. Adsorbed molecular SO_2 is also important, since it can alter the surface of the electrode which will influence the reaction or be responsible for electrode surface poisoning.

4.1.4.3. Surface oxides

At high potentials, metal electrodes are oxidised to form an oxide species that may adsorb onto the surface of the electrode. These metal oxides compete with the bulk electrolyte for surface sites and it is necessary to include the effect these oxide species has on the SO_2 oxidation reaction, since they may play an important role during the reaction and can have an enhancing (may facilitate electron transfer) or an inhibiting effect (may limit surface sites available for adsorption) on the catalytic effect of the catalyst.

Seo & Sawyer (1964) mentioned that an electrode surface stripped of its surface oxide species was desired when an activated surface was required. They then studied the oxidation of SO_2 on Au and Pt and mentioned that the oxidation process occurred via pure electron transfer, as well as electrochemical oxidation by the formed electrode surface oxide species (Seo & Sawyer, 1965) and that repeated oxidation and reduction of the metal surface activated the electrode.

Spotnitz *et al.* (1983) showed that the reduction of surface species was not responsible for activation of electrode, but by varying the higher potential value they showed that it was important to go up to sufficiently high potentials in order to remove adsorbed sulphur species that had formed at low potentials. The removal of surface oxide species, however, was not necessarily responsible for the mentioned activation associated with the peak in the double layer region, since studies had shown, as already discussed, that variation in the lower potential value had an enhancing effect on adsorbed species formation. The fact that the oxidation of SO_2 took place in the potential region where surface oxides formed, made it necessary that the involvement of metal oxides had to be taken into consideration.

The general reaction when SO_2 oxidation takes place on an electrode surface covered with oxide has been proposed by Korzeniewski *et al.* (1987):

$$2SO_{2(ads)} + Pt + 3H_2O \rightarrow SO^{2-}_{4(ads)} + 2H_3O^+ + Pt$$

Appleby & Pinchon (1979) also proposed that the second peak present on cyclic voltammograms was related to oxidation of SO_2 by an adsorbed oxygen species and their experiments also showed the inhibition in the current density at high potentials where the reaction was eventually limited as can be seen in many studies (O'Brien *et al.*, 2010). Most authors explained this by the formation of a metal oxide that covered the surface and hindered the adsorption of bulk SO_2.

Quijada *et al.* (1995) proposed that at the potential where the surface oxide species were initially formed, the oxidation of SO_2 could proceed by charge transfer via the free Pt sites. When the surface was completely covered in adsorbed oxide, the reaction was inhibited.

Where Au is concerned, the surface oxidation occurs at very high potentials and it can be seen very clearly that at the onset of surface oxidation the reaction is inhibited and that during backward sweeps the oxidation of SO_2 is resumed at the potential where the surface is reduced (O'Brien *et al.*, 2010).

The behaviour and influence of electrode surface oxides are not completely understood, but the effect it has on the SO_2 oxidation reaction cannot be ignored. Especially, since if only Au and Pt are compared, on each metal the surface oxides influence the reaction differently. The stability and onset of surface oxide formation will not be the same for each catalyst, and the effect it has on each will differ and has to be taken into consideration when deciding on the experimental parameters.

4.1.5. Focus of the study

Since no studies have been reported in the literature on polycrystalline Rh, all these factors mentioned above have to be taken into consideration when looking at the activity of Rh compared to Pt. The influence of reduced SO_2 species (adsorbed sulphur), as well as adsorbed molecular SO_2, has to be taken into consideration. An appropriate preconditioning method has to be found for Rh, since this may differ considerably from catalysts studied in the literature (which include mainly Pt and Au).

As the ultimate aim was to electro-oxidise dissolved SO_2 gas emitted from a plant stack, for example, initial experiments were carried out whereby SO_2 gas was bubbled through sulphuric acid (0.5 M) solutions for 30 minutes prior to each run. Some experiments were, however, also conducted employing the dissolution of Na_2SO_3 salt in sulphuric acid, whereby SO_2 gas was produced 'in situ', so as to be able to compare the data obtained with that from literature, which largely reported on the use of Na_2SO_3 salt in sulphuric acid. This reaction can be represented as follows:

$$Na_2SO_3 + H_2SO_4 \rightarrow SO_{2(g)} + H_2O + Na_2SO_4$$

CV experiments will be used firstly to investigate the influence of different starting potentials, since adsorbed sulphur that is formed at lower potentials from reduction of SO_2 may enhance

the reaction. From this investigation, an appropriate starting potential will be chosen from onset potentials, peak potentials and peak current densities obtained for further experiments.

LP experiments will be conducted employing a rotating disk electrode (RDE) during which different rotation rates will be investigated so as to conduct a kinetic analysis for the catalysts. K-L, Levich and Tafel analysis techniques will be employed to calculate the number of electrons transferred, kinetic current density, as well as the Tafel slope. Onset potentials and peak current densities will also be used to be able to compare the activity and kinetics of the two catalysts toward the SO_2 oxidation reaction.

4.2. EXPERIMENTAL

4.2.1. Electrochemical setup

A standard three electrode setup was used in the electrochemical experiments (see Figure 2.6 in Chapter 2). The working electrodes were Rh or Pt rotating disk electrodes (Pine instruments). The counter electrode was a Pt wire and the reference electrode a saturated Calomel (0.241 V vs SHE) electrode. All potentials referred to in this study are given versus the Standard Hydrogen Electrode (SHE). A potentiostat (Bio Logic science VSP instrument) was used to control the potential on the working electrode. All experiments were carried out at 25 ˚C and atmospheric pressure. A Julabo F12 temperature controller was used to regulate the temperature of the electrochemical cell.

The XRD graphs for the Rh and Pt working electrodes can be seen in Figure 2.7 in Chapter 2 where the polycrystallinity of the catalysts was confirmed.

4.2.2. Preconditioning procedures

Preconditioning of the electrodes is extremely important to ensure reproducible results. A suitable procedure was established by a series of experiments during which the reproducibility of a combination of preconditioning procedures was tested (a combination of CV and CA experiments). The best preconditioning procedure was found to be as follows: Electrode was first polished using 5.0 µm and then 0.05 µm alumina polishing solutions. Electrode was then sonicated in ultrapure water for 5 minutes and thereafter rinsed with water and dried, using a nitrogen stream. A CV was then carried out on the electrode in 0.5 M H_2SO_4 solutions (98%

Merck) electrolytes in the potential range -0.06 V < E < 1.74 V to electrochemically clean the electrode. The end potential was chosen high enough to be able to completely oxidise any possible sulphur species or other intermediate species formed during the reaction that might be adsorbing strongly to the surface. 20 cycles were done at a sweep rate of 50 $mV.s^{-1}$ on each electrode to ensure that the surfaces were the same each time before an experiment was done. For both Rh and Pt, it was found that another set of polishing and cyclic voltammetry might be needed in order to completely restore the electrode to its original state and remove all adsorbed species.

This whole procedure was done prior to each run.

4.2.3. Comparison between electrolyte saturated with SO_2 gas and sodium sulfite

Experiments were carried out in sulphuric acid (0.5 M) solutions saturated with SO_2 gas (Afrox) by bubbling for 30 minutes prior to each run. The exact same was also done in a sulphuric acid (0.5 M) solution to which a 0.1 M Na_2SO_3 solution was added prior to each run, in order to achieve a concentration of 0.1 M SO_2 in the electrolyte solution. The sulphuric acid solution was deaerated by bubbling nitrogen for 10 minutes prior to adding the appropriate amount of Na_2SO_3 solution just before the experiment was run.

4.2.4. Variation of lower potential value (E_{LOW})

CV experiments were done at a sweep rate of 10 $mV.s^{-1}$ with different lower potential limits (0.5 M H_2SO_4), since from literature it was evident that species formed at low potentials influenced the oxidation reaction and had the ability to enhance the oxidation of SO_2. These different starting potentials were done on Rh and Pt in order to determine the one most suited for further studies (RDE experiments). The different potentials that were used in this study were as follows: 0.0 V, 0.1 V, 0.2 V, 0.3 V and 0.4 V.

4.2.5. Rotating disk electrode (RDE) experiments

From the CV results obtained by varying the starting potential, a suitable potential was chosen as the ideal starting potential for the reaction (0.3 V for Rh and 0.1 V for Pt). This potential was chosen for Rh since it showed a well-defined peak and also had a higher current density than 0.4 V. The peak potential was also the lowest of all the different starting potentials. For Pt, 0.1 V showed the highest current density with acceptable reproducibility.

Different rotation rates were studied for use in Levich- and Koutecky-Levich analysis. These experiments were also carried out in 0.5 M H_2SO_4 containing either saturated SO_2 (obtained by bubbling pure SO_2 gas) or 0.1 M SO_2 (obtained by adding Na_2SO_3 to the electrolyte). The following different rotation rates were studied: 100 rpm, 400 rpm, 900 rpm and 1600 rpm.

4.3. RESULTS AND DISCUSSION

4.3.1. Cyclic voltammetry

The CVs of clean Rh and Pt surfaces in 0.5 M H_2SO_4 can be seen in Figure 4.3.

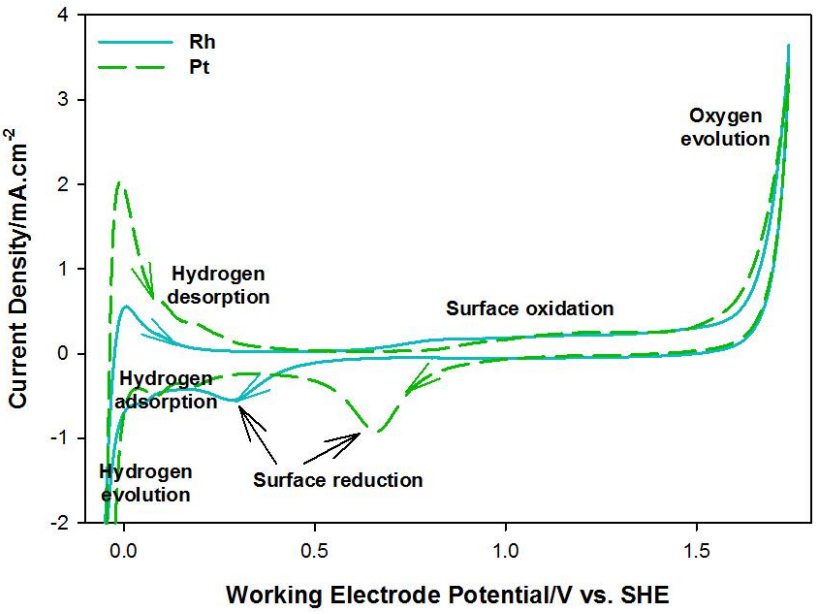

Figure 4.3: CVs of Rh and Pt in 0.5 M H_2SO_4 at a scan rate of 50 mV.s^{-1}

The typical features that could be seen on both electrodes include hydrogen evolution, hydrogen adsorption and desorption as well as surface oxidation and reduction. At high potentials, water oxidation could be observed and as already mentioned in the experimental section it was deemed necessary to go up to sufficiently high potentials to allow water oxidation in order to completely remove adsorbed sulphur species. The intensity of this feature also indicates if there are still adsorbed species present, together with inhibited hydrogen adsorption and desorption peaks. If the current density of the water oxidation is not as high as can be seen in Figure 4.3, some other species may be present that occupy surface sites that otherwise would have been employed for the oxidation of water.

4.3.2. Variation of lower potential value (E_{LOW})

From the literature survey it was evident that the potential value at which the LP is started has a significant effect on the reaction, since SO_2 is reduced at low potentials to form sulphur that adsorbs onto the electrode surface. This adsorbed sulphur species may have an enhancing effect on the SO_2 oxidation reaction. Therefore, a study of the effect of different starting potentials was included and compared on both catalysts.

4.3.2.1. SO_2 gas

The results for the different E_{LOW} values on Rh and Pt in a sulphuric acid electrolyte (0.5 M) saturated with SO_2 gas can be seen in Figure 4.4.

It could be seen that the potential at which the experiment is started, has a significant influence on the reaction. For both Rh and Pt, the current density, as well as the peak potential, was influenced. This is due to the formation of different amounts of adsorbed sulphur onto the catalysts' surfaces which influences the reaction mechanism in the sense that the current density is enhanced/inhibited and a shift in the peak potential is seen either to larger or smaller values.

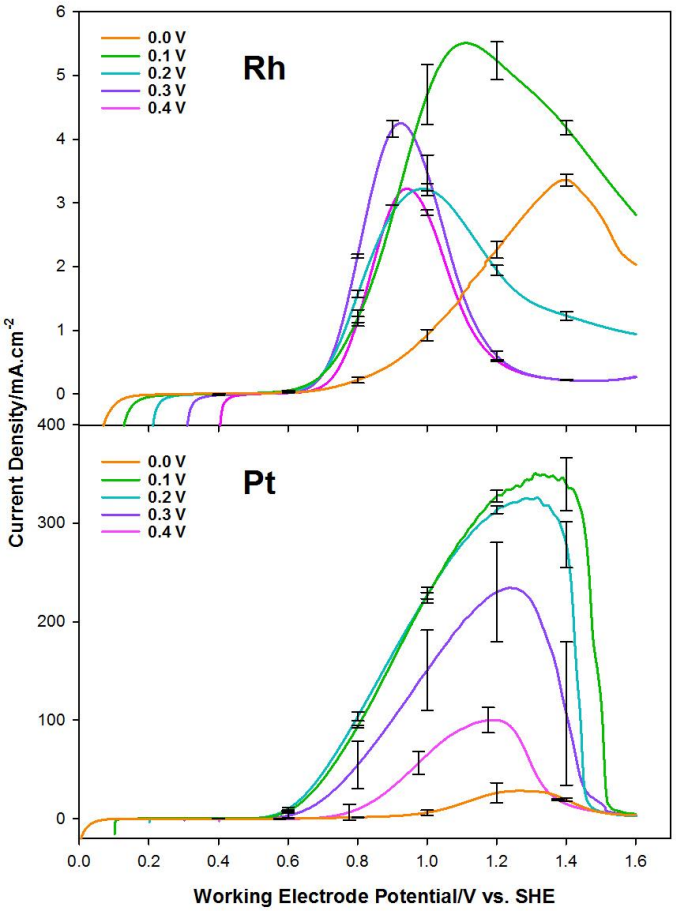

Figure 4.4: **CVs (forward sweep only) on Rh and Pt to show the influence of different E_{LOW} values on the SO_2 oxidation reaction in 0.5 M H_2SO_4 saturated with SO_2 gas at a scan rate of 10 $mV.s^{-1}$**

Figure 4.5 shows a comparison between the onset potentials and peak potentials for Rh and Pt at the different E_{LOW} values. This graph was added to aid in the decision of which starting potential to choose for use in further RDE studies.

It is clear that for Rh and Pt a decrease in onset potential can be seen with the lower E_{LOW} values, except for 0.0 V which gives the highest onset potential, probably due to excessive formation and adsorption of sulphur. When comparing the peak potentials of Rh and Pt a general decrease is seen with an increase in the E_{LOW} value, with the lowest value for both catalysts at 0.3 V.

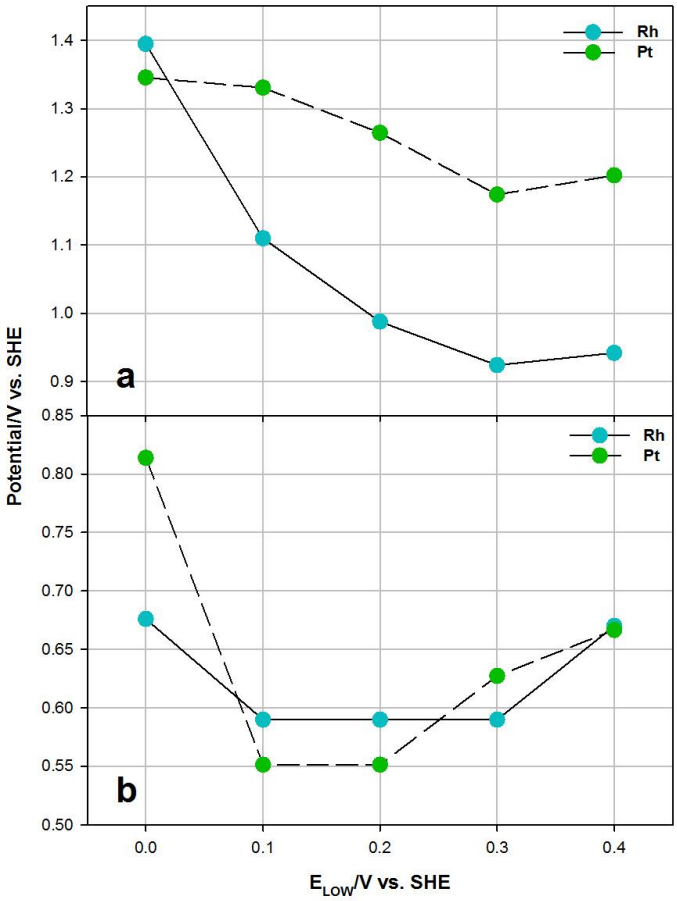

Figure 4.5: **(a) Onset potentials and (b) peak potentials on Rh and Pt corresponding to the different E_{LOW} values in the sulphuric acid electrolyte (0.5 M) saturated with SO_2 gas**

Compared to Rh, Pt shows lower onset potentials which indicates that the reaction is initiated earlier. Comparison of peak potentials reveals that Rh shows lower values than Pt. However, the much higher current density achieved by Pt is already an indication that Rh may not be a very desirable catalyst for the SO_2 oxidation reaction due to very slow reaction kinetics.

4.3.2.2. Na_2SO_3 salt

Figure 4.6 shows the CVs done on Rh and Pt at different E_{LOW} values in a sulphuric acid solution to which a 0.1 M Na_2SO_3 solution was added in order to achieve a SO_2 concentration of 0.1 M.

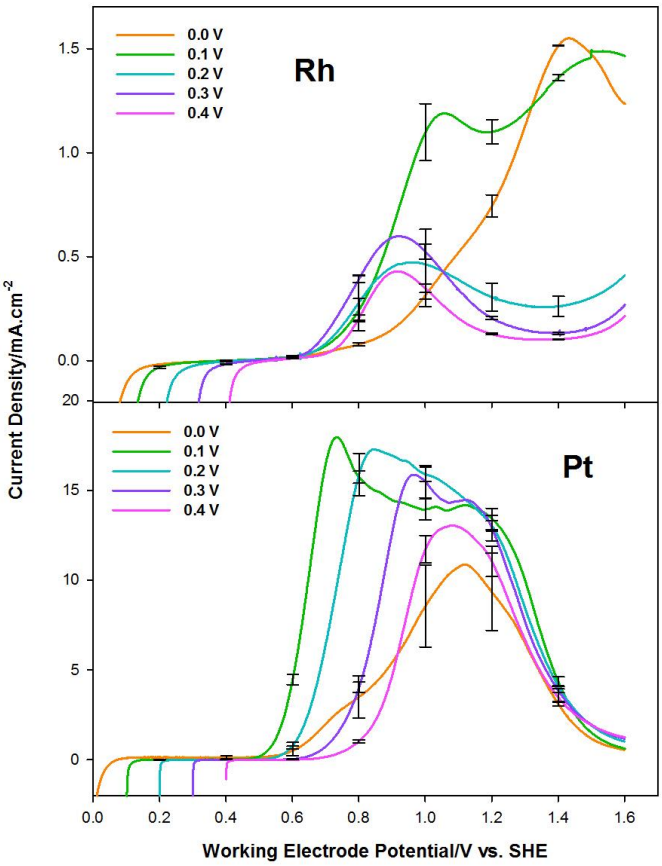

Figure 4.6: CVs (forward sweep only) on Rh and Pt to show the influence of different E_{LOW} values on the SO_2 oxidation reaction in 0.5 M H_2SO_4 containing 0.1 M SO_2 at a scan rate of 10 mV.s^{-1}

For Rh a very similar trend can be observed as when using an electrolyte saturated with SO_2 gas and the reaction occurring on Rh is extremely dependent on the value of E_{LOW}. The current density is much lower, but this may be due to a lower concentration of SO_2 present in the solution which might cause less adsorption and allow for two peaks to be formed in the two regions. The only difference worth mentioning, is that for 0.1 V when using the Na_2SO_3 salt solution, two peaks are observed instead of one. The current density of 0.0 V has also increased in comparison with the other E_{LOW} values, which may be due to less adsorption products as a result of the lower concentration of SO_2 present in the electrolyte solution while in the saturated SO_2 solution too much adsorbed sulphur may have formed which inhibited the reaction.

For Pt, however, very different behaviour is observed than when using the electrolyte saturated with SO_2 gas. Firstly, two features are observed, which correlates with literature results in that two regions of oxidation are observed, as discussed in Section 4.1.3. The first of these regions is in the double layer region and the second in the region where surface oxides are present. This is in contrast to the results obtained in the electrolyte saturated with

SO_2 gas where only one peak could be observed. The presence of adsorbed sulphur species formed from reduction of SO_2 clearly causes a peak in the double layer region as already mentioned.

As far as onset potentials are concerned, for Rh the lowest value was found at 0.2 V and for Pt, 0.1 V (see Figure 4.7).

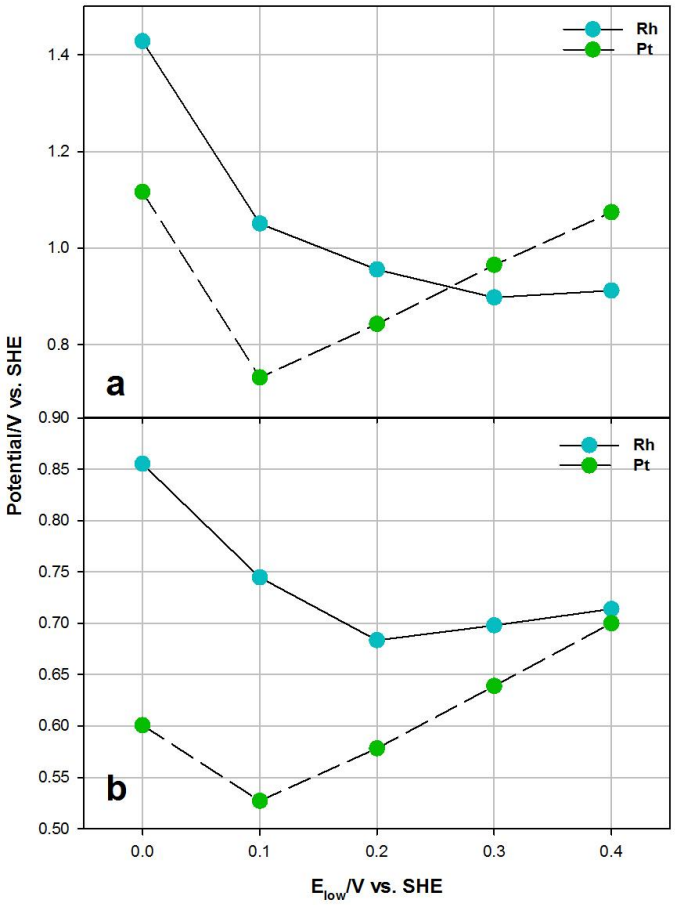

Figure 4.7: (a) Onset potentials and (b) peak potentials on Rh and Pt corresponding to the different E_{LOW} values in the sulphuric acid electrolyte (0.5 M) containing 0.1 M SO_2 from generated from Na_2SO_3

The lowest peak potential for Rh is found at 0.3 V and for Pt, again 0.1 V. The current density also decreases together with the shift in potentials as the E_{LOW} values are increased. This may be due to less formation of adsorbed sulphur species at higher potentials and less enhancement of the reaction.

In this electrolyte solution, the results obtained on Pt were much closer to what has been reported in the literature where two features are observed in two potential regions. Rh still

showed very limited activity when compared to Pt. This, together with higher onset potentials and peak potentials indicates that Rh is not suitable as a catalyst for the SO_2 oxidation reaction.

4.3.3. Rotating disk electrode (RDE) studies

Since Pt showed better results when compared to literature in the sulphuric acid solution to which Na_2SO_3 was added, only the RDE results done in this electrolyte solution will be shown.

The RDE results for Rh and Pt in a 0.5 M H_2SO_4 solution containing 0.1 M SO_2 generated by adding Na_2SO_3 just before each experiment can be seen in Figure 4.8 and 4.9. The RDE study included three E_{LOW} values which included 0.1, 0.2 and 0.3 V. The other values were not used since at 0.0 V too much adsorbed sulphur was present and at 0.4 V too little and the reaction will be inhibited at both these potentials.

As can be seen from Figure 4.8, Rh did not exhibit very good behaviour and a trend of increasing current density with increasing rotation rate was not observed for all of the E_{LOW} values. The current density did not increase significantly enough with rotation of the electrode. The highest current density was achieved at a starting potential of 0.1 V, but with a shift of the peak potential to higher values. At these values, water oxidation occurred and the currents in this potential region were not entirely from the oxidation of SO_2.

These results confirm initial observations that Rh is not suitable as catalyst for the SO_2 oxidation reaction due to low activity and complex mechanisms.

This may be due to adsorbed intermediates that form during the oxidation of SO_2, as well as poisoning of the electrode surface by adsorbed molecular SO_2, described in full during the literature survey. The lack of results that could be used for kinetic analysis on Rh might be due to the already mentioned strong adsorption of SO_2 (as well as SO_2 oxidation products) on the surface of Rh which caused poisoning of the electrode. This might cause the very low activity that was observed for Rh, as well as the limitations during RDE studies where better transport of electrolyte to the electrode surface did not make much difference in the current densities that were able to be reached.

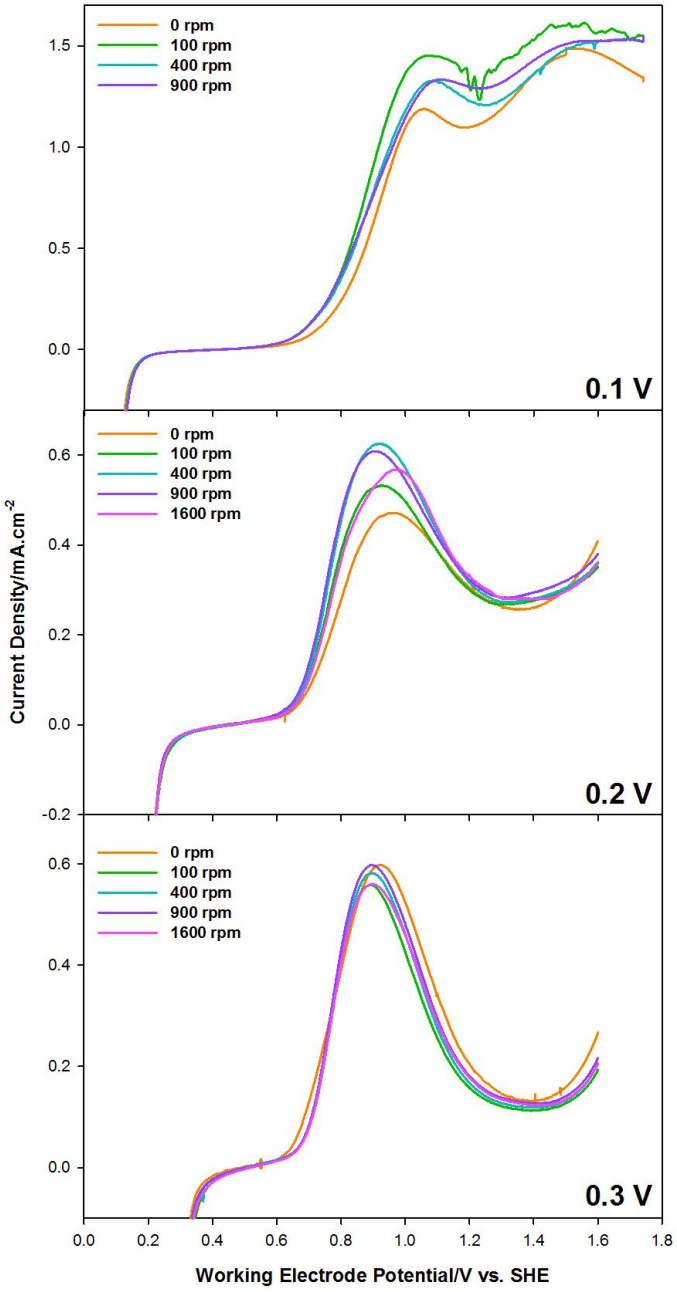

Figure 4.8: **RDE experiments on Rh in 0.5 M H_2SO_4 solution containing 0.1 M SO_2 generated from Na_2SO_3 at different rotation rates**

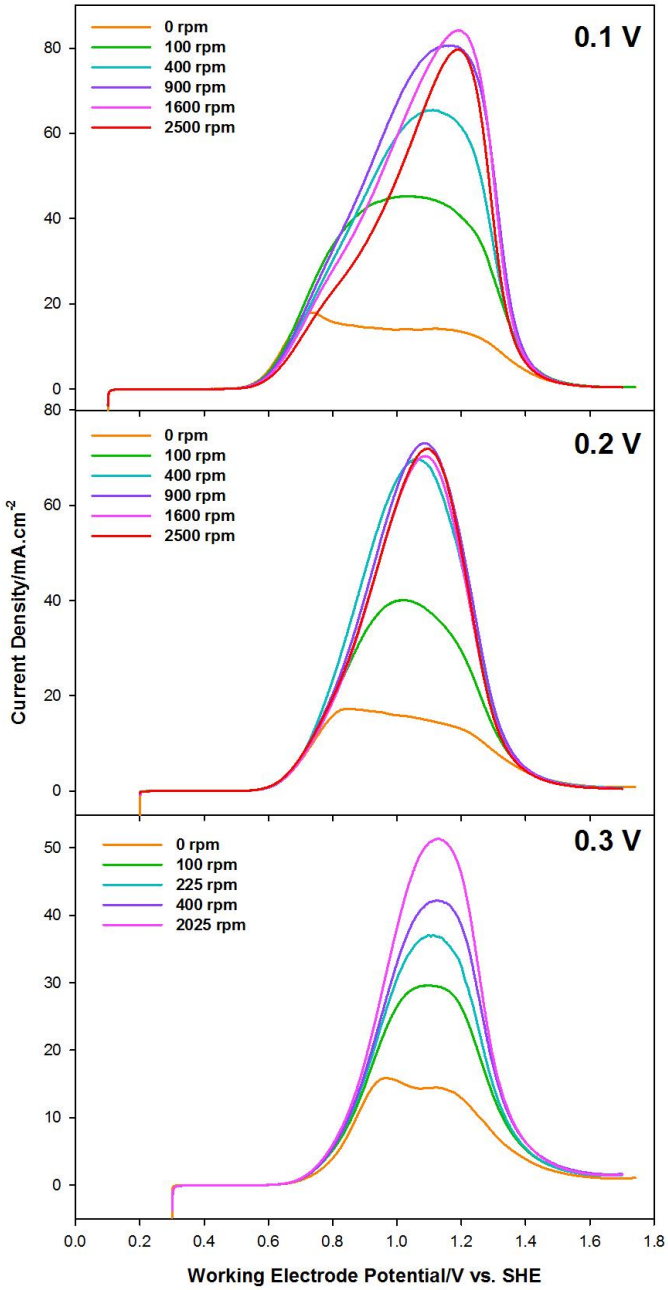

Figure 4.9: **RDE experiments on Pt in 0.5 M H_2SO_4 solution containing 0.1 M SO_2 generated from Na_2SO_3 at different rotation rates**

For Pt it can be seen that for 0.1 V a trend of increasing current density with increasing rotation rate could be observed up until a certain rotation rate (900 rpm) after which the rotation did not influence the current density anymore.

A shift in peak potentials was also observed at higher rotation rates. For 0.2 V this point was reached even sooner and after 400 rpm the current did not increase significantly. At a starting

potential of 0.3 V, however, a good trend of increasing current density with increasing rotation rate could be observed together with good reproducibility (see results with error bars more clearly in Figure 4.10). These results can be used in further Levich and K-L analyses.

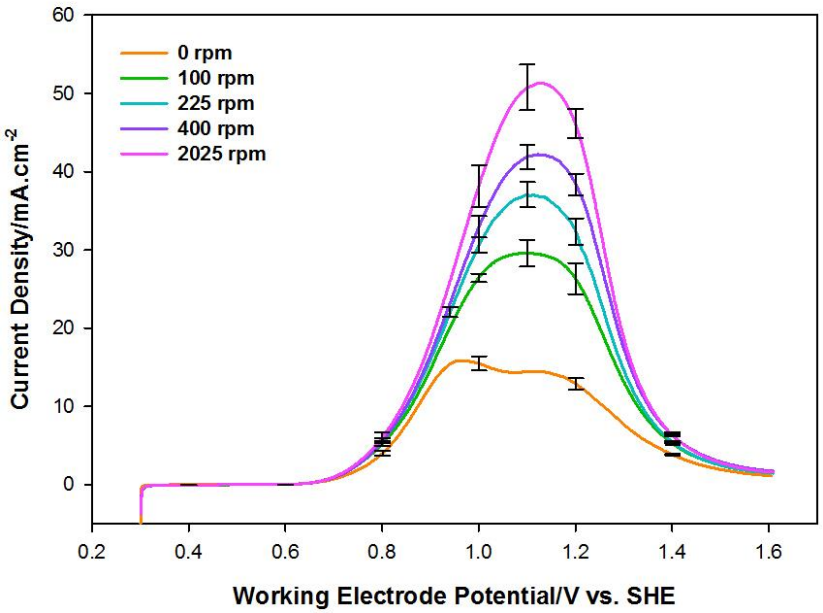

Figure 4.10: RDE experiments on Pt in 0.5 M H_2SO_4 solution containing 0.1 M SO_2 generated from Na_2SO_3 at different rotation rates and a starting potential of 0.3 V

In Section 4.1.4.2 it was mentioned that the presence of adsorbed SO_2 influenced the surface of Pt and might be responsible for many problems encountered. On Au electrodes little or no adsorbed SO_2 was found, as already mentioned, which might be the reason for the good activity of the SO_2 oxidation reaction on Au compared to Pt. These observations may be an explanation for the behaviour of Rh, since the presence of strongly adsorbed SO_2, and its oxidation products, limit the activity of a catalyst. Therefore perhaps the problems encountered on Rh in spite of which type of SO_2 was used and of concentration, might be attributed to very strongly adsorbed SO_2 present on the surface of Rh (even more strongly than for Pt). This observation was confirmed by Kriek *et al.* (2013) where it was shown by means of DFT that SO_2 bonded stronger on Rh than on Pt.

For Pt, the E_{LOW} value is crucial since an appropriate amount of adsorbed sulphur is needed for the reaction to occur optimally. At too low or too high potentials, the reaction will not be enhanced sufficiently since too much or too little adsorbed sulphur will be present.

Generally better results were obtained when using the Na_2SO_3 solution to generate a low concentration of SO_2 gas than when the electrolyte solution saturated with pure SO_2 gas was

used. This might be due to very high adsorption of the gas that led to the formation of excess sulphur on the surface of the electrode. It was also easier to control the concentration of SO_2 in solution each time an experiment was done since a certain amount of Na_2SO_3 was added. This might add to the better reproducibility, as well as easier cleaning of electrodes during the preconditioning procedures.

- **Levich analysis**

The Levich plot for Pt can be seen in Figure 4.11 and this plot was drawn using the peak current densities at the different rotation rates.

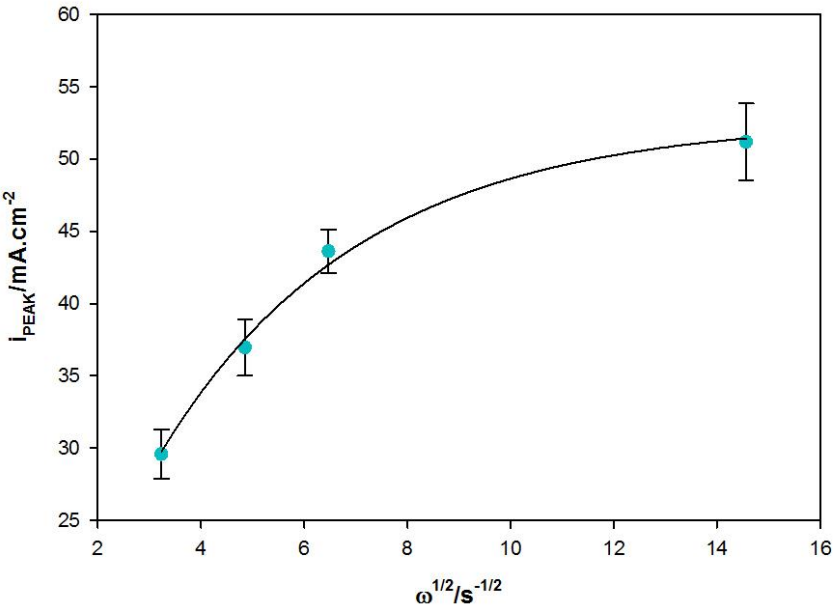

Figure 4.11: Levich plot for Pt in 0.5 M H_2SO_4 at a lower potential value of 0.3 V

A curved line was obtained, which is different to the results from the ORR in Chapter 2 where straight lines were obtained. This is similar to results from O'Brien *et al.* (2012) where they found that Pt gave a curved Levich plot in contrast to a straight line given by Au. They ascribed this to the reaction not being entirely diffusion limited on Pt, in contrast to Au which showed diffusion limitation indicated also by the formation of a plateau region at high potentials where the reaction on Pt eventually became inhibited. This is also true here, since when compared to the oxygen reduction reaction, which showed clear diffusion limitation by the formation of a plateau region, Pt became inhibited at high potentials due to the formation of surface oxide species. This was confirmed by the straight line obtained for the ORR in Levich plots versus the curved line obtained for SO_2 oxidation.

- **K-L analysis**

Mechanistic (number of electrons) and kinetic analysis on Pt were conducted using the Levich, K-L, and Tafel analyses techniques described in full in Chapter 2. This was done using results obtained at a E_{LOW} value of 0.3 V. The K-L plots for Pt can be seen in Figure 4.12.

A series of parallel straight lines were obtained. This is an indication that a single mechanism is followed in the potential range used for the K-L analysis. The calculated number of electrons transferred and kinetic current densities for the potential range studied for K-L analysis are shown in Table 4.1 for Pt.

As can be seen from Table 4.1, the number of electrons transferred on a Pt electrode during the SO_2 oxidation reaction at the different overpotential values are all approximately 2. This corresponds well with the general reaction that occurs during the oxidation of SO_2 where 2 electrons are transferred:

$$SO_{2(aq)} + 2H_2O \rightarrow H_2SO_4 + 2H^+ + 2e^- \quad | \quad E^0 = 0.158V\ (vs.SHE) \quad | \quad (32)$$

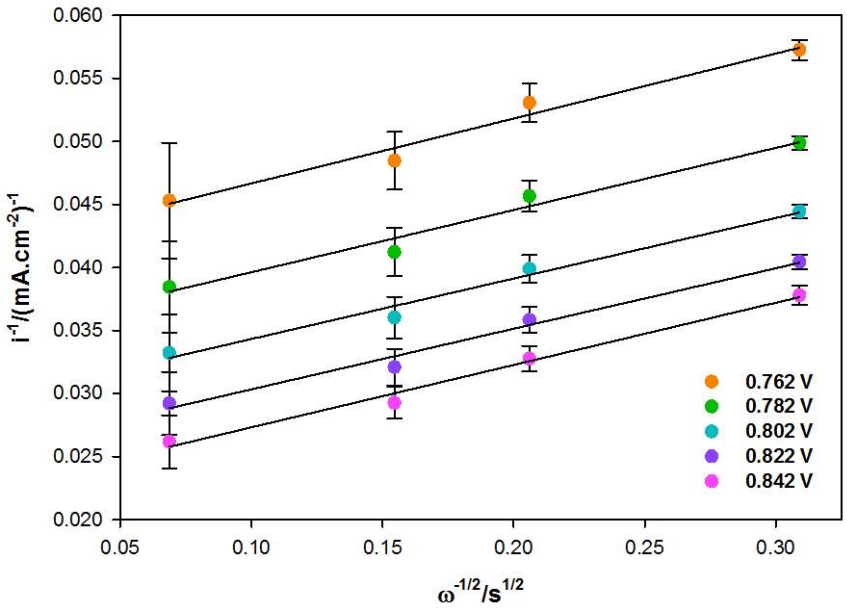

Figure 4.12: **K-L plots for Pt in 0.5 M H_2SO_4 at a starting potential of 0.3 V**

Table 4:1: **Calculated number of electrons transferred for Pt in 0.5 M H_2SO_4 from K-L plots**

Potential (V)	Overpotential (V)	n
0.92	0.762	1.994

0.94	0.782	2.083
0.96	0.802	2.135
0.98	0.822	2.135
1.00	0.842	2.075

- **Tafel analysis**

The Tafel plots for Rh and Pt can be drawn by using the results at 0 rpm at the E_{LOW} value of 0.3 V, since the best results for both catalysts were obtained at this potential. These plots were drawn by plotting the working electrode potential against the logarithm of the current density from which the linear segments were used. The Tafel plots for Rh and Pt can be seen in Figure 4.13.

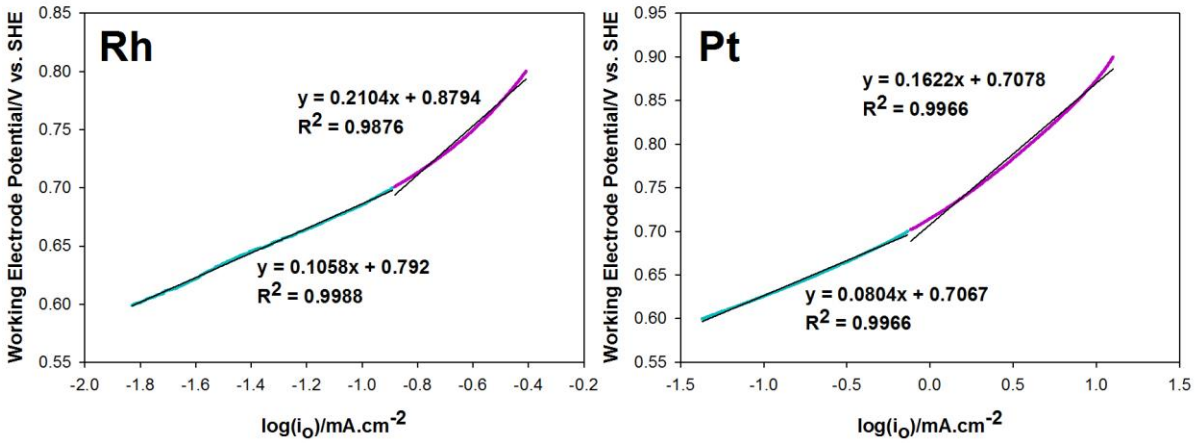

Figure 4.13: Tafel plots for Rh and Pt in 0.5 M H_2SO_4 at a starting potential of 0.3 V

Two Tafel slopes could be obtained for both catalysts. For Rh, a Tafel slope of 105.8 mV.dec^{-1} was found for potentials between 0.6 V and 0.7 V. For Pt a Tafel slope of 80.4 mV.dec^{-1} was found in the same potential region. At potentials above 0.7 V for both catalysts, the Tafel slope doubled with Rh reaching a value of 210.4 mV.dec^{-1} and Pt 162.22 mV.dec^{-1}. Therefore, at potentials above 0.7 V, the mechanism on each electrode changed. This might be due to the presence of more surface oxide species on the surfaces of the electrodes, which had an effect on the oxidation reaction. Another possibility is more occupation of surface sites by molecular SO_2, which in turn adsorbed strongly and influenced the mechanism of the reaction at these potentials. In comparison, a different mechanism was also present on Rh than on Pt since both values for the Tafel slope were different from the values obtained for both catalysts.

4.4. CONCLUSIONS

4.4.1. Comparison between different forms of SO_2 and different E_{LOW} values

Better results were obtained in the electrolyte solution where Na_2SO_3 was added to the sulphuric acid solution than when pure SO_2 gas was bubbled into the solution to form a saturated solution in the sense that Pt showed results more comparable to what was obtained from the literature as mentioned in Section 4.1. The same trend was observed for Rh in both types of electrolyte solutions in that the E_{LOW} value influenced the mechanism followed greatly due to the formation of adsorbed sulphur as seen from peaks at different potential values for the different E_{LOW} values. Sulphur species formed at low potentials which either enhanced or inhibited the reaction, depending on the extent of the adsorption. Further studies were conducted in the electrolyte solution to which the Na_2SO_3 salt was added to form SO_2. The best results were found at 0.3 V for both catalysts.

4.4.2. RDE Studies

Results for Rh did not allow Levich and K-L analyses, since an increase in current density with increasing rotation rate could not be observed. These analyses were done for Pt and the results agreed well with that obtained by O'Brien *et al*. (2012). It was observed that the reaction on Pt was not diffusion limited from the curved plot obtained from Levich analysis. From K-L analysis the number of electrons transferred, corresponded well with the 2 electron oxidation reaction that the SO_2 oxidation reaction follows. Tafel plots were drawn from results at 0 rpm for both catalysts revealing a changing mechanism on both as the potential was taken to higher values. This might be due to the presence of the surface oxide of each catalyst, as well as removal of adsorbed sulphur and adsorption of molecular SO_2. Many of the possible intermediate species may also be responsible. The low current densities achieved by Rh, together with lower onset and peak potentials by Pt, indicate that Rh is not a suitable catalyst for the oxidation of SO_2.

5 CONCLUDING REMARKS

The main focus of this study was to investigate and compare the oxidation of SO_2 on polycrystalline Rh and Pt as catalysts. This reaction occurs at the anode of a sulphur dioxide depolarized electrolyser for the production of hydrogen as a clean and renewable energy carrier. Two other reactions were also included in this study to assist in the characterization of the catalysts. The oxygen reduction reaction was investigated first due to being a well-studied reaction with multiple reaction mechanisms that might occur in a single potential range. The ethanol oxidation reaction was chosen as another reaction for preparation before attempting the SO_2 oxidation reaction since it was a much more complex reaction with multiple reaction pathways and intermediate species that might play a part during the reaction. These two reactions assisted in understanding why certain problems might be encountered on each electrode and served as a good foundation from which further studies could be conducted.

5.1. Oxygen Reduction Reaction

In acidic electrolyte it was shown that Pt exhibited better catalytic activity than Rh from onset potentials and limiting current densities. Rh achieved a limiting current density of 0.291 $mA.cm^{-2}$ at an onset potential (overpotential) of 0.568 V where Pt achieved a limiting current density of 0.229 V at an onset potential (overpotential) of 0.44 V. Despite the higher current density achieved on Rh, the limiting current density was reached much quicker on Pt. A change in the mechanism operating on Pt was observed as the overpotential was increased as seen from the number of electrons transferred from Levich ($n = 2.9$) and K-L ($2.9 < n < 3.4$) analyses. For Rh, a change in mechanism was also observed from the number of electrons transferred from Levich ($n = 3.5$) and K-L ($n = \sim4$) analyses. Levich analysis also revealed that the ORR was diffusion limited on each catalyst (from linearity of these plots). The difference in values observed between the two catalysts also indicated that a different mechanism was followed on Rh, compared to Pt. The difference in values obtained from Tafel analysis confirms confirmed that there was a different mechanism followed on each catalyst (221.3 $mV.dec^{-1}$ for Pt vs. 168.8 $mV.dec^{-1}$ for Rh).

In alkaline electrolyte Rh exhibited very similar behaviour to that of Pt. A slightly higher limiting current density was obtained on Rh (0.228 $mA.cm^{-2}$) than on Pt (0.201 $mA.cm^{-2}$) at onset potentials (overpotentials) close to that obtained on Pt (0.327 V for Rh vs. 0.270 V for Pt). The limiting current density achieved by Rh was also reached quicker in alkaline electrolyte compared to in acidic electrolyte. Similar as in acidic electrolyte, a changing mechanism was

operative on each catalyst's surface as the overpotential was increased as seen from the number of electrons transferred from Levich (n = 3.5 for Rh and n = 3.1 for Pt) and K-L (4 < n < 4.3 for Rh and 0.41 < n < 0.49 for Pt) analyses. The mechanism was also different for each catalyst, which could be confirmed by Tafel analysis (178.1 mV.decade^{-1} for Pt vs. 278 mV.decade^{-1} for Rh).

5.2. Ethanol Oxidation Reaction

Rh showed very limited catalytic activity compared to Pt in acidic electrolyte for the EOR as shown from the very smaller peak current densities achieved. The reaction was initiated earlier on Rh than on Pt (0.2 V for Rh vs. 0.3 V for Pt). Rh showed similar behaviour than Pt in the sense that the same features were present for both catalysts which might indicate that a similar mechanism was operative on both catalysts. This was confirmed by the similar Tafel slopes obtained for both catalysts (209.9 mV.dec^{-1} for Rh and 226.1 mV.dec^{-1} for Pt). However, the low reaction kinetics present on Rh indicated that it did not show much promise as catalyst for the EOR in acidic media. However, the lower onset potential achieved on Rh confirmed that it showed promise for use as co-catalyst to improve the performance of Pt.

In alkaline electrolyte two different concentrations of KOH were investigated (1 M and 0.1 M) and much higher current densities were obtained in the 1 M KOH, as well as a shift in the peak potentials to higher values. More suppression of currents was observed in the hydrogen adsorption/desorption region in the 0.1 M KOH for both catalysts which might be due to better adsorption of EtOH and its dissociation products in this concentration of electrolyte (which also allowed higher current densities to be reached). Poor reproducibility was, however, obtained when using this concentration of electrolyte and further studies were conducted in the 1 M KOH electrolyte solution. During RDE studies a decrease in current density was observed for Pt as the electrode was rotated due to low adsorption of EtOH and products formed during the oxidation of EtOH. An initial increase was observed for Rh whereafter the current density also decreased with increased rotation of the electrode. This suggested that to some extent adsorption of EtOH occured on Rh. This could be confirmed by a higher i_f/i_b ratio which indicated that more complete oxidation of adsorbed species (formed during the forward scan from oxidation of EtOH) occurred during the backward scan. Therefore, the presence of adsorbed species played a larger role on Rh when compared to Pt. Differences observed from Tafel slopes indicated that the same mechanism was not followed on both catalysts since only one Tafel slope was present on Rh (165.1 mV.decade^{-1}) and two were present on Pt (123.1 mV.decade^{-1} in a lower potential region and 192.4 mV.decade^{-1} in a higher potential region).

5.3. SO_2 Oxidation Reaction

Different types of electrolyte were used in the study of the SO_2 oxidation reaction; pure gas bubbled into an acid solution to create a solution saturated with SO_2 and a sulphuric acid solution to which Na_2SO_3 salt was added to generate a SO_2 concentration of 0.1 M. These two types of electrolyte solutions were compared at different E_{LOW} values since SO_2 underwent reduction to produce sulphur at low potentials which adsorbed onto the surface and influenced the reaction mechanism. An enhancement was seen at lower E_{LOW} values where more of these adsorbed sulphur species were present. When the E_{LOW} value was taken to too low values (< 0.2 V) too much adsorbed sulphur was formed which inhibited the reaction on each catalyst. Better results were obtained by Pt in the electrolyte solution where Na_2SO_3 salt was added to the sulphuric acid solution in the sense that the results agreed better to what was observed in literature. Rh showed similar behaviour in both types of electrolytes used, and the mechanism was influenced significantly by the different E_{LOW} values. Further evaluation of catalysts was done in the sulphuric acid solution to which the Na_2SO_3 salt was added to generate SO_2.

During RDE studies it was shown that Rh did not exhibit good behaviour since an increase in current density could not be achieved by increasing the rotation rate at any of the E_{LOW} values. Further evaluation (Levich and K-L analyses) was done on Pt to show that good behaviour which agreed with literature could be obtained in the system used in our laboratories. During Levich analysis it was shown that Pt did not exhibit diffusion limitation. K-L analysis revealed a number of electrons transferred close to 2, which confirmed that the SO_2 oxidation reaction during which 2 electrons were transferred was occurring on the surface of Pt. Levich analysis was done on both catalysts from the results obtained at 0 rpm and two Tafel slopes were obtained for each catalyst. The Tafel slopes changed from 105.8 $mV.dec^{-1}$ for Rh and 80.4 $mV.dec^{-1}$ for Pt at potentials below 0.7 V to 210.4 $mV.dec^{-1}$ for Rh and 162.2 $mV.dec^{-1}$ for Pt above 0.7 V. This increase in Tafel slope for both catalysts could be ascribed to a change in mechanism for each catalyst at high potentials which could be attributed to a change in the surface due to adsorption of SO_2 or intermediate species formed during its oxidation, formation of surface oxide or removal of adsorbed sulphur species.

Rh did not show good activity due to very low current densities achieved when compared to Pt (0.598 $mA.cm^{-2}$ for Rh vs. 15.873 $mA.cm^{-2}$ for Pt). This could be ascribed to stronger adsorption of molecular SO_2 onto the surface of Rh when compared to Pt which was confirmed by Kriek *et al.* (2013) from DFT results.

5.4. Summary

It was shown that Rh showed similar behaviour than Pt during the study of the reduction of oxygen although a different mechanism was probably followed on each catalyst. During the study of the oxidation of ethanol it was shown that adsorbed species played a more significant role on Rh than on Pt even in different types of electrolyte solutions together with low activity. For the oxidation of SO_2, it seemed that adsorbed species (sulphur, SO_2 as well as intermediates formed during oxidation of SO_2) were responsible for the low activity observed on Rh compared to Pt. Therefore, it seems that the poor catalytic activity observed on Rh for the ethanol oxidation reaction and the SO_2 oxidation reaction might be due to susceptibility of this catalyst to surface poisoning due to the presence of strongly adsorbed species, either the reagents present in the electrolyte solution or products formed during the electrochemical oxidation of these reagents.

Finally, Rh did not show much promise for use as catalyst on its own or as a co-catalyst for the oxidation of SO_2 due to various reasons. Very low catalytic activity, as could be seen from the very low current densities, was achieved. Strong adsorption of SO_2 and possibly intermediate species formed during the oxidation of SO_2 which poisoned the electrode surface and which created even more complications for an already complicated reaction.

Bibliography

ANTOLINI, E. 2007. Catalysts for direct ethanol fuel cells. *Journal of power sources*, 170:1-12.

APPLEBY, AJ & PINCHON, B. 1979. The mechanism of the electrochemical oxidation of sulfur dioxide in sulfuric acid solutions. *Journal of Electroanalytical Chemistry*, 95:59-71.

ATKINS, D & DE PAULA, J. 2006. Atkins' Physical Chemistry. Oxford: Oxford University Press. 1064p.

BARD, AJ & FAULKNER, LR. 2001. Electrochemical methods: fundamentals and applications. United States of America: John Wiley & Sons.

BATISTA, EA, MALPASS, GRP, MOTHEO, AJ & IWASITA, T. 2004. New mechanistic aspects of methanol oxidation. *Journal of Electroanalytical Chemistry*, 571:273-282.

DE SOUZA, JPI, QUEIROZ, SL, BERGAMASKI, K, GONZALEZ, ER & NART, FC. 2002. Electro-oxidation of ethanol on Pt, Rh and PtRh electrodes. A study using DEMS and in-situ FTIR techniques. *Journal of Physical Chemistry B*, 106:9825-9830.

FANG, X, WANG, L, KANG SHEN, P, CUI, G & BIANCHINI, C. 2010. An in situ Fourier transform infrared spectroelectrochemical study on ethanol electrooxidation on Pd in alkaline solution. *Journal of power sources*, 195:1375-1378.

GENSHAW, MA, DAMJANOVIC, A & BOCKRIS, J.O.M. 1967. The role of hydrogen peroxide in oxygen reduction at rhodium electrodes. *The Journal of Physical Chemistry*, 71:3722-3731.

GORENSEK, MB, STASER, JA, STANFORD, TG & WEIDNER, JW. 2009. A thermodynamic analysis of the SO_2/H_2SO_4 system in SO_2-depolarized electrolysis. *International journal of hydrogen energy*, 34:6089-6095.

GORENSEK, MB & SUMMERS, WA. 2009. Hybrid sulfur flowsheets using PEM electrolysis and a bayonet decomposition reactor. *International journal of hydrogen energy*, 34:4097.

GUPTA, SS & DATTA, J. 2006. A comparative study on ethanol oxidation behaviour at Pt and PtRh electrodeposits. *Journal of electroanalytical chemistry*:65-72.

HAYES, JR, ZELLER, DJ & FRIESEN, C. 2008. The influence of platinum surface morphology on the electrooxidation of methanol in alkaline solutions. *ECS Transactions*, 13(23):41-54.

KORZENEWSKI, C, MCKENNA, W & PONS, S. 1987. An in situ infrared study of the oxidation of sulfur dioxide on platinum electrodes. *Journal of Electroanalytical Chemistry*, 235:361-368.

KOWAL, A, GOJKOVIC, SLj, LEE, K-S, OLSZEWSKI, P & SUNG, Y-E. 2009. Synthesis, characterization and electrocatalytic activity for ethanol oxidation of carbon supported Pt, Pt-Rh, Pt-SnO2 and Pt-Rh-SnO2 nanoclusters. *Electrochemistry communications*, 11:724-727.

KRIEK, RJ, VAN RAVENSWAAY, JP, POTGIETER, M, CALITZ, A, LATES, V, BJORKETUN, ME, SIAHROSTAMI, S & ROSSMEISL, J. 2013. SO_2 - an indirect source of energy. *The Journal of The Southern African Institute of Mining and Metallurgy*, 113:593-604.

KUTZ, RB, BRAUNSCHWEIG, B, MUKHERJEE, P, BEHRENS, RL, DLOTT, DD & WIECHOWSKI, A. 2011. Reaction pathways of ethanol electrooxidation on polycrystalline platinum catalysts in acidic electrolytes. *Journal of catalysis*, 278:181-188.

LAI, SCS, KLEIJN, SEF, OZTURK, FTZ, VAN REES VELLINGA, VC, KONING, J, RODRIQUEZ, P & KOPER, MTM. 2010. Effects of electrolyte pH and composition on the ethanol electro-oxidation reaction. *Catalysis Today*, 154:94-104.

LAI, SCS & KOPER, MTM. 2009. Ethanol electro-oxidation on platinum in alkaline media. *Physical chemistry chemical physics*, 11:10466-10456.

LAMY, C, LIMA, A, LERHUN, V, DELIME, F, COUTANCEAU, C & LEGER, J-M. 2002. Recent advances in the development of direct alcohol fuel cells (DAFC). *Journal of power sources*, 105:283-296.

LAMY, C, ROUSSEAU, S, BELGSIR, EM, COUTANCEAU, C & LEGER, JM. 2004. Recent progress in the direct ethanol fuel cell: development of new platinum-tin electrocatalysts. *Electrochimica acta*, 278:3901-3908.

LAURSEN, AB, MAN, IC, TRINHAMMER, OL, ROSSMEISL, J & DAHL, S. 2011. The Sabatier Principle Illustrated by Catalytic H_2O_2 Decomposition on Metal Surfaces. *Journal of Chemical Education*, 88:1711-1715.

LAURSEN, AB, VARELA, AS, DIONIGI, F, FANCHIU, H, MILLER, C, TRINHAMMER, OL, ROSSMEISL, J & DAHL, S. 2012. Electrochemical Hydrogen Evolution: Sabatier's Principle and the Volcano Plot. *Journal of Chemical Education*, 89:1595-1599.

LIANG, ZX, ZHAO, TS, XU, JB & LD, Zhu. 2009. Mechanism study of the ethanol oxidation reaction on palladium in alkaline media. *Electrochimica acta*, 54:2203-2208.

LU, PWT & AMMON, RL. 1980. An investigation of electrode materials for the anodic oxidation of sulfur dioxide in concentrated sulfuric acid. *Journal of The Electrochemical Society*, 127(12):2610-2616.

LU, PWT & AMMON, RL. 1982. Sulfur dioxide depolarized electrolysis for hydrogen production: Development status. *International Journal of Hydrogen Energy*, 7(7):563-575.

MARKOVIC, NM, GASTEIGER, HA, ROSS, PN, JIANG, X, VILLEGAS, I & WEAVER, MJ. 1995. Electro-oxidation mechanisms of methanol and formic acid on Pt-Ru alloy surfaces. *Electrochimica Acta*, 40:91-98.

MARKOVIC, NM & ROSS JR, PN. 2002. Surface science studies of model fuel cell electrocatalysts. *Surface Science Reports*, 45:117-229.

MARTINOVIC, JM, SEPA, DB & VOJNOVIC, MV. 1988. Kinetics of electrochemical reduction of oxygen at rhodium. *Electrochimica Acta*, 33:1267-1272.

MORAES, IR, WEBER, M & NART, FC. 1997. On the structure of adsorbed sulfur dioxide at the platinum electrode. *Electrochimica Acta*, 42(4):617-625.

MORAES, IR, WEBER, M & NART, FC. 1997. On the structure of adsorbed sulfur dioxide at the platinum electrode. *Electrochimica Acta*, 42:617-625.

NORSKOV, JK, ROSSMEISL, J, LOGADOTTIR, A & LINDQVIST, L. 2004. Origin of the Overpotential for Oxygen Reduction at a Fuel-Cell Cathode. *Journal of Physical Chemistry B*, 108:17886-17892.

O'BRIEN, JA, HINKLEY, JT & DONNE, SW. 2012. Electrochemical oxidation of aqueous sulfur dioxide II. Comparative studies on platinum and gold electrodes. *Journal of the electrochemical society*, 159(9):F585-F593.

O'BRIEN, JA, HINKLEY, JT, DONNE, SW & LINDQUIST, S-E. 2010. The electrochemical oxidation of aqueous sulfur dioxide: A critical review of work with respect to the hybrid sulfur cycle. *Electrochimica Acta*, 55:573-591.

PLETCHER, D. 2009. A First course in electrode processes 2nd edition. Cambridge: The Royal Society of Chemistry. 301p.

QUIJADA, C, HUERTA, FJ, MORALLON, E, VAZQUEZ, JL & BERLOUIS, LEA. 2000a. Electrochemical behaviour of aqueous SO_2 at polycrystalline gold electrodes in acidic media: a voltammetric and in situ vibrational study. Part 1. Reduction of SO_2: deposition of monomeric and polymeric sulfur. *Electrochimica Acta*, 45:1874-1862.

QUIJADA, C, MORALLON, E, VAZQUEZ, JL & BERLOUIS, LEA. 2000b. Electrochemical behaviour of aqueous SO_2 at polycrystalline gold electrodes in acidic media. A voltammetric and in situ vibrational study. Part II. Oxidation of SO2 on bare and sulphur-modified electrodes. *Electrochimica Acta*, 46:651-659.

QUIJADA, C, RODES, A, VAZQUEZ, JL, PEREZ, JM & ALDAZ, a. 1995a. Electrochemical behaviour of aqueous SO_2 at Pt electrodes in acidic medium. A voltammetric and in situ Fourier transform IR study part I. Oxidation of SO2 on Pt electrodes with sulphur-oxygen adsorbed species. *Journal of Electroanalytical Chemistry*, 394:217-227.

QUIJADA, C, RODES, A, VAZQUEZ, JL, PEREZ, JM & ALDAZ, A. 1995b. Electrochemical behaviour of aqueous sulphur dioxide at polycrystalline Pt electrodes in acidic medium. A voltammetric and in-situ FT-IR study Part II. Promoted oxidation of sulphur dioxide. Reduction of sulphur dioxide. *Journal of Electroanalytical Chemistry*, 398:105-115.

QUIJADA, C, VAZQUEZ, JL & ALDAZ, A. 1996. Study of sulfur adlayers on polyoriented platinum electrodes: influence of the electrocatalysis of the SO_2 oxidation reaction. *Journal of Electroanalytical Chemistry*, 414:229-233.

QUIJADA, C, VAZQUEZ, JL, PEREZ, JM & ALDAZ, A. 1994. Voltammetric behaviour of irreversibly adsorbed SO_2 on a Pt(111) electrode in sulphuric acid medium. *Journal of Electroanalytical Chemistry*, 372:243-250.

SAMEC, Z & WEBER, J. 1975. Study of the oxidation of SO_2 dissolved in 0.5M H2SO4 on a gold electrode - I stationary electrode. *Electrochimica Acta*, 20:403-412.

SAMEC, W & WEBER, J. 1975a. Study of the oxidation of SO_2 dissolved in 0.5M H2SO4 on a gold electrode - II. A rotating disc electrode. *Electrochimica Acta*, 20:413-419.

SAMEC, Z & WEBER, J. 1975b. Study of the oxidation of SO_2 dissolved in 0.5M H2SO4 on a gold electrode-1 Stasionary electrode. *Electrochimica Acta*, 20:403-412.

SAWYER, DT & DAY, RJ. 1963. Kinetics for oxygen reduction at platinum, palladium and silver electrodes. *Electrochimica Acta*, 8:589-594.

SCOTT, K & TAAMA, WM. 1999. An investigation of anode materials in the anodic oxidation of sulphur dioxide in suphuric acid solutions. *Electrochimica Acta*, 44:3421-3427.

SEO, ET & SAWYER, DT. 1964. Determination of sulfur dioxide in solution by anodic voltammetry and by UV spectrophotometry. *Journal of Electroanalytical Chemistry*, 7:184-189.

SEO, ET & SAWYER, DT. 1965. Electrochemical oxidation of dissolved sulfur dioxide at platinum and gold electrodes. *Electrochimica Acta*, 10:239-252.

SEPA, DB & VOJNOVIC, MV. 1981. Reaction intermediates as a controlling factor in the kinetics and mechanism of oxygen reduction at platinum electrodes. *Electrochimica Acta*, 26:781-793.

SHAO, MH, HUANG, T, LIU, P, ZHANG, J, SASAKI, K, VUKMIROVIC, MB & ADZIC, RR. 2006. Palladium monolayer and palladium alloy electrocatalysts for oxygen reduction. *Langmuir*, 22:10409-10415.

SHEN, SY, ZHAO, TB & XU, JB. 2010. Carbon supported PtRh catalysts for ethanol oxidation in alkaline direct ethanol fuel cell. *International journal of hydrogen energy*:12911-12917.

SONG, C & ZHANG, J. 2008. PEM Fuel Cell Electrocatalysts and Catalyst Layers Fundamentals and Applications. Springer.

SPOTNITZ, RM, COLUCCI, JA & LANGER, SH. 1983. The activated electro-oxidation of sulphur dioxide on smooth platinum. *Electrochimica Acta*, 28:1053-1983.

STREBER, R, PAPP, C, LORENZ, M.P.A., HOFERT, O, DARLATT, E, BAYER, A, DENECKE, R & STEINRUCK, H.-P. 2010. SO_2 adsorption and thermal evolution on clean and oxygen precovered Pt(111). *Chemical Physics Letters*

STRUCK, BD, JUNGINGER, R, BOLTERSDORF, D & GEHRMANN, J. 1980. The anodic oxidation of sulfur dioxide in the sulfuric acid hybrid cycle. *International Journal of Hydrogen energy*, 5:487-497.

SUO, Y & HSING, I-M. 2011. Highly active rhodium/carbon nanaocatalysts for ethanol oxidation in alkaline medium. *Journal of power sources*, 196:7945-7950.

TREIMER, S, TANG, A & JOHNSON, DC. 2002. A Consideration of the Application of Koutecky-Levich Plots in the Diagnosis of Charge-Transfer Mechanisms at Rotated Disk Electrodes. *Electroanalysis*, 14:165-171.

VERMA, A & BASU, S. 2005. Direct use of alcohols and sodium borohydride as fuel in an alkaline fuel cell. *Journal of power sources*, 145:282-285.

VIGIER, F, COUNTANCEAU, C, PERRARD, A, BELGSIR, EM & LAMY, C. 2004. Development of anode catalysts for a direct ethanol fuel cell. *Journal of applied electrochemistry*, 34:439-446.

WAKABAYASHI, N, TAKEICHI, M, ITAGAKI, M, YCHIDA, H & WATANABE, M. 2005. Temperature-dependance of oxygen reduction activity at a platinum electrode in an acidic electrolyte solution investigated with a channel flow double electrode. *Journal of Electroanalytical Chemistry*, 574:339-346.

XU, JB, ZHAO, TS, SHEN, SY & LI, YS. 2010. Stabilization of the palladium electrocatalyst with alloyed gold for ethanol oxidation. *International journal of hydrogen energy*, 35:6490-6500.

Appendix

Table 1: Slopes, Y-Intercepts and kinetic current densities for the ORR in acidic electrolyte for Rh

Potential (V)	Overpotential (V)	Slope	Y-Intercept	R^2 value	n	Kinetic current density ($mA.cm^{-2}$)
0.230	1.000	2.129	0.049	1.000	4.035	20.243
0.250	0.980	2.115	0.062	0.999	4.062	16.129
0.270	0.960	2.110	0.080	0.998	4.070	12.579
0.290	0.940	2.107	0.107	0.995	4.077	9.320
0.310	0.920	2.153	0.146	0.985	3.989	6.849

Table 2: Slopes, Y-Intercepts and kinetic current densities for the ORR in acidic electrolyte for Pt

Potential (V)	Overpotential (V)	Slope	Y-Intercept	R^2 value	n	Kinetic current density ($mA.cm^{-2}$)
0.550	0.680	2.511	0.065	0.998	3.420	15.456
0.570	0.660	2.522	0.085	0.996	3.405	11.710
0.590	0.640	2.585	0.103	0.994	3.322	9.756
0.610	0.620	2.699	0.124	0.988	3.182	8.052
0.630	0.600	2.888	0.151	0.977	2.974	6.631

Table 3: Slopes, Y-Intercepts and kinetic current densities for the ORR in alkaline electrolyte for Rh

Potential (V)	Overpotential (V)	Slope	Y-Intercept	R^2 value	n	Kinetic current density ($mA.cm^{-2}$)
-0.300	0.701	2.110	0.073	0.994	4.320	13.624
-0.320	0.721	2.164	0.061	0.996	4.211	16.420
-0.340	0.741	2.198	0.052	0.996	4.146	19.157
-0.360	0.761	2.251	0.043	0.997	4.048	23.310
-0.380	0.781	2.265	0.038	0.998	4.024	26.042

Table 4: Slopes, Y-Intercepts and kinetic current densities for the ORR in alkaline electrolyte for Pt

Potential (V)	Overpotential (V)	Slope	Y-Intercept	R^2 value	n	Kinetic current density ($mA.cm^{-2}$)
-0.010	0.411	2.043	0.379	0.965	4.461	2.639
-0.030	0.431	2.161	0.274	0.984	4.218	3.644
-0.050	0.451	2.258	0.210	0.989	4.035	4.773
-0.070	0.471	2.317	0.167	0.994	3.934	6.002
-0.090	0.491	2.361	0.135	0.996	3.859	7.418

Calculation of number of electrons from Levich plots:

Levich equation:

$$i_{lim} = 0.620nFAD_0^{2/3}v^{1/6}\omega^{1/2}c^*$$

From Levich equation, isolate n:

$$n = \frac{i_{lim}}{0620FAD_0^{2/3}v^{1/6}\omega^{1/2}c^*}$$

where $slope = \frac{i_{lim}}{\omega^{1/2}}$.

Calculation of numbers of electrons from K-L plots:

K-L equation:

$$\frac{1}{i} = \frac{1}{i_K} + \frac{1}{0.62nFAD_0^{2/3}c^*v^{1/6}\omega^{1/2}}$$

From K-L equation, isolate n:

$$n = \frac{i_{lim}}{0.62nFAD_0^{2/3}c^*v^{1/6}\omega^{1/2}} + \frac{1}{i_K}$$

where $slope = \frac{\omega^{1/2}}{i_{lim}}$ and $y - intercept = \frac{1}{i_K}$